

ABSTRACT

ZHU, JIANCHENG. Approaches to Modify the Protein Resistance of Biodegradable Polyester Brushes. (Under the direction of Christopher B. Gorman).

Polyesters, such as poly(lactic acid) (PLA), poly(glycolide) (PGA) and polycaprolactone (PCL), have drawn a lot of attentions due to their substantial biocompatible property.

Biofouling can inevitably hinder the activity of implanted sensor surface. Usually, even covered with protein resistant coatings, the surface will be attached with proteins within a limited period of time. Hydrophilic polymeric chains, i.e. poly(ethylene glycol) (PEG), were used to cover the sensor surfaces to reduce the non-specific adsorption.

When the biocompatible polymeric layers degrade off, the sensor surface can be refreshed. This new strategy can extend the time in which the sensor is still available. Furthermore, if a gradient thickness can be formed, the underneath substrate can be released and respond to stimuli gradually.

Highly functional PLA materials ought to be developed in nano-ordered morphology with a high level of precision, i.e. polymer brushes. Based on the prepared surface-initiated PLA, PGA, and PCL brushes and their degradation conditions, the synthesis of biocompatible polymer brushes that bind two necessary properties: high-level hydrophilicity (PEG) and fair degradation rates (polyesters) is performed. Those macromolecular chains grown (grafting from) or immobilized (grafting to) are organized to form a water layer within the brushes layer to resist protein, while their backbones, polyesters, degrades relatively fast via a back-biting mechanism.

© Copyright 2015 by Jiancheng Zhu
All Rights Reserved

Approaches To Modify The Protein Resistance Of Biodegradable Polyester Brushes

by
Jiancheng Zhu

A thesis submitted to the Graduate Faculty of
North Carolina State University
in partial fulfillment of the
requirements for the degree of
Master of Science

Chemistry

Raleigh, North Carolina
2015

APPROVED BY:

Christopher B. Gorman

Committee Chair

Jan Genzer

David Shultz

BIOGRAPHY

Jiancheng Zhu graduated from Nankai University and Tianjin University with a B.S. degree in Chemistry and a B.E. degree in Chemical Engineering in 2010. He then began his Master program in Chemistry Department at North Carolina State University in the fall of 2011. There he joined the research group of Christopher B. Gorman where he had the opportunity to work on the surface polymerization project.

ACKNOWLEDGEMENTS

I would like to first thank my advisor, Professor Gorman, for his continuous guidance and help throughout my work during these years. I also thank my committee members, Professor Shultz, Professor Genzer and Professor Pierce, for giving me helpful advices on my research. I thank my group members Menglong, Jingchao, Andrew and Lance for sharing their helpful ideas on my research. Last but not least, I thank my family for their support.

TABLE OF CONTENTS

LIST OF FIGURES	vii
LIST OF TABLES	xi
LIST OF SCHEMES	xii
RESEARCH IDEA AND OBJECTIVE	1
BACKGROUND AND LITERATURE REVIEW	2
A. Biodegradable polymers	2
B. Implanted Biosensors	6
C. Biofouling and attempts at its resolution.....	8
D. Preparation of Polymer Brushes	13
<i>D.1. Surface-initiated polymerization (SIP) (Grafting from)</i>	14
<i>D.2. Grafting to</i>	18
<i>D.3. Physisorption</i>	19
E. Hydrophilicity of bulk PLA and PLA brushes.....	20
<i>E.1. Hydrolysis of PLA, OLA, PLA brushes and other polyesters</i>	20
<i>E.2. Design of hybrid polymer brushes</i>	23
F. Smart Surfaces	23
References:.....	27
RUSLTS AND DISCUSSION	29
A. Reproducing the growth of PLA brushes on silicon surfaces.....	29
<i>A.1. Growth vs. time via ellipsometry</i>	29
<i>A.2. Degradation vs. time via ellipsometry</i>	31
B. Synthesis of PEG ₆ Spirolactide	32
<i>B.1. Reproducing the work of Weck et al.⁴</i>	32
<i>B.2. Polymerization of PEG₆-spirolactide</i>	38
<i>B.3. Enumerating the stereoisomers of PEG₆-Spirolactide</i>	39
C. Synthesis of PEG grafted <i>O</i> -carboxyanhydride	42
<i>C.1. Synthesis of 5-substituted 1,3-dioxolane-2,4-diones</i>	42
<i>C.2. Water sensitivity of 1</i>	43

C.3. Polymerization of OCA in solution and on surfaces	44
D. Synthesis of OEG-Grafted PLA (version II and III)	46
D.1. Synthesis of OEG-Grafted PLA (version II)	46
D.2. Synthesis of OEG-Grafted PLA (version III)	50
References:	53
FUTURE PLANS	54
A. Functional Polylactide-Poly(ethylene glycol) by CuAAC	54
B. Synthetic route for poly(lactide-amino acid)	59
References:	62
EXPERIMENTAL SECTION	63
A. General Considerations	63
B. Reproduced Growth and Degradation Curve of Poly(lactic acid)	64
B.1. Growth of PLA on silicon surface	64
B.2. Degradation of PLA brushes	64
C. PEG ₆ -Grafted PLA: Monomer synthesis and polymerization (All the numbers of molecules are referred to Scheme 10)	65
C.1. Synthesis of Hexaethylene Glycol Methyl Ether 1,2,3- <i>A</i> ² -Triazoline-spiro[6-methyl-1,4-dioxane-2,5-dione-3,2'-bicyclo-[2.2.1]heptanes, PEG ₆ Spirolactide	65
D. Synthesis and polymerization of 5-Phenyl-1,3-dioxolane-2,4-dione [<i>O</i> -carboxyanhydride (OCA)]	77
D.1. Synthesis of 5-Phenyl-1,3-dioxolane-2,4-dione	77
D.2. Test of water sensitivity of 5-Phenyl-1,3-dioxolane-2,4-dione	79
D.3. Polymerization of 5-Phenyl-1,3-dioxolane-2,4-dione	79
E. OEG-Grafted PLA (Version II): Monomer Synthesis and Characterization (All the numbers of molecules are referred to Scheme 16)	79
E.1. Syntheses of 3-(Benzyloxymethyl)-6-methyl-1,4-dioxane-2,5-dione (9)	79
E.2. Attempt at Syntheses of Oligo(ethylene glycol)-grafted Lactide (11)	86
F. OEG-Grafted PLA (Version III): Monomer Synthesis and Characterization (All the numbers of molecules are referred to Scheme 17)	88

<i>F.1. Synthesis of 1-Bromo-7,10,13-trioxatetradecane (16)</i>	88
<i>F.2. Synthesis of 2-Hydroxy-9,12-dioxatridecanoic Acid (18)</i>	89
<i>F.3. Synthesis of 3,6-Bis(7,10,13-trioxatetradecyl)-1,4-dioxane-2,5-dione (19)</i>	93
References:.....	95

LIST OF FIGURES

Figure 1. Schematic of a proposed, smart surface composed of a gradient of degradable polymeric brushes that can gradually release fresh surface to the protein solution.....	1
Figure 2. A typical biosensor architecture and potential analyte species in (A) sample solution, (B) biological recognition layer, (C) transducer that converts interaction of the biological recognition layer with the corresponding substrate into a measurable electrical signal and (D) electrical signal operator for amplification, display and storage. Taken from reference 9.....	6
Figure 3. Carbon nanotube-based enzyme-modified biosensor electrodes using a layer by layer electrostatic self-assembly procedure. Taken from reference 10.....	7
Figure 4. Proteins encapsulation or membrane malfunction lead to malfunction of GOD enzyme biosensor. Taken from reference 11	8
Figure 5. Surface macromolecule structure and binding energy per patch (black for PEG, red for PLL): (A) All covered PEG brushes; (B) full brushes with some buried PLL patches; (C) more buried patches with coiled PEG brushes; (D) dominant PLL patches make PEG lose brush characters and remain in “mushroom” regime. Taken from reference 18	10
Figure 6. Two main approaches of combating surface biofouling: (Left) Hydrophilic polymers (off-white) are grafted on surface to hide it from the cells of body (blue); (Right) Bioactive peptide motifs (off-white) are modified on surface to imitate the function of cell membrane to communicate well with immune cells. Taken from reference 19.....	12
Figure 7. A combination of antibiofouling polymers with bioactive signaling motifs. Taken from reference.....	13
Figure 8. Structure of PHEMA-b-PMMA brushes and the variation of chain lengths. Taken from reference 28.....	17

Figure 9. The height of polymeric chains as a function of grafting density, where N is the degree of polymerization of the polymer and σ the grafting density	25
Figure 10. The solution draining method for preparation of a polymer brush with a gradient in thickness. Taken from reference 2	26
Figure 11. Ellipsometric thickness of PLA brushes from surface silanol groups versus growth time (left) and reproduced plot (right)	30
Figure 12. Ellipsometric thickness of PLA brushes versus degradation time at 37°C under different pH conditions (left) and reproduced plot at 37°C and pH=8 (right)	31
Figure 13. Ellipsometric thicknesses of absorbed BSA on PLA (left) and OEG (right) coated Si surfaces versus incubation time in BSA (PBS, pH 7.4, 10 mM ionic strength, 37 °C) solutions with different concentrations	33
Figure 14. ^1H , ^1H -COSY spectrum of PEG ₆ -spirolactide in CDCl ₃	37
Figure 15. Infrared spectrum of PEG ₆ -spirolactide	38
Figure 16. ^1H NMR spectra illustrating the hydrolysis of 9 over time	44
Figure 17. ^1H NMR spectrum of (3S, 6S)-3-Bromo-3,6-dimethyl-1,4-dioxane-2,5-dione (CDCl ₃)	66
Figure 18. ^1H NMR spectrum of (6S)-3-Methylene-6-methyl-1,4-dioxane-2,5-dione (CDCl ₃)	67
Figure 19. ^1H NMR spectrum of Spiro[6-methyl-1,4-dioxane-2,5-dione-3,2'-bicyclo[2.2.1]hept[5]ene] (CDCl ₃)	69
Figure 20. ^1H NMR spectrum of heptaethylene glycol monomethyl ether tosylate (CDCl ₃). 70	
Figure 21. ^1H NMR spectrum of azido-poly(ethylene glycol) monomethyl ether (CDCl ₃)... 72	

Figure 22. ^1H NMR spectrum of PEG ₆ -spiro-lactide (CDCl_3)	73
Figure 23. ^{13}C NMR spectrum of PEG ₆ -spiro-lactide (CDCl_3)	74
Figure 24. Mass Spectrum of PEG ₆ -spirolactide	75
Figure 25. ^1H NMR spectrum of PEG ₆ -spiro-PLA (acetone- d_6)	76
Figure 26. ^{13}C NMR spectrum of PEG ₆ -spiro-PLA (CDCl_3)	77
Figure 27. ^1H NMR spectrum of crude OCA (CDCl_3) showing the methane protons of the starting material, mandelic acid and the product	78
Figure 28. ^1H NMR spectrum of 3-Benzyloxy-2-hydroxypropionic Acid (CDCl_3).....	80
Figure 29. ^1H NMR spectrum of L- α -Bromopropionyl Chloride (CDCl_3).....	82
Figure 30. ^1H NMR spectrum of 3-(Benzyloxy)-2-(2-bromopropanoyloxy)propanoic Acid (CDCl_3)	83
Figure 31. ^1H NMR and ^{13}C NMR spectrums of 3-(Benzyloxy)-2-(2-bromopropanoyloxy)propanoic Acid (CDCl_3)	86
Figure 32. ^1H NMR spectrum of Hydroxyl Functionalized Lactide (CDCl_3)	87
Figure 33. ^1H NMR spectrum of 1-Bromo-7,10,13-trioxatetradecane (CDCl_3).....	89
Figure 34. ^1H NMR spectra of α -keto ester 17 (CDCl_3).....	90
Figure 35. ^1H NMR spectrum of α -hydroxyl ester (CDCl_3).....	91
Figure 36. ^1H NMR and ^{13}C NMR spectrums of 2-Hydroxy-9,12-dioxatridecanoic Acid (CDCl_3).....	93

Figure 37. ^1H NMR spectrum of 3,6-Bis(7,10,13-trioxatetradecyl)-1,4-dioxane-2,5-dione
(CDCl_3) 94

LIST OF TABLES

Table 1. Comparison of bio-based and petrochemical polymers.....	4
Table 2. Ellipsometric thicknesses (\AA) of OEG-spiro-PLA brushes prepared under different reaction conditions (tin catalyst).....	39
Table 3. Optimization of Reaction Conditions for the Generation of 10.....	49
Table 4. Optimization of Reaction Conditions for the Generation of 11.....	50
Table 5. Optimization of Reaction Conditions for the Generation of 5.....	52

LIST OF SCHEMES

Scheme 1. Chemical structure of PLA, PCL and PGA and their monomers.....	3
Scheme 2. Ring opening polymerization of (a) poly(ϵ -caprolactone) ²² , (b) poly(lactic acid) ²³ , (c) poly(glutamate) ²⁴	15
Scheme 3. Polystyrene brushes prepared by (a) living anionic polymerization ²⁵ and (b) living cationic polymerization ²⁶	16
Scheme 4. Polymer Brushes of PNIPAM grown on gold surfaces by ATRP	17
Scheme 5. Synthetic route for preparation of mSi-PDLA. Taken from reference 20	19
Scheme 6. Rate determining step of acid- and base-catalyzed hydrolysis of polycarbonate and polyester	21
Scheme 7. A possible degradation route of N-(2-hydroxypropyl)methacrylamide (HPMAM) initiated OLA. k_r -random chain scission, k_{bb} -backbiting, k_{HPMAM} -chain scission at the ester near HPMAM. Taken from reference 34	22
Scheme 8. Mechanism of Surface Initiated ROP of Lactide Catalyzed by Sn(Oct) ₂ . Taken from reference 2	29
Scheme 9. Backbiting mechanism for the degradation of PLA brushes.....	32
Scheme 10. Synthetic route to prepare PEG ₆ Spirolactide	33
Scheme 11. Illustration of the diastereoselectivity of the Diels-Alder reaction of molecule 2 and cyclopentadiene (only the most and least favored are shown).....	35
Scheme 12. Diastereogenic Diels-Alder reaction illustrating facial and endo-exo regioisomers	40

Scheme 13. Stereoisomers of Huisgen Cycloaddition (using the exo, syn to 6-methyl product as the starting material).....	41
Scheme 14. One step synthesis of OCA from D,L-mandelic acid and TCF	42
Scheme 15. Mechanism of ROP of LA catalyzed by DMAP.....	45
Scheme 16. Proposed Synthesis of Cyclic Monomer 13 Using an Acid Chloride Coupling .	47
Scheme 17. Synthesis of Cyclic Monomer 7 Using a Diesterfication.....	51
Scheme 18. Derivatization of PCL by combining ROP and CuAAC.....	55
Scheme 19. Synthetic Route for Polylactide-g-poly(ethylene glycol).....	56
Scheme 20. Synthetic route for 2-hydroxy-4-pentynoic acid (molecule 1 in scheme 1a).....	58
Scheme 21. Synthetic route for OEG modified morpholione-2,5-dione and corresponding polymer	60

RESEARCH IDEA AND OBJECTIVE

The ultimate goal of this research is to prepare a dynamic surface that also is reasonably good at avoiding biofouling. Such a surface is a potential platform for implantable sensors or even sensor arrays that can respond to an environmental stimulus gradually. The research idea involves several fundamental concepts. First, biodegradable polymeric brushes are employed. They may be constructed using “grafting to”, “grafting from” or physical adsorption methods. The brushes must be protein-resistant to some degree. The rate of their degradation off of the surface should be well defined and have a rate that is suitably matched to the time scales for sensing and/or protein adsorption. In a sensor array, a gradient thickness of these brushes across the array elements is needed. Varying the time that the monomer solution is in contact with various regions of the surface (and thus the time available for the polymerization reaction) is one good way to prepare a gradient thickness. Although the sensing substrate (gold or Si) will inevitably be contaminated by cell or protein in environment, the designed approach can generate a kind of long-lived biosensor if the process of degradation will slough off the adsorbed proteins (Figure 1).

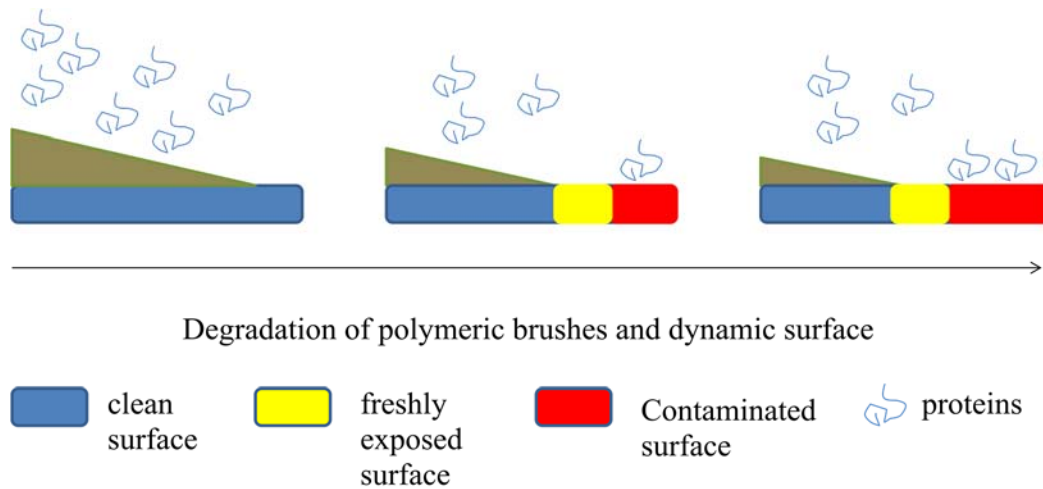


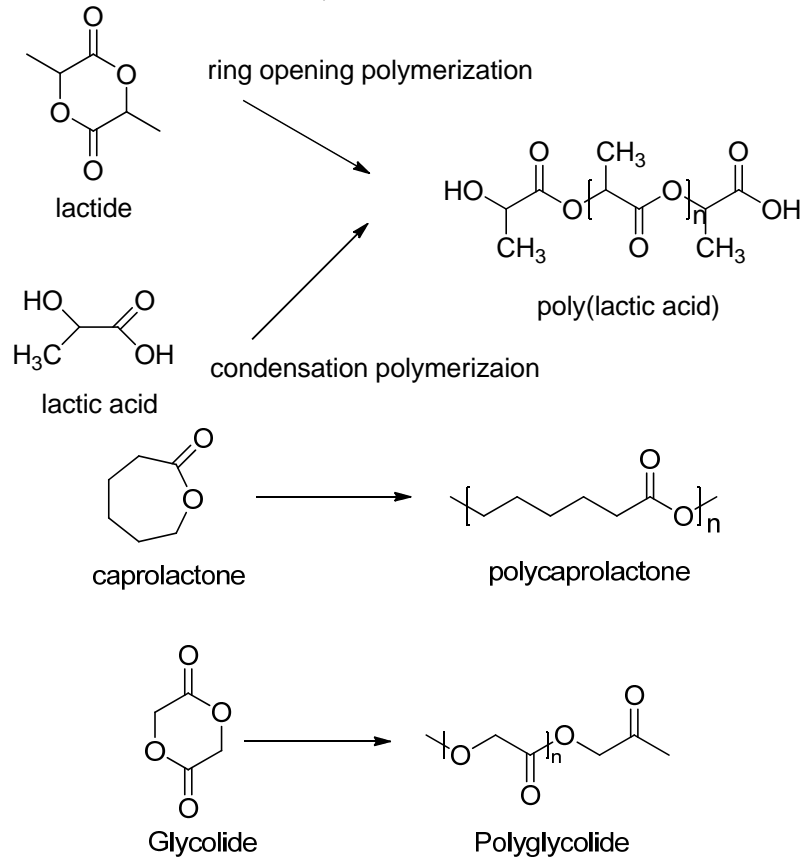
Figure 1. Schematic of a proposed, smart surface composed of a gradient of degradable polymeric brushes that can gradually release fresh surface to the protein solution.

BACKGROUND AND LITERATURE REVIEW

A. Biodegradable polymers

Petrochemical-based plastics are used considerably all over the world. It has been reported that over 300 million tons of petroleum product will be required in the next five years.^{1,2} It also requires large amounts of petroleum and leaves hundreds of millions of tons of carbon dioxide during producing its production. These potential environment and health damages could be reduced by biodegradable polymers which can be converted to various monomers by microorganisms or even simple hydrolysis reaction. Synthetic biocompatible polymers, especially aliphatic polyesters, have excellent mechanical behavior and environment-friendly chemical properties. Poly(lactic acid) (PLA), polycaprolactone (PCL) and polyglycolide (PGA) are good representatives in this catalog (Scheme 1). All of them can be hydrolyzed and biodegraded.

Scheme 1. Chemical structure of PLA, PCL and PGA and their monomers



Bio-based polyesters have been exploited recently because of the depletion of fossil reserves, concerns over greenhouse effects and rising feedstock costs for traditional petrochemical plastics. For example, PLAs are less dependent on petroleum and low-carbon plastics compared with polyethylenes (Table 1). These factors make PLAs much beneficial in replacing conventional petroleum plastics and applying in the area of biomedical engineering.

Table 1. Comparison of bio-based and petrochemical polymers

	Biodegradability	Monomer	Starting Bioproduct ion	Polymerization Condition	Degradation Time	Reference
Poly(lactic acid)	Yes	D,L-lactic acids	Glucose	High monomer purity required, N ₂ atmosphere, over 100°C	Days	3,4
Polyethylene	very slow	ethylene	Ethanol to ethylene	High monomer purity required, N ₂ atmosphere, over 80°C	years	5

Bio-based polyesters are widely applied in several biomedical areas including tissue engineering, drug delivery devices and surgical implants such as sutures.

For drugs that have strong side effects or short half-lives, capsules should be used to deliver them to targeted organs and release them in a controlled manner. The biocompatibility of PLA makes it a good candidate in such application. Different kinds of functional groups can be attached to PLA monomers and these groups can be covalently attached to drug molecules. Recently, Fan and co-workers reported the attachment of 5-fluorouracil on side chains of PLA.⁶ 5-fluorouracil was treated as a model drug and PLA as the drug carrier. This drug/polymer conjugate was then studied in model drug release experiments.

To be used as tissue engineering materials, polyesters should (1) be biodegradable (2) be non-toxic (3) be biocompatible with foreign bodies used in clinical applications such as sensors (4) have a suitable size and multi-porous structure and (5) have reasonable mechanical properties. PGA is a good example for use as man-made scaffold for regeneration of organs or osseous tissue. For example, Hillmyer et al. combined ring opening metathesis polymerization of 1,5-cyclooctadiene and ring opening polymerization of D,L-lactide to produce a triblock ABA copolymers: poly(D,L-lactide)-poly(cyclooctadiene)-poly(D,L-

lactide).⁷ To apply it for osseous tissue regeneration, its tensile properties were tested through applying uniaxial extension on dog-bone shaped structures. The PLA segments elongated before fracture occurred.

Different from the traditional materials used in repair of bone fractures and in surgical sutures, use of PLA, PCL and PGA does not require a second surgical intervention because they are capable of degrading. Thus, there is no need to take out bone screw or stitches. Furthermore, anticatarrhals molecules can be attached to the backbone of polyesters to inhibit inflammation. For example, Guan et al. functionalized caprolactone with hydroxyl groups through preparing a permethoxylated ϵ -caprolactone [(OMe)CL] from a reduced sugar, D-dulcitol. Drug molecules like paclitaxel that can react with hydroxyl could be attached onto the backbone of the corresponding polymers.⁸

B. Implanted Biosensors

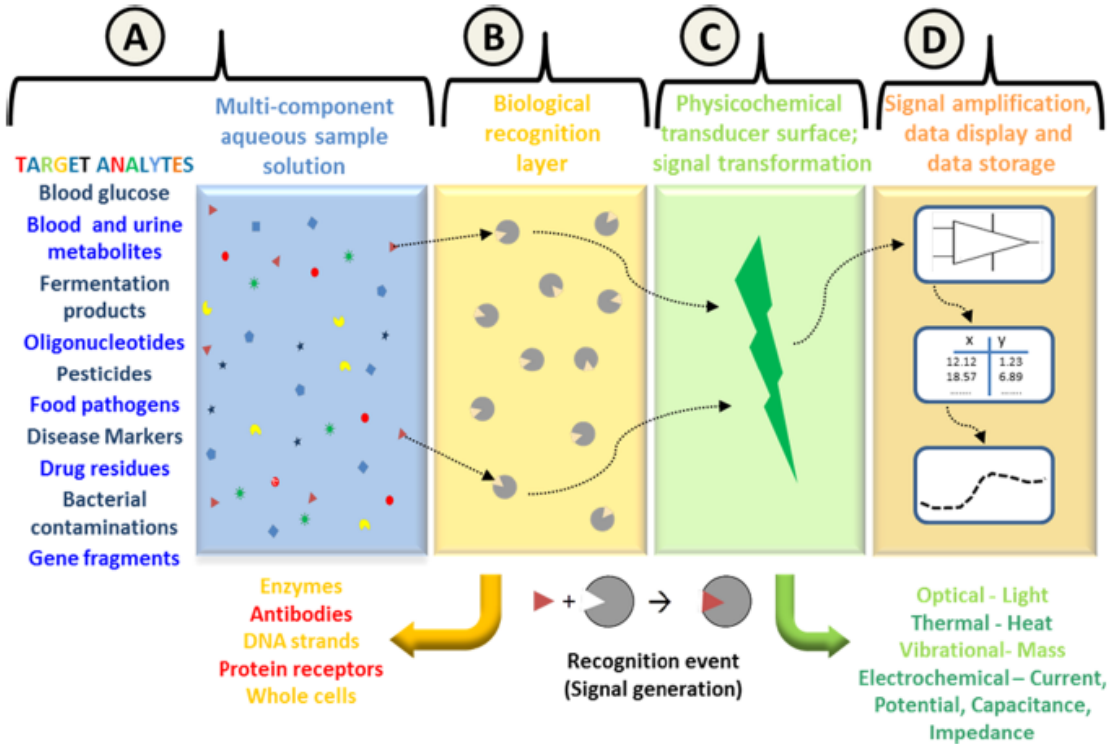
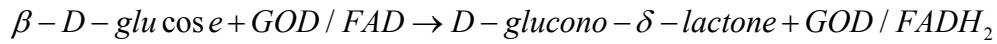


Figure 2. A typical biosensor architecture and potential analyte species in (A) sample solution, (B) biological recognition layer, (C) transducer that converts interaction of the biological recognition layer with the corresponding substrate into a measurable electrical signal and (D) electrical signal operator for amplification, display and storage. Taken from reference 9

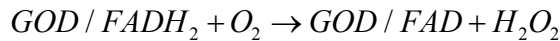
Figure 2 shows the components of a biosensor. Biosensors make use of biological recognition elements (Figure 2B), including enzymes, antibodies and single-stranded DNA that interact with analyte (Figure 2A). The interaction results in generation of an initial biological signal by the recognition layer. Then the transducer transforms it into an electrical signal, which is easier to be qualified (Figure 2C). The operator (Figure 2D) converts that signal into a user-friendly form that can be directly interpreted.

For example, there are three reactions in a glucose oxidase (GOD) enzyme biosensor.¹⁰ Oxidation of α -D-glucose to D-glucono- δ -lactone and reduction of its flavin adenine

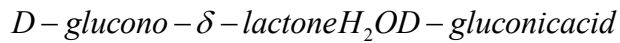
dinucleotide (FAD) prosthetic group happens at the same time (reaction 1). Reoxidation of reduced FAD by dissolved oxygen follows up and generates electroactive byproduct H_2O_2 (reaction 2). D-glucono- δ -lactone is eventually hydrolyzed to gluconic acid (reaction 3). The change in pH and concentration of oxygen and hydrogen peroxide are measured as change in current at a glassy carbon electrode modified with carbon nanotubes (Figure 3).



(1)



(2)



(3)

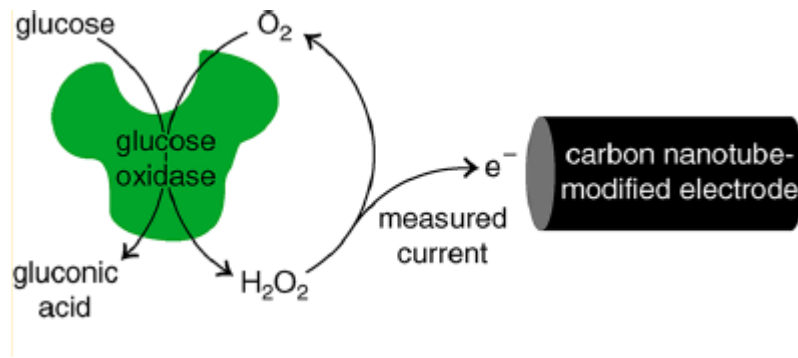


Figure 3. Carbon nanotube-based enzyme-modified biosensor electrodes using a layer by layer electrostatic self-assembly procedure. Taken from reference 10

However, almost all of the biosensors have limited lifetime *in vivo* because of adsorption of proteins on their surfaces. Periodic refreshment of the surface of implants is required or a new biosensor needs to be replaced. Besides the caustic repelling reaction *in vivo*, both of the two strategies are inconvenience for the second surgical interventions are needed. These concerns constitute the so-called surface biofouling problem.

C. Biofouling and attempts at its resolution

To graft biocompatible macromolecules on surfaces is at the forefront of biomedical approach of extending medical implant lifetime. Nonspecific adsorption of protein occurs when an implant first come into contact with blood-based fluid and that inevitable process will finally result in a dead sensor (Figure 4). Research work has been done to show that, even in single protein buffer solutions [usually bovine serum albumin (BSA)] physical protein adsorption occurs that is similar to that on actual implanted biosensors.¹¹

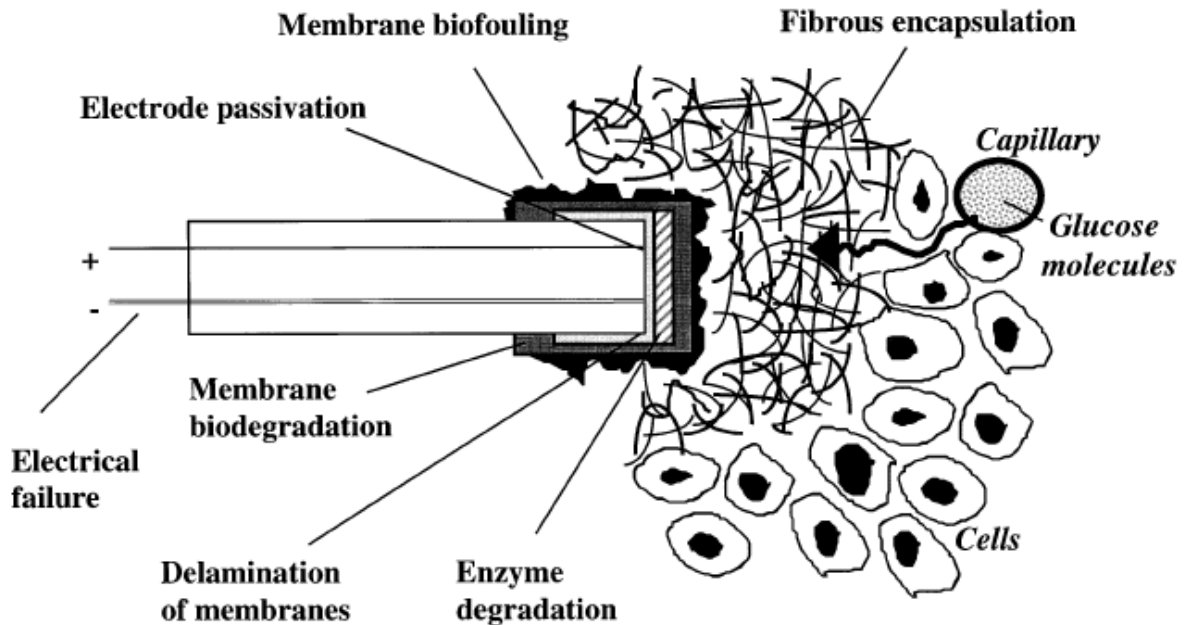


Figure 4. Proteins encapsulation or membrane malfunction lead to malfunction of GOD enzyme biosensor. Taken from reference 11

The interaction between protein and implant surface is quite complex, but still some useful conclusions have been drawn. In a simplified model, two parameters: the intrinsic affinity and bulk concentration of the proteins were considered as the driving force determining the composition of the adsorbed layer from plasma. In a blood-based fluid test, thrombosis

formation led by the platelet adhesion was clearly observed. These behaviors were mainly generated by the response of the immune system, i.e. granulocyte/monocyte activation, fibroblast effect attracted by foreign-body giant cells (FBGCs) and so on.¹² Typically, single macrophages can phagocytose particles up to 5 μ m in size, but when they meet larger ones, macrophages tend to amalgamate to FBGCs and coat the surface of biomaterials. Research showed that cytokines 1L-4 and 1L-13 induced macrophages fusion *in vivo* and *in vitro*.¹³

When the adsorption process is considered from the view of protein properties, in general, the driving force was largely considered as enthalpic interaction due to Van der Waals forces and hydrophobic effects for “soft” proteins.¹⁴ For charged, “hard” proteins, which have limited conformational changes, electrostatic interaction serve as the predominant contributor to adsorption.^{15, 16} Implantable glucose sensors were found to cause considerable infiltration of inflammatory cells at the tissue-sensor interface and a diffusion barrier of exudative fluid around the sensor when used on dogs to monitor the amount of plasma glucose.

Besides the biological factors and the properties of the proteins themselves, the properties of the surfaces themselves also influence protein adsorption. The general rule is that proteins tend to adsorb fastest on a hydrophobic surface. This behavior was illustrated by studying protein adsorption on thiol-based self-assembled monolayers (SAMs) with different tail groups,¹⁷ i.e. methyl (hydrophobic) and hydroxyl (hydrophilic). Increasing hydrophilicity on surfaces may be a potential strategy to circumvent biofouling problems. In addition, for charged proteins, surfaces modified by opposite charges will increase the adsorption strongly.

Surface morphology also has a great impact on biological adhesion. For example, poly(ethylene glycol) (PEG) is used commonly as an anti-biofouling material. The effect of its architecture was studied. When a brush architecture was used, fibrinogen adsorption on poly-L-lysine (PLL) was greater when a more patchy structure (decreased amount of PEG, more exposed PLL) was presented. In this case, protein-patch binding energy increased, which led to more protein adsorbed on surface.¹⁸ A threshold amount of PEG was determined to effectively resist fibrinogen adsorption, when the amount of PEG brushes was reduced

below a certain level, the heads of the PEG brushes coiled back to form a mushroom-like shape (Figure 5). This conformation resulted in the least resistance to protein adsorption.

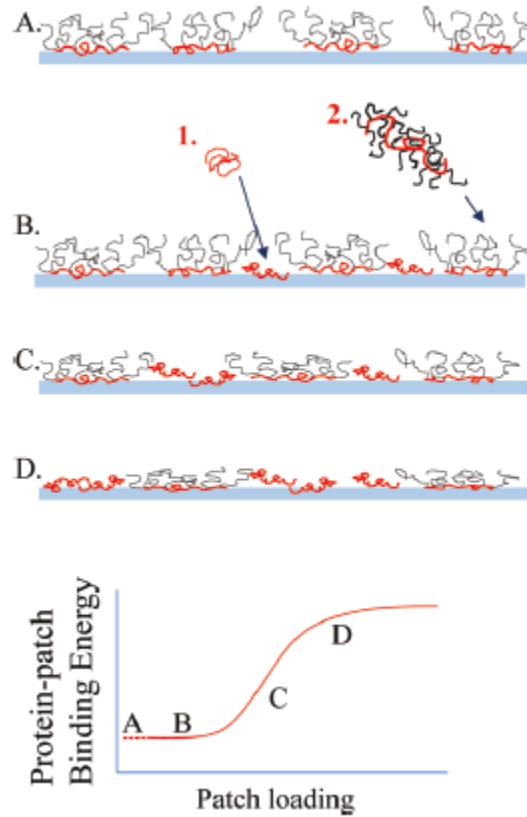


Figure 5. Surface macromolecule structure and binding energy per patch (black for PEG, red for PLL): (A) All covered PEG brushes; (B) full brushes with some buried PLL patches; (C) more buried patches with coiled PEG brushes; (D) dominant PLL patches make PEG lose brush characters and remain in “mushroom” regime. Taken from reference 18

To further explain these behaviors, grafting density was also taken into consideration. Although high loads of PLL lead to both a decreased backfill amount and a decreased thickness of the protein repelling PLL-PEG brushes, the increased fibrinogen adsorption speed in this case was attributed more to the increased mass of PLL, which means increased

grafting density of protein-attracting materials or decreased grafting density of protein-repelling materials, rather than the decreased thickness of the anti-biofouling PLL-PEG brushes. It also supported that a multivalent fibrinogen capture was occurring. Low grafting density concomitant with a mushroom-like shape could lower the anti-biofouling effect even the material coated on the surface is hydrophilic or sterically hindered to non-specific adsorption.

The Debye length also plays an important role on protein adsorption.¹⁸ The Debye length is defined as equation 4. It is inversely proportional to ionic strength. In this equation, I is the ionic strength of the electrolyte, ϵ_0 is the permittivity of free space, ϵ_r is the dielectric constant of the solvent, k_B is Boltzmann's constant, T is the absolute temperature in Kelvin, N_A is Avogadro's number and e is the elementary charge. The units for the Debye length are mole/m³.

At an ionic strength of 0.007 mM, $\kappa^{-1}=4$ nm, and the electrostatic patch-protein interactions were strongest. At an ionic strength of 0.104 mM, $\kappa^{-1}=1$ nm, and the weakest interactions occurred. High load of PLL was required to adsorb fibrinogen. However, as shown in equation 5, the thickness of the polyelectrolyte brushes was inversely proportional to salt concentration. When large amount of salt was added, the brushes collapsed regardless of charge and grafting density due to the very large osmotic pressure exerted on the films. The two effects lead to a competition between ionic strength and steric repulsion.

$$\kappa^{-1} = \sqrt{\frac{\epsilon_r \epsilon_0 k_B T}{2 N_A e^2 I}}$$

(4)

$$H \approx Na(2aD^2C_s)^{-1/3}$$

(5)

Brush height equation, where N is the number of repeating units in the chain, a is the length of the monomers and C_s is the salt concentration.

To combat biofouling on a foreign body, two approaches are ideally involved in tandem (Figure 6). First, hydrophilic, biocompatible polymeric brushes can be grafted on the surfaces of the foreign body to form a non-fouling coating. The water layer formed around these brushes prevents adsorption of protein. Second, the cells of the immune system surrounding the site of implantation must be provided proper stimulation from implanted sensors to trigger adhesion and biofouling. When the sensors have bio-coatings in the form of attached integrin ligands and cytokines, an inherent communicative understanding, i.e. mild bio-material interaction can occur. Bioactive molecules, usually polypeptides, can be used in this strategy.¹⁹

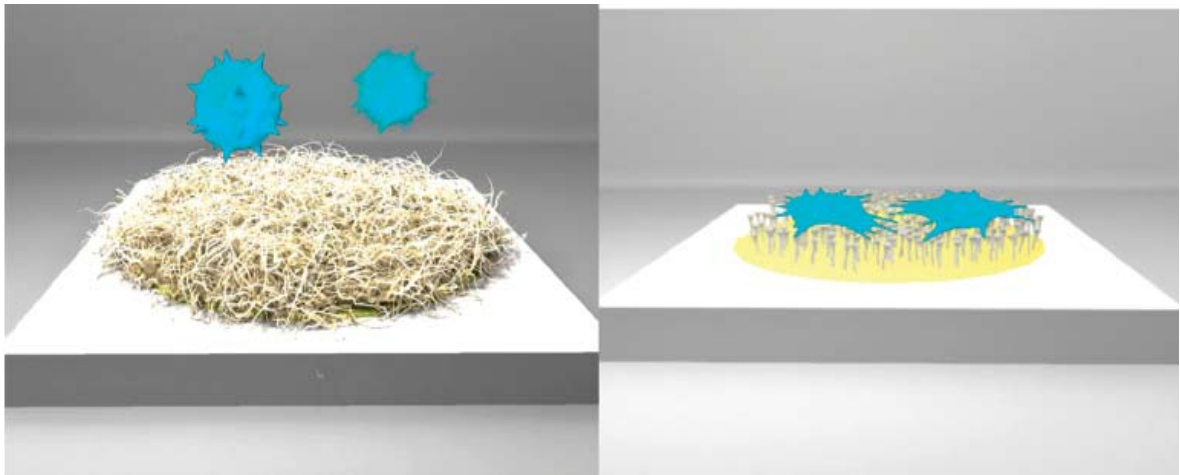


Figure 6. Two main approaches of combating surface biofouling: (Left) Hydrophilic polymers (off-white) are grafted on surface to hide it from the cells of body (blue); (Right) Bioactive peptide motifs (off-white) are modified on surface to imitate the function of cell membrane to communicate well with immune cells. Taken from reference 19

Currently, the combination of the non-fouling PEG moiety with the biomimetic oligopeptide sequences is the new strategy that can further improve the performance of implanted materials (Figure 7). Here in this research project we will mainly focus on the first approach while the second approach serves as complement that could be pursued in future works.



Figure 7. A combination of antibiofouling polymers with bioactive signaling motifs. Taken from reference

D. Preparation of Polymer Brushes

As discussed above, a simplified explanation how polymeric brushes resist biofouling has two components. First, creation of steric repulsion prevents proteins from contacting the surface directly. Second, creation of a hydration layer among macromolecular chains prevents non-specific protein adsorption. Thus, methods for the preparation of polymer brush-modified surfaces are of interest.

Generally, surface modification techniques can be broadly divided into two categories: covalent bonding or physisorption. Covalent bonding anchors polymeric chains to surfaces via chemical bonds between functional groups on the surface and those on polymeric chains. This bonding can be further divided into “grafting from” (also known as surface-initiated polymerization), in which a monomer solution is introduced and polymerization is initiated by functional groups on the surface, and “grafting to”, which pre-formed macromolecular

chains are immobilized on the surface through reaction of their endgroups with groups on the surface.^{20, 21} Generally, however, non-covalent adsorption is reversible, and such brushes are unstable when high shear forces are applied or the surface comes into contact with a solvent that readily dissolves the polymer brush.

D.1. Surface-initiated polymerization (SIP) (Grafting from)

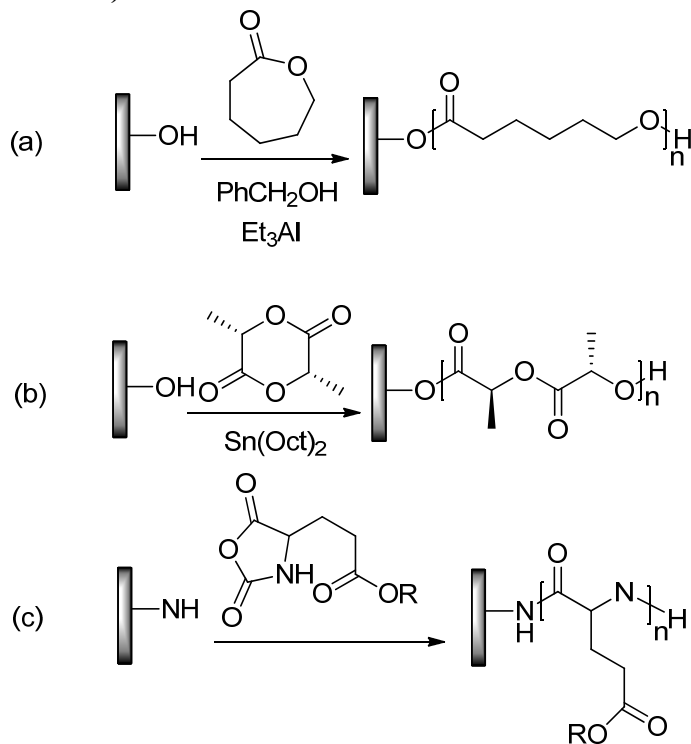
D.1.1. Ring opening polymerization (ROP)

Some commercially available polymers, such as PLA, PCL and PGA, are produced by ring opening polymerization (ROP). Grafting thin layers of these polymers by surface-initiated ROP is quite attractive because parameters as brush density, polydispersity, composition and formation of block copolymers can be well controlled.

Husseman *et al.* used ROP of caprolactone catalyzed by aluminium alkoxide to grow PCL on gold surfaces (Scheme 2a).²² They first modified the gold surfaces with a SAM containing di(ethylene glycol) moieties ending with hydroxyl groups. Within a few hours at room temperature, a 70 nm thick layer was built up. However, the polymerization also occurred in solution, resulting in polymer that could physisorb onto the surface, causing the thickness of the brush to be overestimated. Removal of physisorbed polymer required several washes.

Gorman and Xu reported the growth of PLLA on silica initiated by silanols (hydroxyl groups on silica) and catalyzed by tin (II) octanoate (Scheme 2b).²³ Their principal conclusions were (1) silanols functioned as well as other hydroxyl groups in initiating ROP of lactide; (2) conventional reaction condition of solution polymerization (60°C) were not ideal for SIP. Instead, room temperature was more suitable. Although the percentage of conversion was low, this is not relevant for the growth of a surface confined, polymer brush. Over 10 nm thick polymer brushes were obtained on both gold and silica surfaces.

Scheme 2. Ring opening polymerization of (a) poly(ϵ -caprolactone)²², (b) poly(lactic acid)²³, (c) poly(glutamate)²⁴



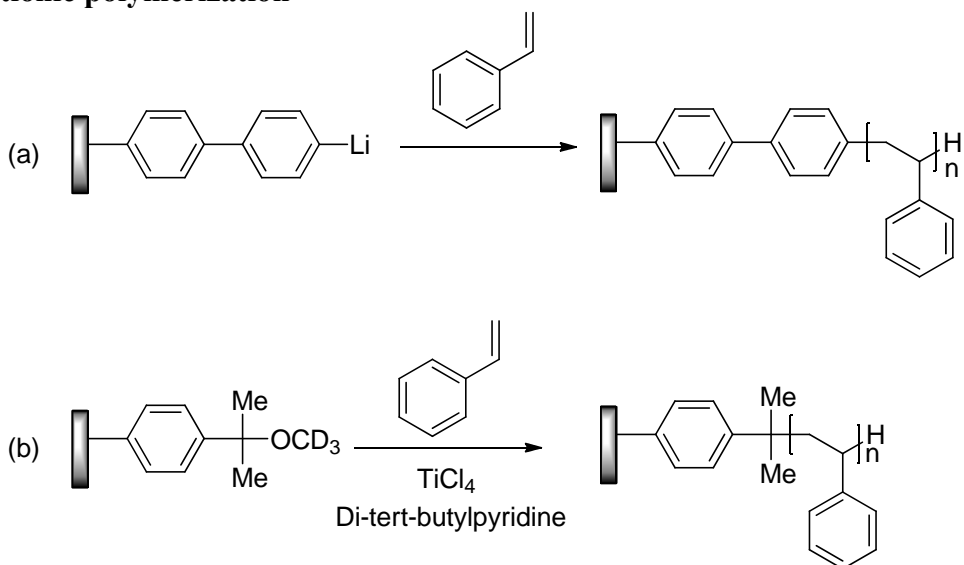
Schouten and co-workers grew poly(L-glutamate) on silica wafers and glass slides (Scheme 2c).²⁴ The monomers applied were N-carboxy anhydrides (NCA) of L-glutamates which also underwent ROP initiated by amine groups. They obtained 40 nm thick layers at room temperature in a few hours. The “living” nature of this polymerization was supported by re-initiation of the polymerization to add a second block of polymer on top of the first.

D.1.2. Cationic/anionic polymerization

Jordan *et al.* utilized living anionic polymerization conditions to grow polystyrene chains on gold surfaces (Scheme 3a). They first prepared a SAM layer containing bromobiphenyl groups. Then sec-butyllithium was employed to convert the initial SAM into a biphenyllithium-containing layer. After adding styrene and three days reaction time, uniform polymeric layers with 18 nm thickness were obtained.²⁵

Zhao and Brittain grew PS chains on silica surfaces through living cationic polymerization (Scheme 3b). SAM deposited on silica wafer was terminated with cumyl methyl ether moieties. A proton scavenger, di-tert-butylpyridine was added to decrease the solution polymerization of PS. Brushes of 30 nm thickness were polymerized on a silica surface in 1h at -78°C . Low temperature was used to minimize chain transfer reaction.²⁶

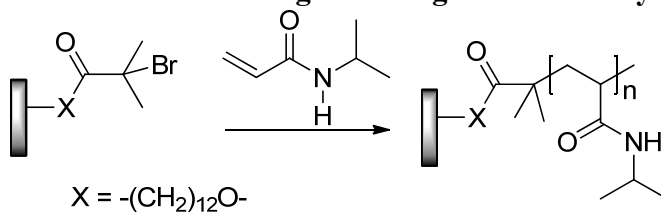
Scheme 3. Polystyrene brushes prepared by (a) living anionic polymerization²⁵ and (b) living cationic polymerization²⁶



D.1.3. Atom transfer radical polymerization (ATRP)

Atom transfer radical polymerization has several advantages for the synthesis of polymer brushes. It is compatible with many functional groups. It produces polymers with a low polydispersity and it tolerates mild reaction conditions (no rigorously dry environment is required). Huck et al. used aqueous ATRP to grow poly(N-isopropylacrylamide) (PNIPAM) on gold surfaces (Scheme 4).²⁷ The topography, morphology, stiffness and adhesion of this kind of polymeric brushes showed reversible changes consistent with a phase transition.

Scheme 4. Polymer Brushes of PNIPAM grown on gold surfaces by ATRP



Genzer et al. grew A-B block copolymers of poly(2-hydroxyethyl methacrylate)-b-poly(methyl methacrylate) (PHEMA-b-PMMA) on silica wafers decorated with a monolayer of initiator for atom transfer radical polymerization: (11-(2-bromo-2-methyl)-propionyloxy) undecyl-trichlorosilane (BMPUS). The significant feature of this work was that the chain length of PHEMA and PMMA was systematically varied in orthogonal directions on the surface (Figure 8). Such structures were systematically used to map out the influence of the block length on surface morphologies of PHEMA-b-PMMA in response to selectively collapsing the top (PMMA) block of the copolymer.²⁸

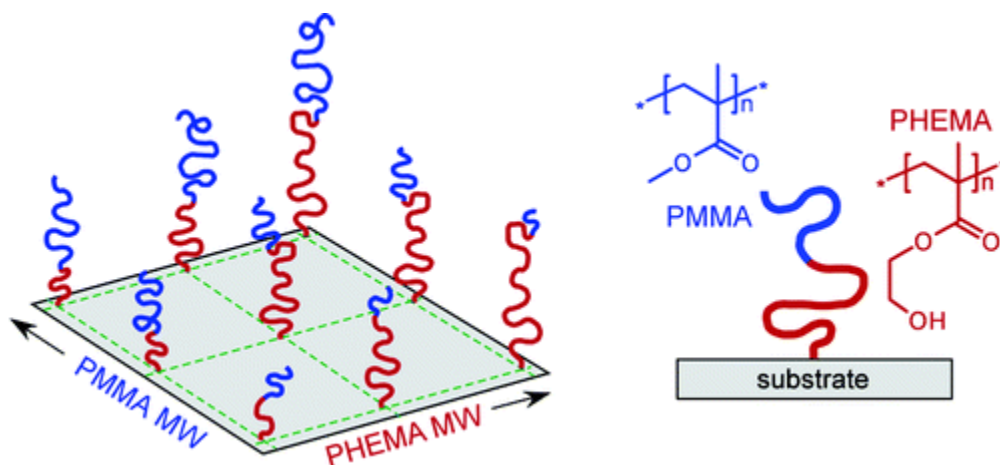


Figure 8. Structure of PHEMA-b-PMMA brushes and the variation of chain lengths. Taken from reference 28

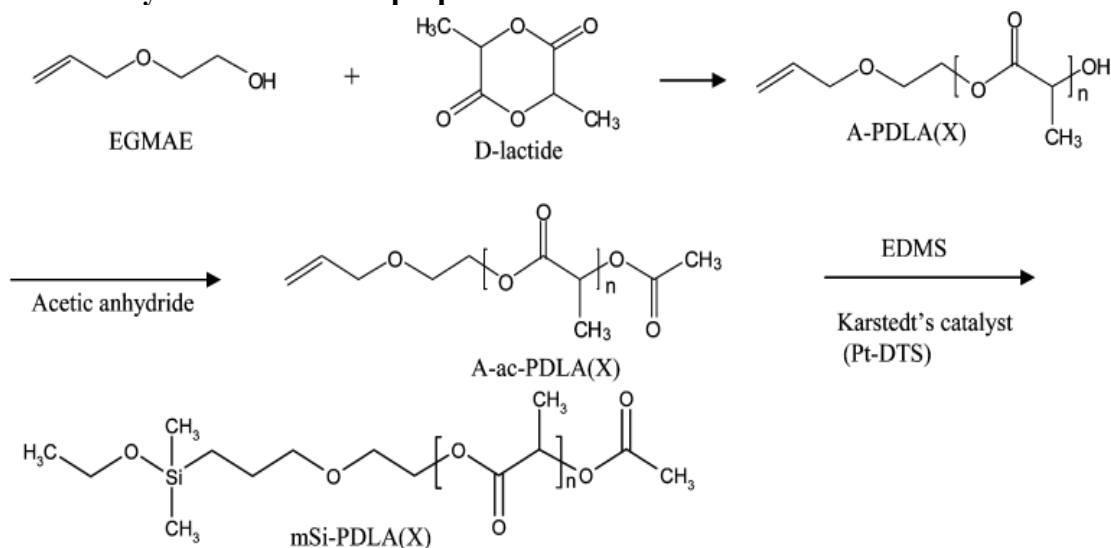
D.2. Grafting to

The so-called “grafting to” method bonds covalently the terminal functional groups of synthesized polymeric chains with the activated sites on substrates. Some kinds of polymeric brushes that are difficult to be grown on surfaces by the “grafting from” method can be performed by a “grafting to” method.

Although L-lactide has been used as monomer to build biocompatible brushes on substrates i.e. the SIP of PLLA on gold surfaces by Xu et al. and Choi et al.^{23, 29} There are also studies of PLLA and PDLA brushes prepared by the “grafting to” method.

Kimura synthesized monoethoxydimethylsilyl-terminated PDLAs that had different molecular weights and immobilized them homogeneously through Si-O-Si bond on silicon wafers (Scheme 5).²⁰ After immobilization of PDLA, solutions of PDLA and PLLA in DCM were applied to the surface to form the homochiral and stereocomplexed bilayer polymeric brushes respectively. They supposed the “hydrogen bonding” between O=C- and CH₃ was the connection between the two layers and that was proved by the lower change of $\nu(\text{O}=\text{C})$ peak in infrared spectrum.³⁰ Although this work is flawed (e.g. CH₃ is not a hydrogen bond donor), their work showed how to prepare nano-ordered surface morphologies with PLA materials.

Scheme 5. Synthetic route for preparation of mSi-PDLA. Taken from reference 20



D.3. Physisorption

Physisorption relies on weak, non-covalent interactions such as electrostatic or hydrophobic interactions. In one example, polymeric brushes modified with polypeptides containing a net positive charge were always adsorbed on negatively charged surfaces via electrostatic interactions. Textor and co-workers built PLL-g-PEG brushes on silicon wafers coated with a niobium pentoxide layer. After different grafting densities were tested, it was calculated that 100% grafting ratios worked best in resisting protein adsorption.³¹ Spin coating was the main method they used to prepare the physisorbed polymer layers. In this technique, a polymer solution was placed at the center of the flat surface, then the surface was rotated at high speed to spread the polymer solution by centrifugal force. At the same time, the solvent evaporated, leaving a uniform, thin film on the surface.

Remaining on a surface for a long time is required for the polymeric brushes to resist biofouling. Compared with physisorption, covalent attachment strategies require harsh reaction conditions and are time-consuming. However, it has been found that non-covalently adsorbed, biodegradable PCL, PEG, PLA as well as a non-biodegradable nondegradable poly(urethane), PET cause an inflammatory response and promoted thrombosis presumably

due to non-efficient coverage. Thus, SIP is the better choice for preparing polymer brushes that resist biofouling.

E. Hydrophilicity of bulk PLA and PLA brushes

E.1. Hydrolysis of PLA, OLA, PLA brushes and other polyesters

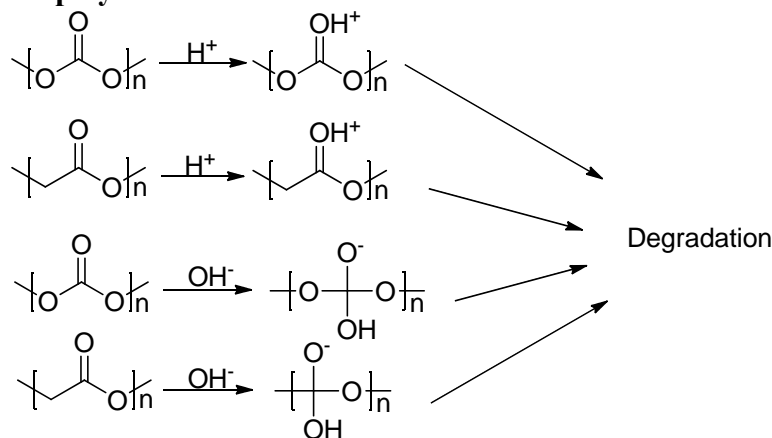
It is valuable to study the hydrolytic degradation of bulk polyesters to understand, for example, how they can be applied in drug delivery devices to realize controlled drug-release. The most obvious process for the degradation of polyesters is via hydrolysis of the ester groups resulting in random chain scissions. This process can be catalyzed by acid or base. Acid-catalysis activates the oxygen of the carbonyl group, making it more electrophilic. It then becomes more susceptible to attack by the relatively weak nucleophile, water. Base-catalysis takes advantage of the relatively strong nucleophile, hydroxide, and the reaction occurs without any activation of carbonyl (Scheme 6). Thus, it is reasonable to get segments or monomers from polyesters when strongly acidic or basic aqueous solutions are provided.

However, polymeric brushes require different reaction conditions compared with bulk polymers. The so-called “backbiting” mechanism is considered as the main route of PLA brushes degradation in mild basic and relative high temperature environment. The biodegradable polymeric layer will slough off the adsorbed proteins during the disconnection of brushes from the surface. Hence, the surface can be thoroughly refreshed and live longer *in vivo*. To apply polymers that have moderate degradation rate and well studied mechanism on surfaces is a reasonable way to realize the so-called “dynamic surface”.

Kim et al. investigated the hydrolytic degradation of poly(propylene carbonate) (PPC), PCL and PLA.³² The general conclusion was that fast reaction was observed under acidic (pH<1.0) or basic (pH>13.0) conditions (Scheme 6). Under moderate acidic, basic and neutral conditions almost no degradation was observed. The rate of degradation under strongly acidic pH followed the trend: PPC<<PLA<PCL. Under strongly basic conditions, the trend was PCL<<PLA<PPC. The differences of the three polymers were attributed to the different

nucleophilicities of their carbonyl oxygen atoms. Nucleophilicity (O of C=O): PCL>PLA>>PPC. Electrophilicity (C of C=O): PPC>PLA>PCL. These trends agree with the relative rates of hydrolytic degradation of the three polymers.

Scheme 6. Rate determining step of acid- and base-catalyzed hydrolysis of polycarbonate and polyester

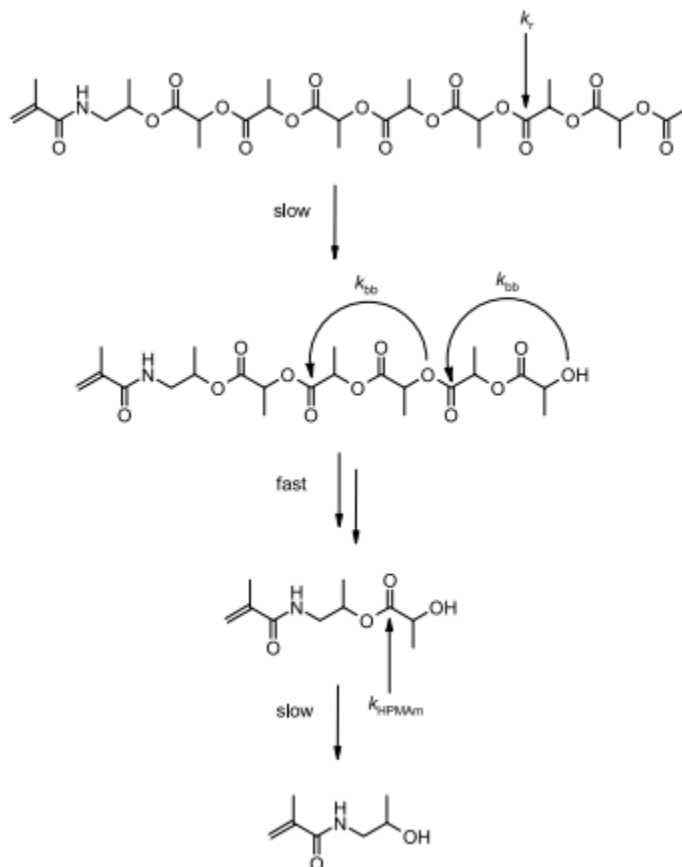


Lee et al. studied the degradation behavior of poly(D,L-lactide-co-glycolide) (PLGA) with different molecular weights (8000 and 33,000 g/mol) using various buffer solutions (pH 3.0, 5.0, 7.0 and 9.0 of phosphate buffered saline, pH 5.8 of distilled water).³³ The degradation of PLGA depended more on the pH value than molecular weight as determined by the *in vitro* release of LA and GA respectively, although the PLGA with lower molecular weight did degrade slightly faster than higher molecular weight samples. More acidic solutions provided more rapid production of the LA and GA monomers. Solution with a pH value of 3.0 gave the fastest production of monomer. Furthermore, GA was released faster than LA which is reasonable due to its higher hydrophilicity.

Good solubility in water leads to faster degradation. Oligomers and polymeric brushes of lactic acid are soluble in water to some extent. Degradation behavior of PLA brushes can be better understood by probing such behavior of oligo(lactic acid)s (OLAs). Nostrum et al.

made the kinetic and mechanistic analysis of the hydrolysis process of OLA.³⁴ They and others determined that chain end scission by backbiting (Scheme 7) is the main mechanism of hydrolysis of hydroxyl-terminated OLA. When protecting groups as acetyl were added to the terminal hydroxyl of OLA, random chain scission became the rate limiting step of degradation.

Scheme 7. A possible degradation route of N-(2-hydroxypropyl)methacrylamide (HPMAM) initiated OLA. k_r -random chain scission, k_{bb} -backbiting, k_{HPMAM} -chain scission at the ester near HPMAM. Taken from reference 34



The “backbiting” degradation mechanism was proposed to be the most rapid one for PLA brushes.³⁴ Xu and Gorman studied the degradation behavior of PLA brushes immersed in

buffered, aqueous solutions by tracking their ellipsometric thickness as a function of time.³⁵ PLA brushes degraded relatively rapidly in moderately basic (pH=8) aqueous solution and relatively high temperature (37°C). However, almost no reaction was observed under acidic conditions. Presumably, basic conditions deprotonated the terminal hydroxyl group so it could attack a carbonyl to form lactide, the monomer from which PLA was synthesized.

E.2. Design of hybrid polymer brushes

As discussed above, forming a water layer to block the interaction between proteins and surfaces has been considered to be an important function molecule that resists protein adsorption. Gesine et al. emphasized the importance of PEG to be utilized as protein resistor for so many hydrogen bonding acceptors rather than donors were presented in the backbone of PEG.³⁶ In their study, dendritic glycerol-based brushes were synthesized and good protein resisting effects were observed.

Inspired by the necessity of hydrophilicity and biodegradability in designing hybrid antibiofouling brushes, the strategy of combining biodegradable monomer molecules with oligo(ethylene glycol) is proposed. For example, in the first route, norbornene bridge was expected to connect the methyl group of lactide and terminal azide group of OEG through Diels-Alder reaction and $[2_s+4_s]$ cycloaddition respectively. If this modified lactide can be successfully planted onto substrates, it will take advantages of the two compositions: forming water layer while degrading from surfaces. Other monomers as *O*-carboxyanhydrides can also be designed into such synthetic strategies and will be presented in experimental section and future work.

F. Smart Surfaces

Smart surfaces can change their properties in response to outside stimuli. This behavior may be useful in addressing the problem of biofouling. As shown in figure 1, after a gradient

thickness of a biodegradable brush is built on surfaces and is placed in contact with a protein environment, polymeric brushes degrade spontaneously and release fresh substrate gradually (regime from right end of polymeric layer to red area) under the proper degradation conditions. Instead of being adsorbed by proteins on the whole surface, this strategy uncovers functional area continuously. If this was placed on an array of biosensors, perhaps, at a given time, one would find a sensor element that was uncovered (in which the brush had degraded) yet had not been inactivated by adsorption of protein. This approach could be a way to generate a long-lived device.

Controlling grafting density is one approach to prepare a brush with a gradient thickness. As discussed above, low grafting density always leads to the coiled formation of polymeric brushes, which is the so-called mushroom regime, while high grafting density results in macromolecular chains interacting with each other and standing up on surfaces (Figure 9). By altering the density of initiators on the surface and growing brushes from the discrete to the compact regime, a gradient thickness could be achieved.

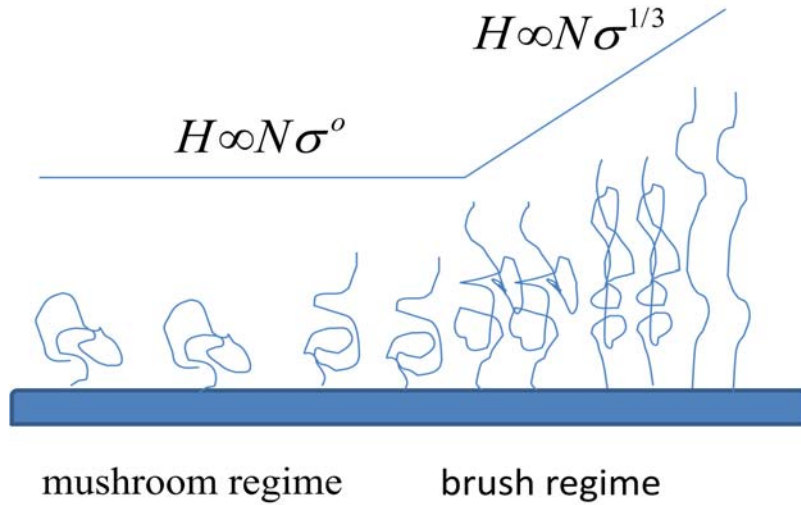


Figure 9. The height of polymeric chains as a function of grafting density, where N is the degree of polymerization of the polymer and σ the grafting density

Altering the molecular weight of the polymer by varying reaction time is another option. If a substrate covered by hydroxyl initiators is immersed into the monomer (lactide) solution, a systematic decrease in contact time between the monomer solution and the surface can be made by continuous draining of the solution by a micropump. In this way, it is envisioned that polymeric brushes with a gradient in length can be prepared by varying the draining rate (Figure 10).

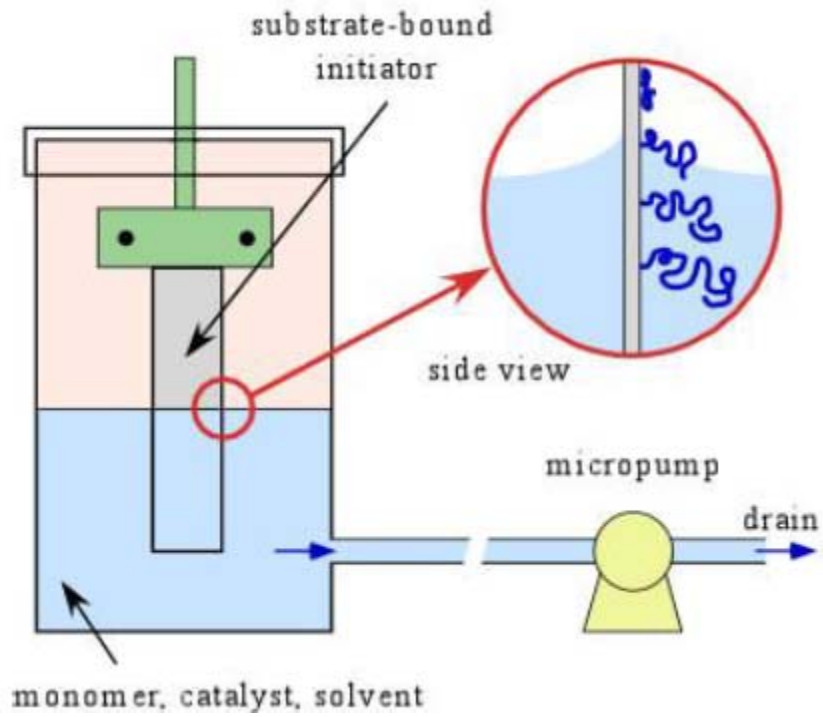


Figure 10. The solution draining method for preparation of a polymer brush with a gradient in thickness. Taken from reference 2

References:

- (1) Halden, R. U. *Annual review of public health* **2010**, *31*, 179.
- (2) Simon, C. J.; Schneider, F. Business Data and Charts 2009/2010. PlasticsEurope Market Research Group (PEMRG): Frankfurt/Consultic Marketing & Industrieberatung GmbH: Alzenau, Germany.
- (3) Jem, K. J.; van der Pol, J. F.; de Vos, S. *Plastics from Bacteria, Natural Functions and Applications*; Springer: Heidelberg, 2010; pp 323_346.
- (4) Benninga, H. *A History of Lactic Acid Making: A Chapter in the History of Biotechnology*; Kluwer: Dordrecht, Boston and London, 1990.
- (5) Huang, H. *Natural Functions and Applications*; Springer: Heidelberg, 2010; pp 389_404.
- (6) Fan, CL (1995). *Gāoděng xuéxiào huàxué xuébaò (0251-0790)*, *16*, p. 973.
- (7) Pitet, L. M.; Hillmyer, M. A. *Macromolecules* **2009**, *42*, 3674.
- (8) Urakami, H.; Guan, Z. *Biomacromolecules* **2008**, *9*, 592.
- (9) Suginta, W.; Khunkaewla, P.; Schulte, A. *Chemical Reviews* **2013**, *113*, 5458.
- (10) Hobbs, J. M.; Patel, N. N.; Kim, D. W.; Rugutt, J. K.; Wanekaya, A. K. *J. Chem. Educ.* **2013**, *90*, 1222.
- (11) Hucknall, A.; Rangarajan, S.; Chilkoti, A. *Advanced Materials* **2009**, *21*, 2441.
- (12) Franz, S.; Rammelt, S.; Scharnweber, D.; Simon, J. C. *Biomaterials* **2011**, *32*, 6692.
- (13) Xia, Z.; Triffitt, J. T. *Biomedical materials* **2006**, *1*, R1.
- (14) Malmsten, M., *J. Colloid Interface Sci.* **1998**, *207*, (2), 186-199.
- (15) Norde, W., *Adv. Colloid Interface Sci.* **1986**, *25*, (4), 267-340.
- (16) Haynes, C. A.; Sliwinsky, E.; Norde, W., *J. Colloid Interface Sci.* **1994**, *164*, (2), 394-409.
- (17) Sigal, G. B.; Mrksich, M.; Whitesides, G. M., *J. Am. Chem. Soc.* **1998**, *120*, (14), 3464-3473.
- (18) Gon, S.; Santore, M. M. *Langmuir* **2011**, *27*, 15083.
- (19) Meyers, S. R.; Grinstaff, M. W. *Chem Rev* **2012**, *112*, 1615.

- (20) Nakajima, H.; Nakajima, M.; Fujiwara, T.; Lee, C. W.; Aoki, T.; Kimura, Y. *Macromolecules* **2012**, *45*, 5993.
- (21) Edmondson, S.; Osborne, V. L.; Huck, W. T. *Chem. Soc. Rev.* **2004**, *33*, 14.
- (22) Husemann, M.; Mecerreyes, D.; Hawker, C. J.; Hedrick, J. L.; Shah, R.; Abbott, N. L. *Angewandte Chemie International Edition* **1999**, *38*, 647.
- (23) Xu, L.; Gorman, C. B. *Journal of Polymer Science Part A: Polymer Chemistry* **2010**, *48*, 3362.
- (24) Wieringa, R. H.; Siesling, E. A.; Geurts, P. F. M.; Werkman, P. J.; Vorenkamp, E. J.; Erb, V.; Stamm, M.; Schouten, A. J. *Langmuir* **2001**, *17*, 6477.
- (25) Jordan, R.; Ulman, A.; Kang, J. F.; Rafailovich, M. H.; Sokolov, J. *J. Am. Chem. Soc.* **1999**, *121*, 1016.
- (26) Zhao, B.; Brittain, W. J. *Macromolecules* **1999**, *33*, 342.
- (27) Jones, D. M.; Smith, J. R.; Huck, W. T. S.; Alexander, C. *Advanced Materials* **2002**, *14*, 1130.
- (28) Tomlinson, M. R.; Genzer, J. *Langmuir* **2005**, *21*, 11552.
- (29) Choi, I. S.; Langer, R. *Macromolecules* **2001**, *34*, 5361.
- (30) Zhang, J.; Sato, H.; Tsuji, H.; Noda, I.; Ozaki, Y. *Macromolecules* **2005**, *38*, 1822.
- (31) Michel, R.; Pasche, S.; Textor, M.; Castner, D. G. *Langmuir* **2005**, *21*, 12327.
- (32) Jung, J. H.; Ree, M.; Kim, H. *Catal. Today* **2006**, *115*, 283.
- (33) Yoo, J. Y.; Kim, J. M.; Seo, K. S.; Jeong, Y. K.; Lee, H. B.; Khang, G. *Bio-Med Mater Eng* **2005**, *15*, 279.
- (34) de Jong, S. J.; Arias, E. R.; Rijkers, D. T. S.; van Nostrum, C. F.; Kettenes-van den Bosch, J. J.; Hennink, W. E. *Polymer* **2001**, *42*, 2795.
- (35) Xu, L.; Crawford, K.; Gorman, C. B. *Macromolecules* **2011**, *44*, 4777.
- (36) Gunkel, G.; Weinhart, M.; Becherer, T.; Haag, R.; Huck, W. T. *Biomacromolecules* **2011**, *12*, 4169.

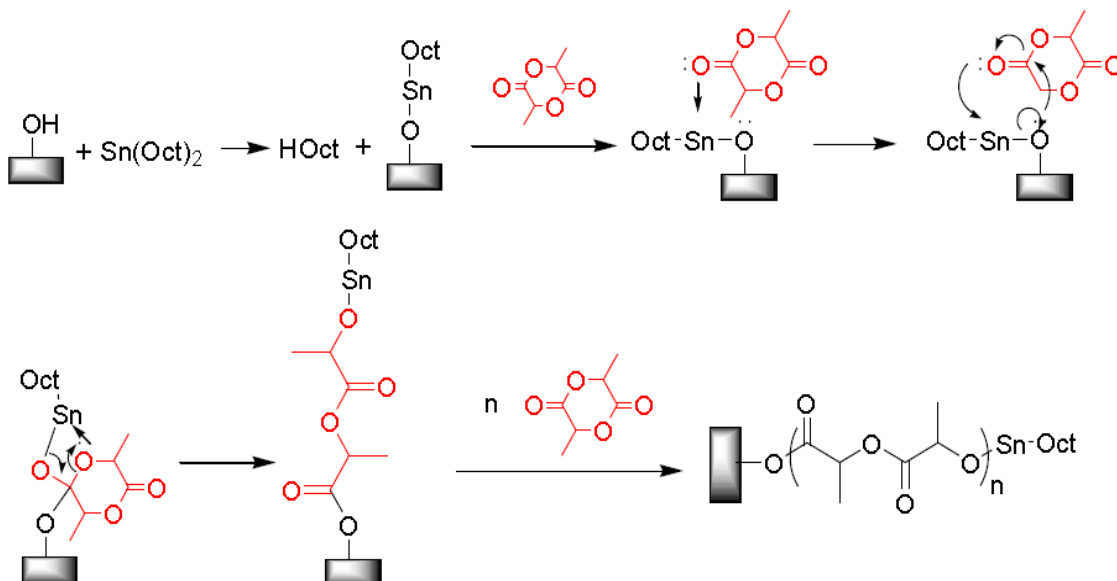
RUSLTS AND DISCUSSION

A. Reproducing the growth of PLA brushes on silicon surfaces

A.1. Growth vs. time via ellipsometry

The silicon substrates were treated by Piranha solution (a 70/30 v/v mixture of concentrated sulfuric acid and 30 % aqueous hydrogen peroxide) and ultraviolet ozone (UVO) cleaner sequentially. The used silica wafers were soaked in Piranha solution for several hours. After cleaned up by ethanol and dried, they were oxidized by UVO for 30 min to prepare the surface silanol groups. These functional groups could be used as initiators for the ROP of lactide as described previously.¹ A tetrahydrofuran (THF) solution of Lactide (1M) and Sn(Oct)₂ catalyst (1mM) was incubated with the substrates at room temperature for various reaction times. The mechanism of for this reaction is shown in Scheme 8. The surface hydroxyl groups react with Sn(Oct)₂ to bond them on surface with tin alkoxide bond. Then carbonyl groups of monomer insert into Sn-O bond, breaking ester bonds, opening the six membered rings and propagating the polymer chains.

Scheme 8. Mechanism of Surface Initiated ROP of Lactide Catalyzed by Sn(Oct)₂. Taken from reference 2



The thicknesses of samples before and after grafting were measured by ellipsometry and their differences were assigned as the thickness of the grafted polymeric layers. All reactions were started at the same time but each silicon chip was taken out of the THF solution, and its thickness was individually measured at different time points. The resulting growth curve is shown in Figure 11 (right) and compared to growth curves previously obtained (Figure 11, left). Although the growth curve (right) was not quite fitted with the published result (left) at the beginning, the thickness over 100 Å obtained at the end showed that the surface ROP of lactide initiated by silanol groups was highly reproducible and the tin salt, which was relatively small and accessible to surface, was a very effective catalyst.

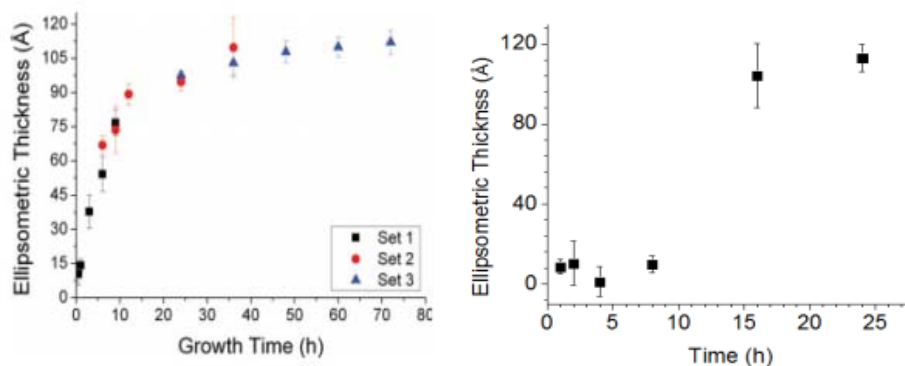


Figure 11. Ellipsometric thickness of PLA brushes from surface silanol groups versus growth time (left) and reproduced plot (right)

A.2. Degradation vs. time via ellipsometry

Next, experiments were performed to demonstrate that the resulting PLA brushes could be degraded with similar kinetics to those illustrated previously^{2,3}. PLA brushes samples with ca. 10 nm thicknesses were soaked in phosphate buffer solution at pH = 8 and at 37 °C. The thicknesses of samples before and after degradation reaction at each time were measured by ellipsometry. The resulting degradation curve is shown in Figure 12. The degradation curve (right) fitted the published results (left) quite well. The decreasing tendency of thickness indicated that the backbone of PLA could be used as bio-coating materials of smart surface.

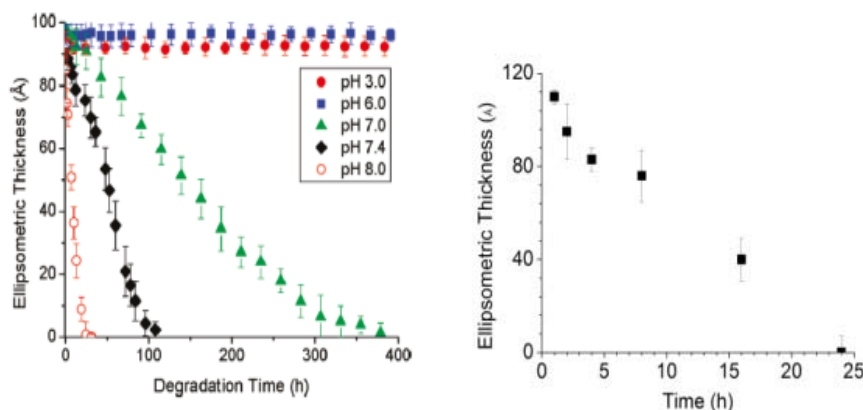
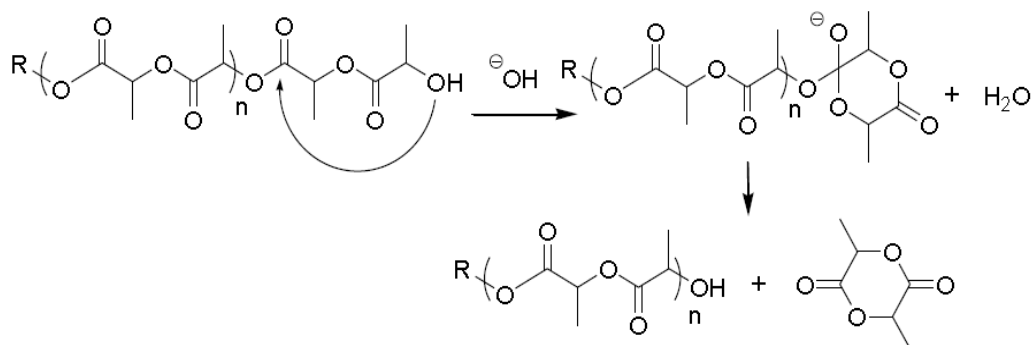


Figure 12. Ellipsometric thickness of PLA brushes versus degradation time at 37°C under different pH conditions (left) and reproduced plot at 37°C and pH=8 (right)

The degradation of PLA brushes has previously been argued to follow a “backbiting” mechanism as shown in Scheme 9. The alcohol/alkoxide then attacks the carbonyl group, breaking the ester bond via a tetrahedral intermediate. A lactide molecule is formed and leaves the macromolecule losing one repeating unit. The backbiting mechanism is thought to occur in the basic environment required by the degradation reaction. As a result, the PLA brushes sloughed off the silicon substrate within 25 h showing a fair rate of degradation which is important for use in antibiofouling dynamic surfaces.

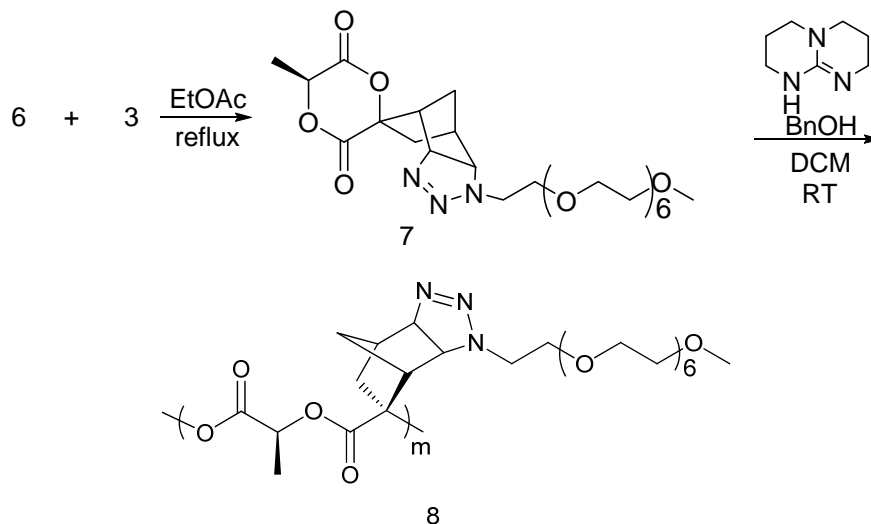
Scheme 9. Backbiting mechanism for the degradation of PLA brushes



B. Synthesis of PEG₆ Spirolactide

B.1. Reproducing the work of Weck et al.⁴

Hu et al. showed that OEG brushes had excellent antibiofouling effect while PLA brushes absorbed proteins quite fast previously (Figure 13).⁵ Although performed bad in biodegradation, based on their good antibiofouling effect, OEG brushes were still widely applied on biosensor surface coating in general.⁶ To realize the smart surface, a synthetic route to an OEG appended lactide was proposed.



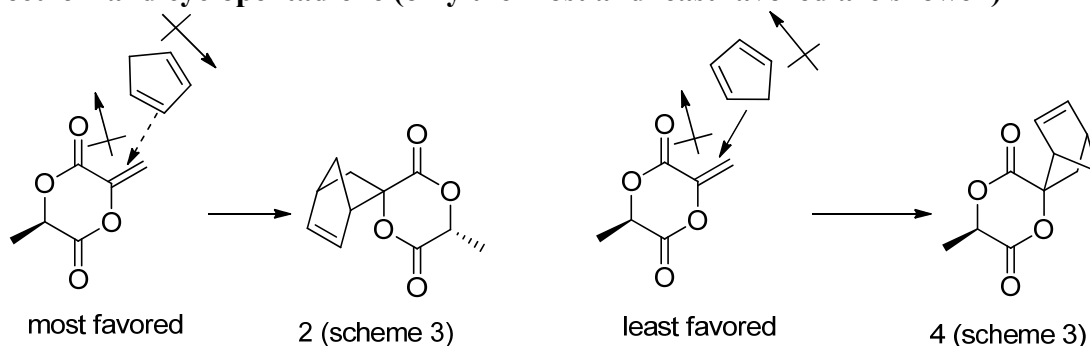
The OEG-appended lactide that was chosen for synthesis followed the procedure reported by Weck et al. Previous to this work, Hillmyer et al. reported the synthesis of spiro[6-methyl-1,4-dioxane-2,5-dione-3,2'-bicyclo[2.2.1]hept[5]ene] (**3**, scheme 10).⁷ Weck et al. subsequently utilized this molecule to prepare the final product, PEG₆-Grafted PLA, after preparing azido-poly(ethylene glycol) monomethyl ethers (**6** and **8**).

The greatest difficulty throughout the synthesis was avoiding the ring opening of LA. Thus, all reactions were run under nitrogen protection and most purifications by column chromatography on silica gel were done with pre-dried stationary phase and were protected by anitrogen atmosphere. In the first step of the synthesis, 3-methylene-6-methyl-1,4-dioxane-2,5-dione (**2**) was prepared following the procedure originally reported by Scheibelhoffer et al.⁸ Bromination and elimination were performed sequentially on L-lactide (¹H NMR, Figure 17 and 18). Then molecule **2**, a captodative alkene (an alkene substituted with both an electron donating group and an electron withdrawing group) was used as a dienophile in a Diels-Alder reaction, and the tricyclic compound **3** was successfully prepared by refluxing in benzene overnight. This reaction time was longer than that originally reported (within 12 h). In running this reaction, it is noted that a dienophile with only electron withdrawing groups on it would be a better candidate. Based on the Frontier

Molecular Orbital (FMO) theory, in the model of normal Diels-Alder reaction, Highest Occupied Molecular Orbital (HOMO) of diene interacts with Lowest Unoccupied Molecular Orbital (LUMO) of dienophile. Electron withdrawing groups on dienophile can lower down the energy of LUMO. Thus, the energy gap between $\text{HOMO}_{\text{diene}}\text{-LUMO}_{\text{dienophile}}$ can be minimized

Four stereoisomers are possible in the synthesis of **3**. Isomer **2** was identified as the preferred cycloadduct (Scheme 11). The diastereofacial selectivity was caused by the 4-methyl group that directed the approach of cyclopentadiene opposite to it in order to reduce steric repulsion. The *exo* Diels-Alder product was dominant because smaller dipole moment was favored in the anti-Alder model (Scheme 11). In the region between 5 to 6 ppm of the ^1H NMR spectrum of molecule **3** (Figure 19 with highlights), the largest peaks are assigned to the major stereoisomer **2**.

Scheme 11. Illustration of the diastereoselectivity of the Diels-Alder reaction of molecule 2 and cyclopentadiene (only the most and least favored are shown)



The cycloaddition between PEG-azide **6** and **3** which contains a norbornene moiety is an accessible synthetic strategy toward PEG-spiro-lactide. This $[2_s+4_s]$ reaction has some advantages such as short reaction time and high conversion. To further study the reactivity of 1,3-dipolar cycloaddition of **6** and **3**, the reaction of 1-azidoadamantane and **3** was examined by Weck et al. The formation of Δ^1 -1,2,3-triazoline ring can be demonstrated by the two

doublets at 4.83 and 3.56 ppm in the ^1H NMR spectrum. This model reaction gave the grafting of PEG side chains on L-lactide with norbornene moiety through $[2_s+4_s]$ cycloaddition a sound foundation.

PEG₆-azide (**6**) was synthesized by sequential tosylation and azidation of heptaethylene glycol monomethyl ether (^1H NMR, Figure 20 and 21). Then, the reaction between **3** and **6** was carried out in refluxing ethyl acetate for 5 days to give the desired product, PEG₆-spiro-lactide **7**. No metal catalyst was used in order to eliminate metal-toxicity and keep biocompatibility of the products. Two new doublets at 4.91 and 3.65 ppm were supposed to be observed in the ^1H NMR spectrum of the reaction product, indicating the formation of Δ^1 -1,2,3-triazoline ring. These are similar to the reported diagnostic peaks of two Δ^1 -1,2,3-triazoline ring protons of azidomantane-spirolactide. Only the doublet at 4.91 ppm can be observed in product **7**, however. The second signal overlaps with that of the PEG chain (Figure 22). In the $^1\text{H},^1\text{H}$ -COSY NMR spectrum of **7**, the doublet at 3.65 is observable, however (highlighted in Figure 14). In the ^{13}C NMR (Figure 23), two diagnostic peaks at around 167 ppm corresponded to the two carbonyl groups on the lactide ring indicating the six-membered ring of lactide was retained during the synthetic and purification steps. The mass spectrum of **7** showed a major peak at 574 corresponding to its molecular weight (Figure 24). The transformation of azide group can be further demonstrated by infrared spectroscopy (Figure 15). No peak was observed around 2100 cm^{-1} . This region belongs to the diagnostic peak of the azide group.

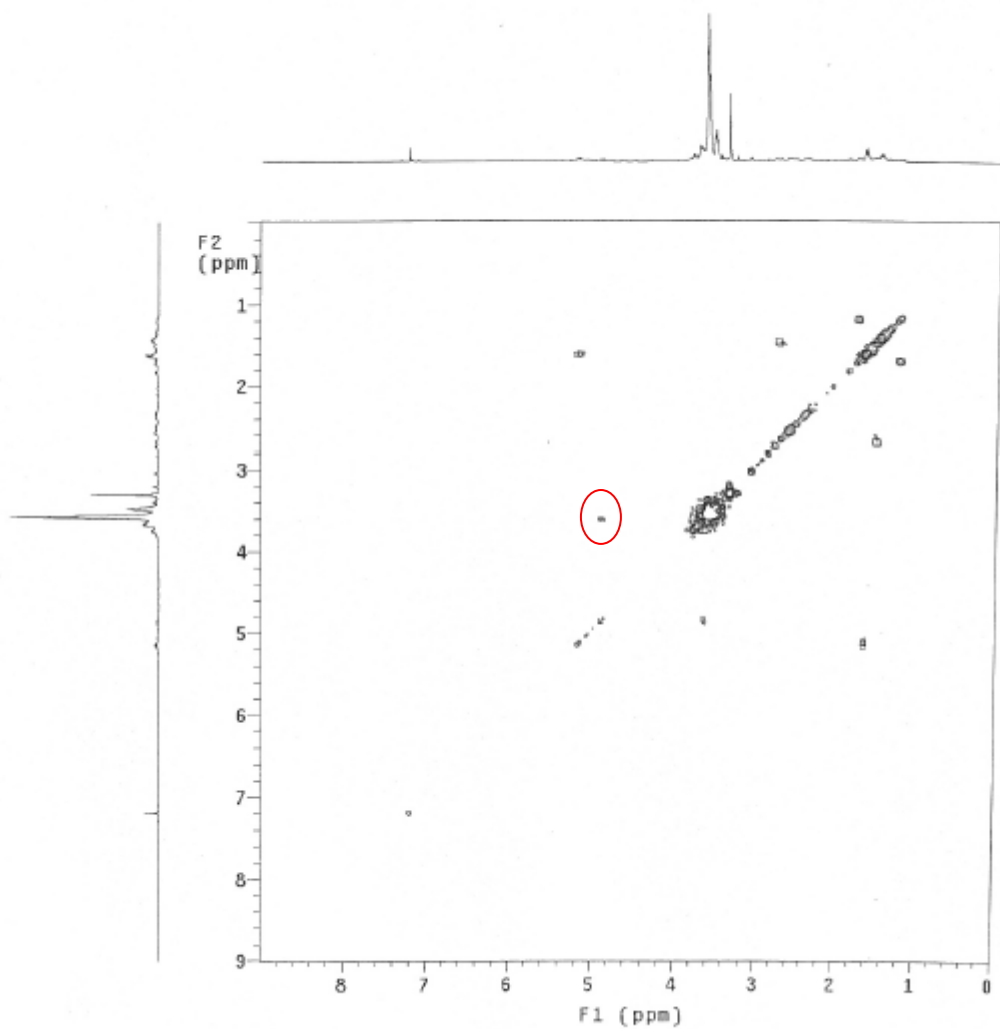


Figure 14. ^1H , ^1H -COSY spectrum of PEG₆-spirolactide in CDCl_3

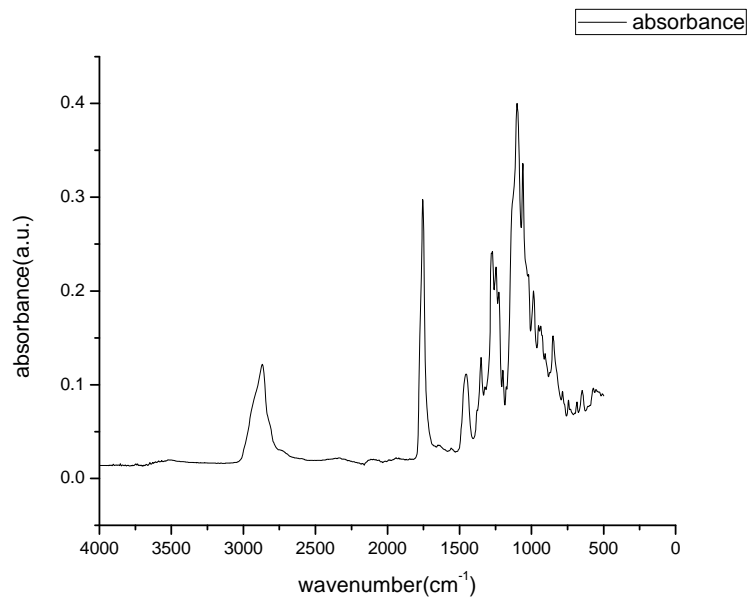


Figure 15. Infrared spectrum of PEG₆-spirolactide

B.2. Polymerization of PEG₆-spirolactide

B.2.1. ROP of PEG₆-spirolactide in solution

After synthesizing the target monomer, ring opening polymerization (ROP) in solution and surface initiated polymerization (SIP) were investigated. Weck et al. did not report any separation of the diastereomers of **7**, and no further separation was attempted here. ROP of lactide requires high purity monomer, so monomer **7** was triply recrystallized from benzene. ROP of **7** in solution was performed at room temperature in methylene chloride using triazabicyclodecene (TBD) as the catalyst and benzyl alcohol (BnOH) as the initiator. The ratio of monomer to TBD to BnOH was 100:0.5:1.

The isolated yield of polymer was 373 mg (49%) after purification by dialysis in DCM. The polymer was further characterized by ¹H NMR and ¹³C NMR spectrums.

The broaden peaks shown in ^1H NMR spectrum (Figure 25) were consistent with the structure of the proposed polymer. Molecular weight determined by end-group analysis was hard to process due to the low concentration of benzyl group.

B.2.2. Attempts at polymerization on a surface, and characterization by ellipsometry

For SIP of **7**, the experimental procedure was the same as that used in reproducing the growth of PLA on silicon surface except that (1) lactide was replaced with PEG₆-spirolactide and (2) both TBD and Sn(Oct)₂ were tested as catalysts (Experimental Section). TBD OAc was demonstrated as an effective catalyst/initiator in bulk/solution polymerization of lactide.⁹ It can be easily prepared by reacting TBD with glacial acetic acid. Unfortunately, no apparent growth of the polymeric brushes were observed under different reaction conditions (Table 2). Further experiments of SIP of lactide catalyzed by TBD or TBD OAc were carried out but still no significant growth has been observed. This result is the same obtained by Xu on the SIP of lactide. It is believed that the TBD molecule is too bulky to effectively initiate polymerization from the silica surface.²

Table 2. Ellipsometric thicknesses (Å) of OEG-spiro-PLA brushes prepared under different reaction conditions (tin catalyst)

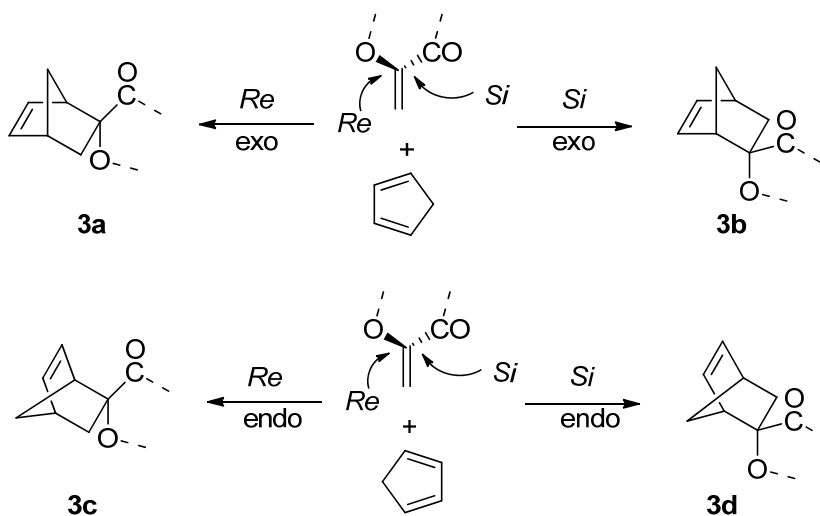
Reaction Time(h) Temp (° C)	24	48	72	96
25	25 Å	32 Å	23 Å	NA
40	26 Å	35 Å	24 Å	36 Å
60	24 Å	25 Å	35 Å	NA

B.3. Enumerating the stereoisomers of PEG₆-Spirolactide

PEG₆-spirolactide is an ideal monomer that combines good hydrophilicity of oligo(ethylene glycol) and fair degradation rate of poly(lactic acid). However, the 16 diastereomers of the final product prohibit its potential application as surface polymeric brushes. These stereoisomers came from the asymmetric Diels-Alder reaction (to produce **3**) (Scheme 12) and the Huisgen (1,3-dipolar) cycloaddition (to produce **7**) (Scheme 13).

The Diels-Alder reaction yields four stereoisomers. These come from either exo or endo attack of the diene to either the Re or Si face of the dienophile. These four possibilities are shown in Scheme 3.

Scheme 12. Diastereogenic Diels-Alder reaction illustrating facial and endo-exo regioisomers

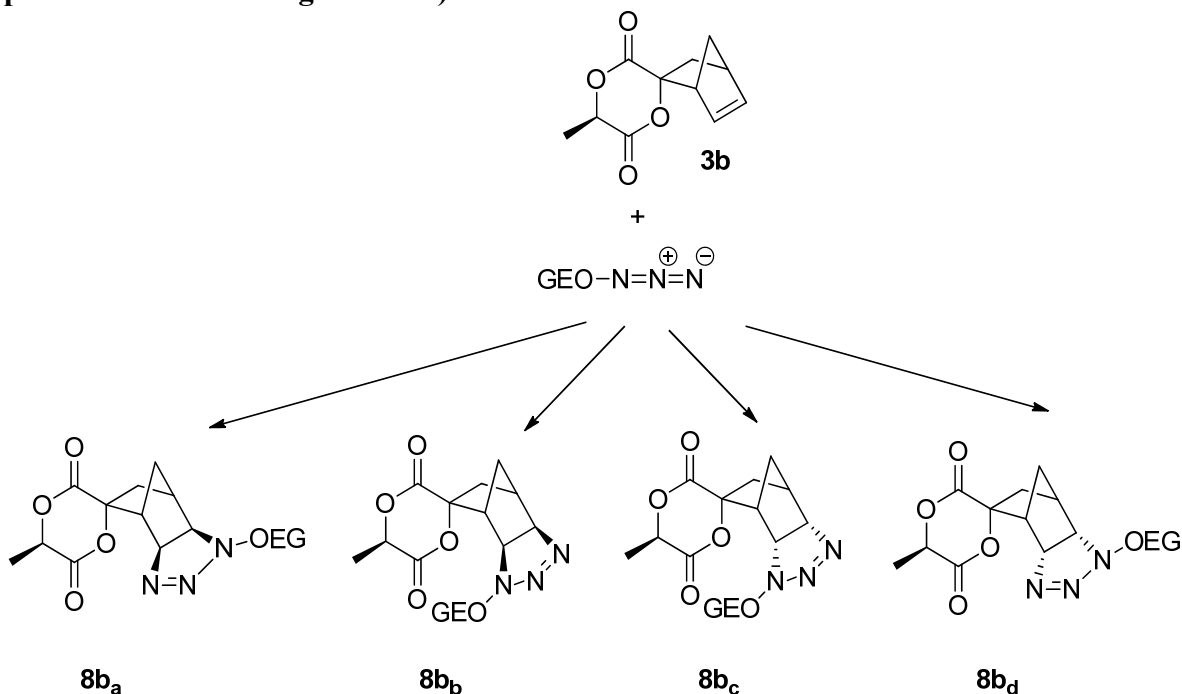


Usually, asymmetrically substituted dienophiles, as (6S)-3-Methylene-6-methyl-1,4-dioxane-2,5-dione in this case, have enantiotopic faces and a pair of enantiomers comprise the product (Scheme 12). However, the 4-position of the norbornene on the lactide ring is a stereogenic center and thus makes the modified molecule diastereogenic. Thus, for example in the case of exo addition, the two products (**3a** and **3b**, scheme 12) based on facial selectivity are diastereomers, not enantiomers. Although based on Alder's Endo Rule, the kinetic product, the endo one, is preferred, since no Lewis acid catalyst or high pressure was introduced, the amount of endo and exo products should be comparable. Consequently, four diastereoisomers should be generated in this step.

Huisgen cycloaddition is a regioselective reaction when the different direction of R group on 1,3-dipole is taken into consideration. Furthermore, for any one isomer of Diels-Alder

reaction the two faces of the double bond of norbornene are diastereogenic. Thus, for each diastereomer shown in Scheme 12 can generate four diastereoisomers (Scheme 13).

Scheme 13. Stereoisomers of Huisgen Cycloaddition (using the *exo*, *syn* to 6-methyl product as the starting material)



An electron withdrawing group on the dipolarophile and/or the use of a copper salt as catalyst each usually facilitates the $[2_s+4_s]$ cycloaddition. Any impurity that is difficult to remove, however, could disrupt the growth of brushes on surface and hinder biocompatibility. As a result, just the two starting materials and solvent were used here. These conditions are thought to be responsible for the long reaction time, 5 days, was required to complete the Huisgen cycloaddition.

The existence of this large number of diastereomers became an increasing concern during the course of this project because monomer purity appears to be very important for successful brush growth. Any diastereomeric mixture likely will be less pure overall than a sample containing only one stereoisomer. As an example of this concern, (3*S*)-*cis*-3,6-Dimethyl-1,4-

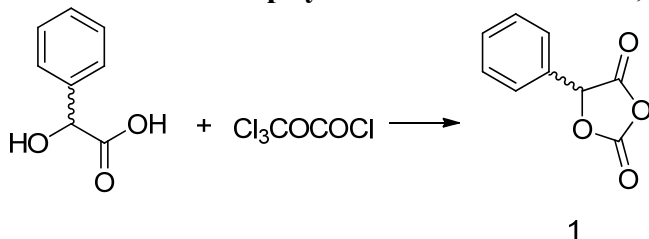
dioxane-2,5-dione (L-LA) worked well in the growth of polymer brushes by SIP (Figure 11). However, when D,L-LA monomer was used in SIP, no brush was formed. As a result, alternate monomers were considered and are discussed below.

C. Synthesis of PEG grafted *O*-carboxyanhydride

C.1. Synthesis of 5-substituted 1,3-dioxolane-2,4-diones

It was decided that a monomer with a more accessible synthetic route and has simpler purification procedure was worth considering for SIP to produce a biodegradable polyester. A monomer that would not be composed of diastereoisomers was also desirable. It was thought that *O*-carboxyanhydride (OCA) monomers might have these criteria. There is no report of the SIP of any OCA monomers, however. Thus, to understand the synthesis, hydrolysis and polymerization (ROP and SIP) of *O*-carboxyanhydride (OCA) based monomers, a model molecule was made and polymerized. The synthesis of 5-substituted 1,3-dioxolane-2,4-diones (OCA, **1**, Scheme 14) was carried out following the reported work of Toyooka et al.¹⁰ Previously, **1** was synthesized from mandelic acid and phosgene with low yield. Thus, trichloromethyl chloroformate (TCF) was used for the synthesis of *N*-carboxy α -amino acid anhydride in place of phosgene. A solution of TCF in THF was refluxed with an equimolar amount of mandelic acid for 6 h. After concentration under reduced pressure and solidified on addition of hexane, the solid was crystallized from diethyl ether to give **1** (¹H NMR, Figure 27).

Scheme 14. One step synthesis of OCA from D,L-mandelic acid and TCF



C.2. Water sensitivity of **1**

Not having worked with OCA monomers, their relative stability in the presence of water was unknown. To determine how stable an OCA monomer was in water, compound **1** was dissolved in CDCl₃ with a drop of D₂O in a NMR tube. The ¹H NMR spectrum of the mixture was taken at several time points (Figure 16). Mandelic acid, the hydrolysis product of OCA, was apparent after 2h but amount of hydrolysis of compound **1** was still less than 50% after 24 h. This result showed that OCA was durable in a moist environment for a short period of time.

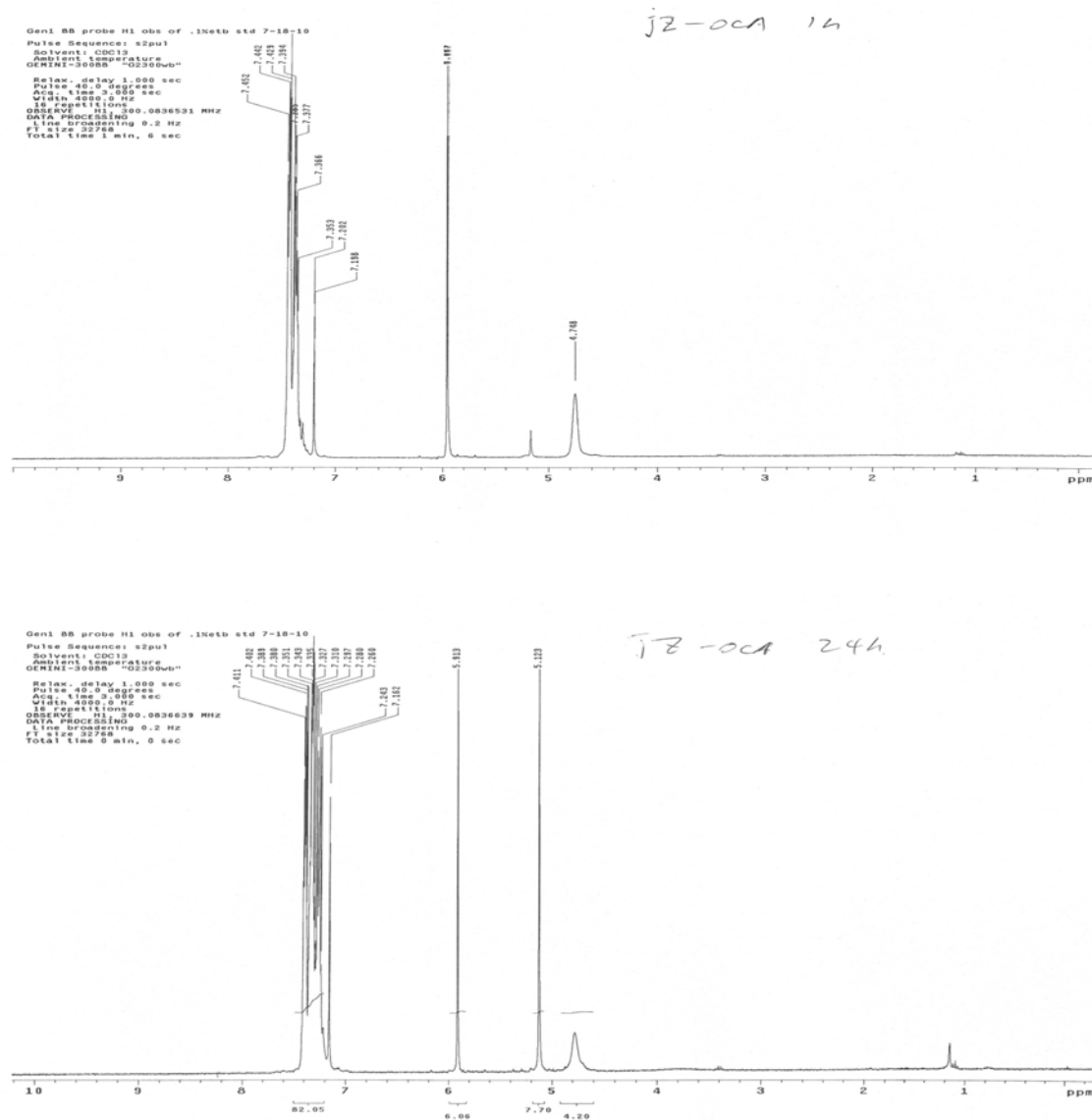


Figure 16. ^1H NMR spectra illustrating the hydrolysis of **9** over time

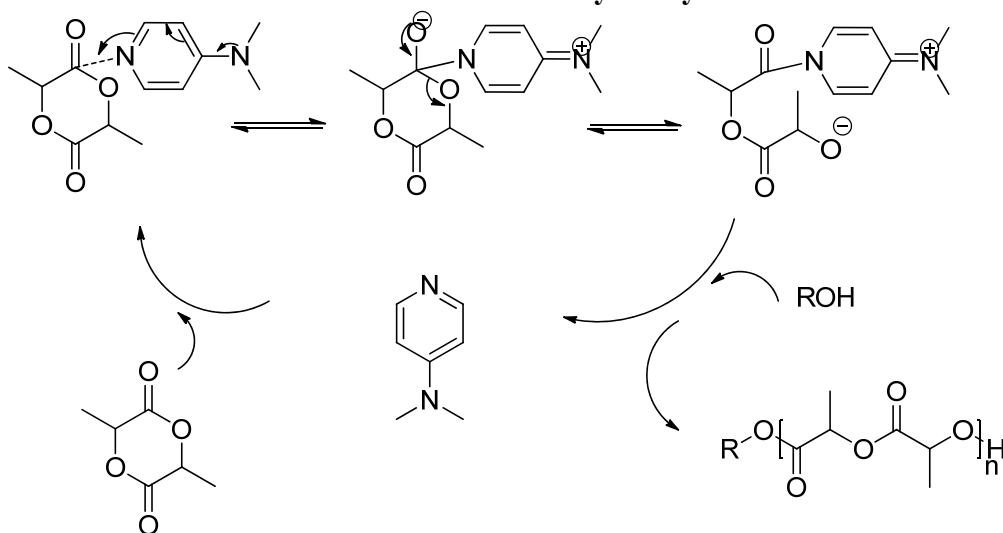
C.3. Polymerization of OCA in solution and on surfaces

The ROP and SIP of 5-Phenyl-1,3-dioxolane-2,4-dione (**1**) were then studied. For ROP of **1** in DCM, dimethylamino pyridine (DMAP) and BnOH were evaluated as catalyst and initiator. The mechanism of DMAP-catalyzed ROP is presented in scheme 15: DMAP

attacks the carbonyl group of the monomer and then is replaced by alcohol. The polymer formed serves as a macroinitiator for the next cycle of propagation. Initiation with DMAP and alcohol showed good control of ROP of **1** with a molecular weight $M_n > 9$ KDa and narrow molecular weight distribution ($PDI < 1.25$) as reported previously.¹¹ $Sn(Oct)_2$ was also tried as catalyst for the polymerization, however, the singlet at 4.9 ppm showed no reaction happened. (Diagnostic Peak: **1** at 5.9 ppm; mandelic acid at 4.9 ppm in 1H NMR)

The experimental procedure used for SIP of **1** was the same as reported previously for the growth of PLA brushes on silicon surfaces except DMAP was used as catalyst (see Experimental Section). Unfortunately, no apparent thickness increase was observed on the Si surface, but polymer was found in the THF solution. This result was attributed to (1) the amount of impurity, mandelic acid, in solution exceeded the amount of silanol surface initiators and (2) DMAP is a bulky catalyst that may not be ideal for SIP.

Scheme 15. Mechanism of ROP of LA catalyzed by DMAP



Considering the numerous diastereomers and the unsuitable catalyst, the synthetic route of PEG₆-spiro lactide will probably be abandoned. Nevertheless, the synthesis of PEG grafted

OCA is still worth to continue since it is synthetically more approachable and has much less stereoisomers. PEG side chains will be grafted at the benzene position of OCA and the catalytic effect of tin salt will be tested for its potential application on Si surfaces. GPC will be used to characterize these polyesters.

D. Synthesis of OEG-Grafted PLA (version II and III)

D.1. Synthesis of OEG-Grafted PLA (version II)

Although attempts at surface-initiated polymerization of PEG₆-spiro lactide were disappointingly unproductive, the goal of synthesizing a PEG-appended monomer has not been abandoned. In the literature, several side-chain-functionalized lactide analogues were synthesized through the incorporation of L-alanine and side-chain protected L-amino acids. The experience of preparing PEG₆-spiro lactide indicated that the purity of the monomer is important to SIP, so that any gel-like monomers with long PEG side chains or those that are produced as a mixture of diastereomers would be disadvantageous to obtaining a pure monomer and to the subsequent surface polymerization. Herein, the design of a new synthetic route was based on two considerations: avoiding the installation of long side chains onto the side-arm of lactide and preparing diastereomerically pure monomers.

acidic solution. The yield depended on the rate of addition. The highest yield reached 70%. (S)-2-bromopropionyl chloride (**5**) was prepared following the procedure originally reported by Langer et al.¹³ The amine group of L-alanine was transformed to bromide through diazotization in HBr solution. Then, the carboxylic acid was transformed to acid chloride using thionyl chloride. Because molecule **5** is relatively cheap to produce, it was prepared on a large scale. During the process of purification, the product solution was divided into several parts and each was purified individually.

Before the coupling reaction, molecule **2** was further purified by azeotropic distillation of any water present. Because the coupling reaction was performed under acidic conditions and the α -proton of acid chloride was enolizable, racemization was expected in this step. After the employment of the Finkelstein reaction on molecule **7**, the diastereomeric mixture was treated with a dilute solution of *N,N*-diisopropylethylamine (DIEA) in acetone. Byproducts of cyclization were easily removed by a short silica column to produce molecule **8** in 30% yield. The diastereomeric mixture was then separated using premium grade silica column to avoid decomposition of lactide ring. Both the (S,S) and (S,R) diastereomers were investigated in the further steps and showed the same reactivity.

The proposed attachment of the OEG chain involved alkanethiol chemistry reported by Queneau et al.¹⁴ In the presence of sodium hydride, tosyl lactide (**11**) could react with poly(ethylene glycol) terminated with thiol group (**12**) via a S_N2 reaction to get the final monomer (**13**). Due to the possible lability of the ester linkages in the lactide, strong nucleophiles, such as alkoxide, were avoided.

However, challenges were met when the deprotection of **9** and tosylation of **10** were performed. The deprotection reaction exhibited poor reproducibility and long reaction time. To prepare molecule **10**, a solution of benzylactide **9** in methanol was treated with palladium on charcoal (10%) under a hydrogen atmosphere at room temperature. Decomposition of lactide ring was discovered within 24 h and a similar result was obtained when other protic solvents were employed (Table 3, entry 3). Thus, the aprotic solvents were explored. Only in one instance, the use of THF lead to the desired product with 90-100% yield after vigorous

stirring for 3 days. Usually this reaction is reported to require minutes to hours for other substrates. Moreover, no reaction was obtained when brand new Pd/C catalyst was used for the second time even with careful storage. Thus, the investigation was focused on the use of other heterogeneous, hydrogenation catalysts. However, none of them gave better results in terms of time and yield.

Table 3. Optimization of Reaction Conditions for the Generation of 10

Entry	<i>T</i> (°C)	Catalyst	Solvent	Product ^a
1	25	Pd/C (10%, new)	THF	Y
2	25	Pd/C (10%, new)	Ethyl Acetate	N
3	25	Pd/C (10%, new)	Methanol	RO
4	25	Pd/C (10%)	THF	N
5	25	Pd/C (5%, new)	THF	N
6	25	Pt/C (10%, new)	THF	N
7	25	Pd(OH) ₂ /C (20%)	THF	N

^a Y=yes, N=none, RO=ring opening

Molecule **11** was difficult to obtain under basic conditions required for the tosylation reaction (Table 4). Although molecule **12** was readily prepared following the procedure reported by Snow¹⁵, the challenges met in the preparation of molecules **10** and **11** made the further investigation of this synthetic route less viable.

Table 4. Optimization of Reaction Conditions for the Generation of 11

Entry	Base ^a	<i>T</i> (°C)	Product ^b
1	TEA	0	N
2	DIEA	0	N
3	Pyridine	0	N
4	DIEA	25	N
5	Pyridine	25	N

a TEA=triethyl amine DIEA=*N,N*-diisopropylethylamine

b N=none

D.2. Synthesis of OEG-Grafted PLA (version III)

The second molecular design based on the strategy of Baker et al. was then considered¹⁶. Considering the possible lability of the ester groups in the lactide, this approach was designed to attach the side-arms first and then assemble the lactide ring.

time was no more than 1h (but the reaction still needed to be tracked by ^1H NMR every 5min, especially after 30min, to determine when to stop) (Table 5, entry 4). After hydrolysis and extraction from ether, α -hydroxy acid **18** was obtained in 47 % yield. This molecule was then dimerized by dehydration in toluene with a catalytic amount of p-toluenesulfonic acid and a Barrett trap. Although the gel-like monomer **6** was purified by recrystallization and reduced-pressure distillation (180 °C/3 mTorr) in the literature, attempts to distill the monomer resulted in polymerization. This challenging purification may lead us to try to prepare analogues that have shorter aliphatic bridges, which may make them easier to isolate, in further investigations.

Table 5. Optimization of Reaction Conditions for the Generation of 5

Entry	NaBH ₄ , equiv ^a	T (°C)	Time (min)	Solvent	Peak (3/4ppm, aft rxn) ^b
1	4	0	30	Ethanol	N/N
2	3	0	30	Ethanol	N/N
3	2	0	30	Ethanol	N/S
4	1.5	0	30	Ethanol	N/P
5	1	0	45	Ethanol	S/P
6	0.5	0	60	Ethanol	S/P
7	1.5	25	30	Ethanol	S/P
8	1.5	0	30	THF	N/P

a Mole equivalence

b Peaks around 3 and 4 ppm correspond to the α -ketone and ester groups. N=none, S=small, P=preserved

References:

- (1) Xu, L.; Gorman, C. B. *Journal of Polymer Science Part A: Polymer Chemistry* **2010**, *48*, 3362.
- (2) Xu L, Ph.D. dissertation, North Carolina State Univ., **2011**
- (3) Xu, L.; Crawford, K.; Gorman, C. B. *Macromolecules* **2011**, *44*, 4777.
- (4) Castillo, J. A.; Borchmann, D. E.; Cheng, A. Y.; Wang, Y.; Hu, C.; Garcia, A. J.; Weck, M. *Macromolecules* **2012**, *45*, 62.
- (5) Hu X., Ph.D. dissertation, North Carolina State Univ., **2013**
- (6) Meyers, S. R.; Grinstaff, M. W. *Chem Rev* **2012**, *112*, 1615.
- (7) Jing, F.; Hillmyer, M. A. *J. Am. Chem. Soc.* 2008, *130*, 13826–13827.
- (8) Scheibelhoffer, A. S.; Blose, W. A.; Harwood, H. J. *Polym. Prepr. (Am. Chem. Soc., Div. Polym. Chem.)* **1969**, *10*, 1375–1380.
- (9) Li, H.; Zhang, S.; Jiao, J.; Jiao, Z.; Kong, L.; Xu, J.; Li, J.; Zuo, J.; Zhao, X. *Biomacromolecules* **2009**, *10*, 1311.
- (10) Toyooka K.; Takeuchi, Y.; Kubota, S. *Heterocycles* Vol. 29, No 5, **1989**
- (11) Lu, Y.; Yin, L.; Zhang, Y.; Zhonghai, Z.; Xu, Y.; Tong, R.; Cheng, J. *ACS macro letters* **2012**, *1*, 441.
- (12) Gerhardt, W. W.; Noga, D. E.; Hardcastle, K. I.; Garcia, A. J.; Collard, D. M.; Weck, M. *Biomacromolecules* **2006**, *7*, 1735.
- (13) Barrera, D. A.; Zylstra, E.; Lansbury, P. T.; Langer, R. *Macromolecules* **1995**, *28*, 425.
- (14) Xavier, N. M.; Rauter, A. P.; Queneau, Y. *Top Curr Chem* **2010**, 295: 19–62.
- (15) Snow, A. W.; Foos, E. E. *Synthesis* 2003, No. 4, Print: 18 03 2003.
- (16) Jiang, X.; Smith III, M. R.; Baker, G. L. *Macromolecules* **2008**, *41*, 318-324.

FUTURE PLANS

A. Functional Polylactide-Poly(ethylene glycol) by CuAAC

The recently developed robust, efficient and orthogonal (REO) technique applied on soft materials provides an opportunity to study the modification of functionalities, architectures and molecular size of well-defined, discrete macromolecules or nanoscale structures. These reactions include pyridyl disulfide, Michael addition, a copper “click” reaction, the thiol-ene reaction and the Diels-Alder reaction.¹ The Diels-Alder reaction has shown reasonable ability to connect PEG with lactide, as discussed above in the experimental section. Although hindered by the diastereoisomers of LA-spiro-OEG, the strategy of combining hydrophilic PEG and biodegradable polyesters into one hybrid polymer is still the primary approach for antibiofouling polymeric brushes.

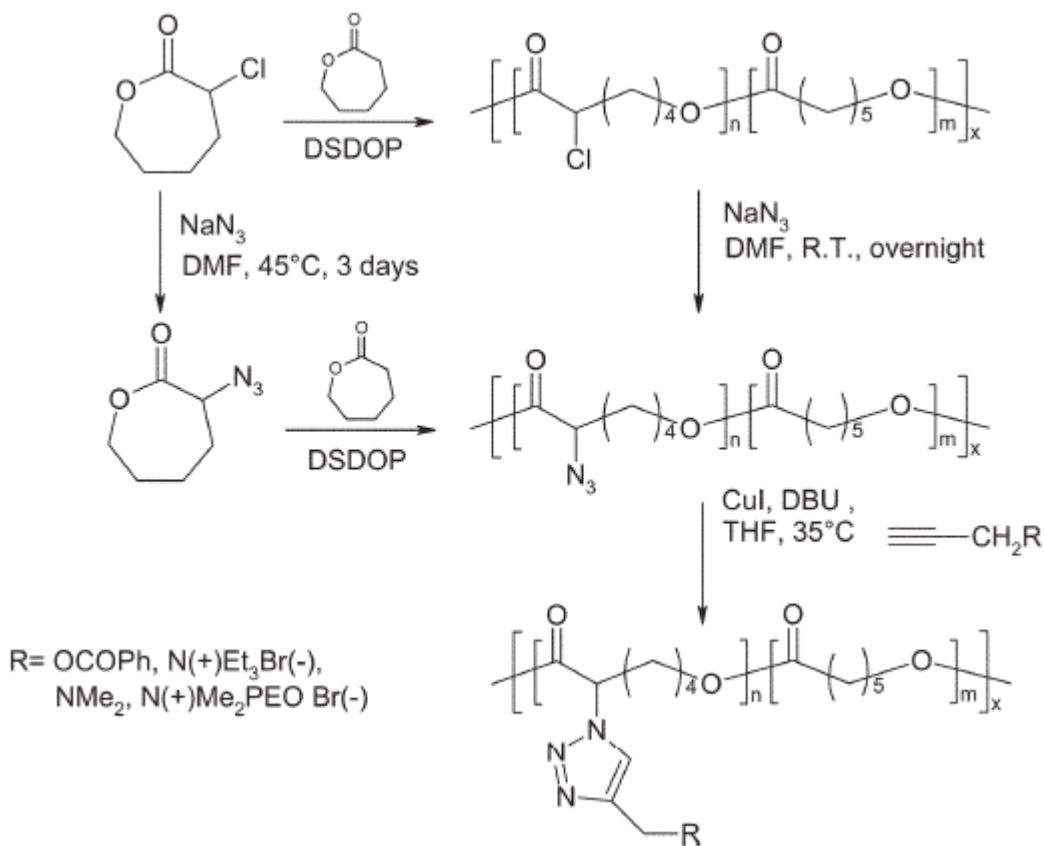
Rather than attaching OEG groups to the monomer, it is proposed to determine if polymer brushes composed of degradable polyesters can be modified with OEG groups after they are synthesized. To do this, the copper-catalyzed azide/alkyne cycloaddition (CuAAC) reaction is chosen because it successfully circumvents the problems of endo-exo and facial selectivity of Diels-Alder reaction. Besides these advantages, CuAAC also has good tolerance of functionality, moderate conditions, high yield and simple purification. These features make CuAAC a powerful method in synthetic polymer chemistry.

There are several ways to utilize CuAAC to modify polymers. CuAAC (1) can be used on chain end functional homo/copolymers to connect two macromolecules; (2) the triple bond or azide functional groups can be added onto monomers first and the click reaction can be conducted in the both the pre- or post-polymerization; (3) star or cross-linked polymers can be prepared through click reaction started from initiators modified by several triple bonds.

CuAAC has already been applied on biodegradable polymers. For example, Lecomte and co-workers successfully grafted α -MeO, *w*-alkyne-PEO ($M_{n,NMR}=5800$) onto poly(α N₃ECL-co-ECL) by combining ring-opening copolymerization with click chemistry (Scheme 16).² The post-polymerization was conducted under mild reaction conditions (THF, 35°C, 2h, copper

iodide and DBU) and the preparation of azido monomer took only 3 days under higher temperature.

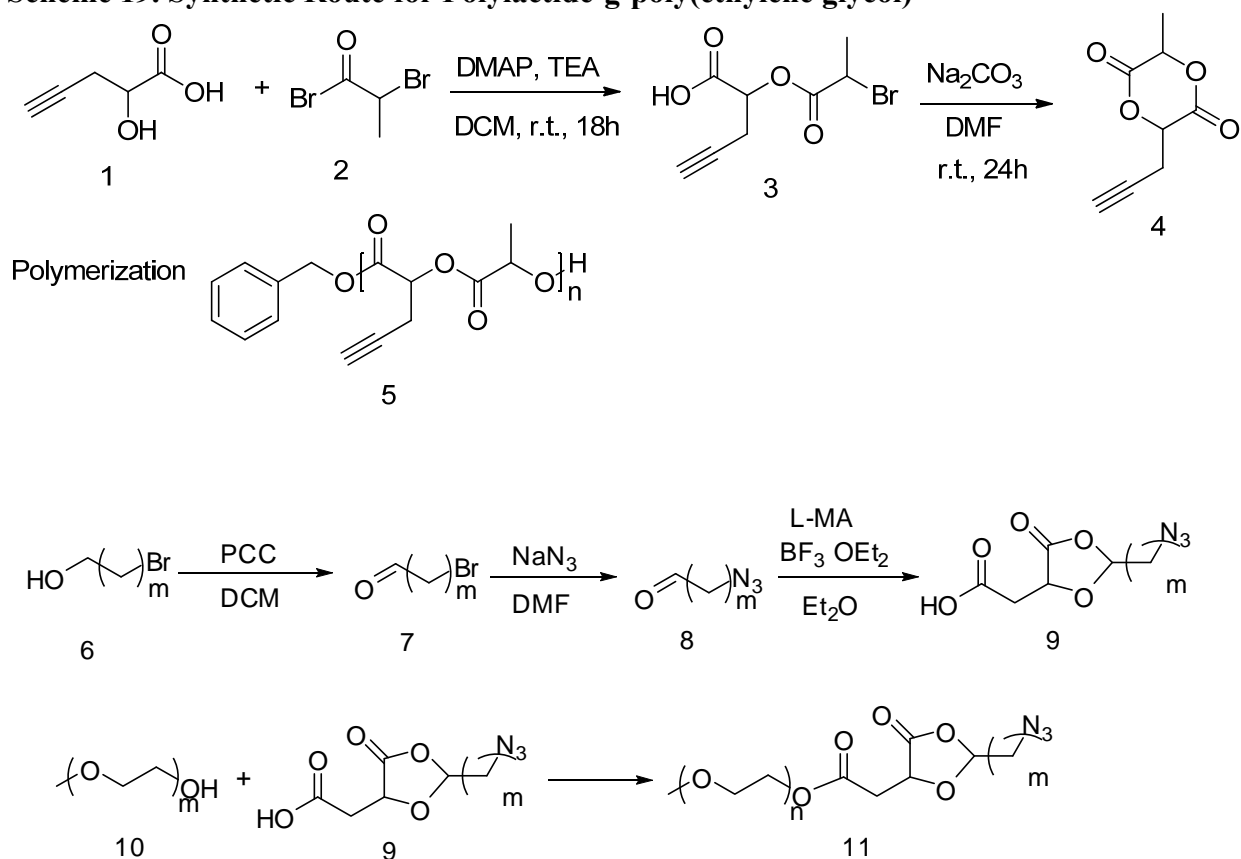
Scheme 18. Derivatization of PCL by combining ROP and CuAAC

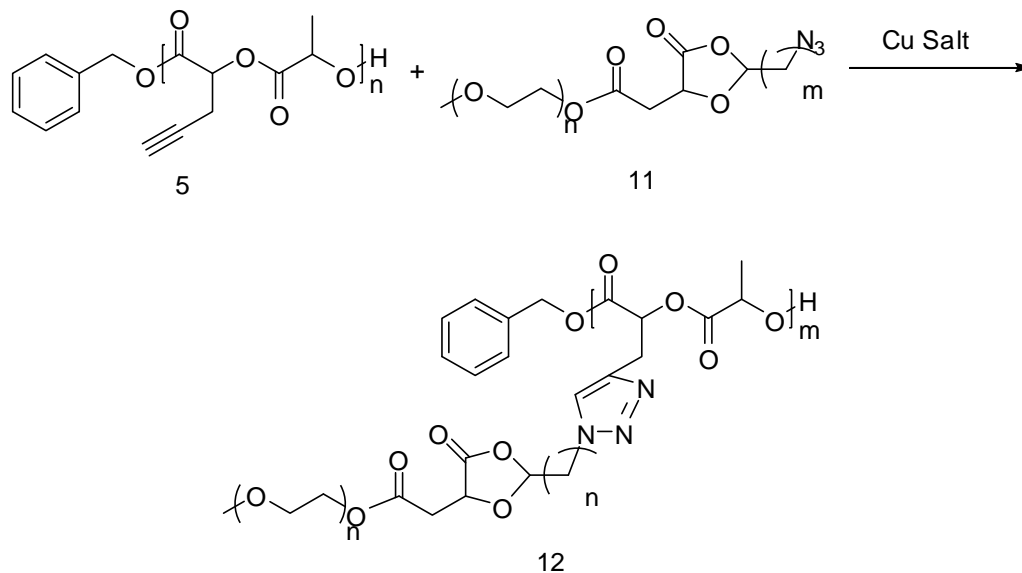


The well-studied “backbiting” degradation mechanism of PLA brushes plus the mild degradation conditions (room temperature, moderate basic solution) make the strategy of “PLA+OEG” still our primary choice. The work of Cheng et al. will be used as reference.³ As shown in scheme 17, carbon triple bonds were grafted onto the backbone of PLA initiated by alcohol (molecule **5**) (or silanol groups on surfaces). After several simple steps of organic synthesis, azide-functionalized PEG (11) can be connected to **5**. The grafting density of OEG

can be tuned by altering the ratio of starting materials. However, when the CuAAC reaction is applied polymeric brushes grafted to surfaces, no matter whether this is performed pre- or post-grafting, it will make the reactivity of the desired monomers questionable. The strategy of pre-grafting the chains might make the monomer bulkier and might make the approach to the surface difficult. While the strategy of post-grafting the chains (after SIP of 4) also suffers difficulties, the density of azide functional groups will be relatively low since steric hindering effect will lower down their reacting possibility (mushroom morphology of PLA chains, sterically hindered by each other).

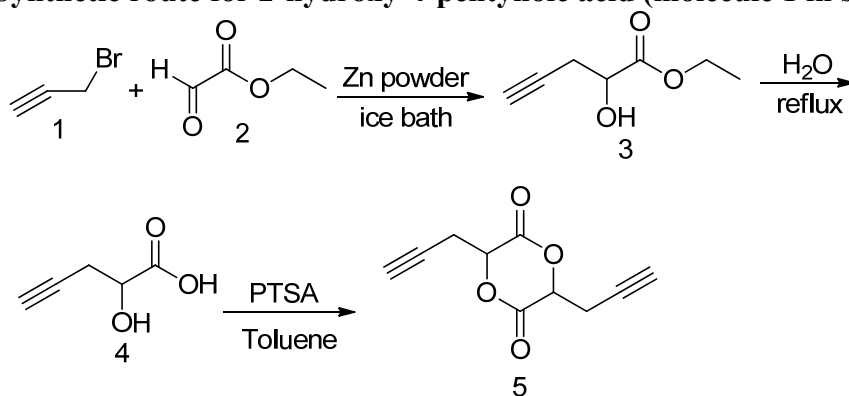
Scheme 19. Synthetic Route for Poly(lactide-g-poly(ethylene glycol))





The preparation of molecule **1** is based on the work of Smith et al. (Scheme 18).⁴ Propargyl bromide (**1**) and freshly distilled ethyl glyoxylate (**2**) undergo a Reformatsky reaction in the presence of activated zinc powder to generate ethyl 2-hydroxy-3-butynoate (**3**). Purification by silica gel is necessary. Molecule **3** is hydrolyzed in refluxing water to give 2-hydroxy-3-butynoic acid (**4**). Then there are two possible routes: cyclization to give **5** (Scheme 17) by refluxing **4** with catalytic *p*-toluenesulfonic acid in toluene or reaction of **4** with 2-bromopropionyl bromide (**2**, Scheme 17) followed by cyclization in DMF catalyzed by Na_2CO_3 . When it is desirable to introduce OEG polymeric chains with large molecular weights, the high density of alkyne groups in the backbone precursor polymer is not necessary due to the bulky azide-functionalized grafting-onto agent, as discussed by Cheng et al. As a result, the monomer **4** in Scheme 17 is our primary choice but monomer **5** in Scheme 18 is also worth examining when OEG when fewer repeating units are desired.

Scheme 20. Synthetic route for 2-hydroxy-4-pentynoic acid (molecule 1 in scheme 1a)



As shown in Scheme 17, functionalized PLA (**5**) with pendent acetylene functionalities will be prepared by the synthesis of mono-acetylene LA monomer **4** followed by ROP of **4**. Molecule **4** will be obtained by a two-step organic synthesis starting from 1, 2-hydroxy-4-pentynoic acid. The “grafting-onto” azide-functionalized agent **12** will be prepared in four-step organic synthesis starting from 6-bromo-1-hexanol. The resulting molecule **12** has a hydrolysable cycloacetal group between azide group and OEG. By tuning the hydrolysis reaction conditions, bond cleavage can happen both at the PLA backbone or the cycloacetal group. The cycloacetal group is acid-sensitive and has hydrolysis reactivity increases with acidity. Cheng et al. tested several conditions for the hydrolysis of polylactide-g-paclitaxel-poly(ethylene glycol) in aqueous buffer solutions with pH of 5.5 and 7.4 at 37°C. The conclusion was that, under acidic conditions, cycloacetal hydrolysis was faster than hydrolysis of ester groups of molecule **12** or PLA. The hydrolysis of PLA backbone happened within 7 days. The cycloacetal groups are helpful to quantify the difference of antibiofouling effect between PLA and PLA-OEG brushes although the pH or temperature of hydrolysis may change when these conditions are applied to brushes on surfaces.

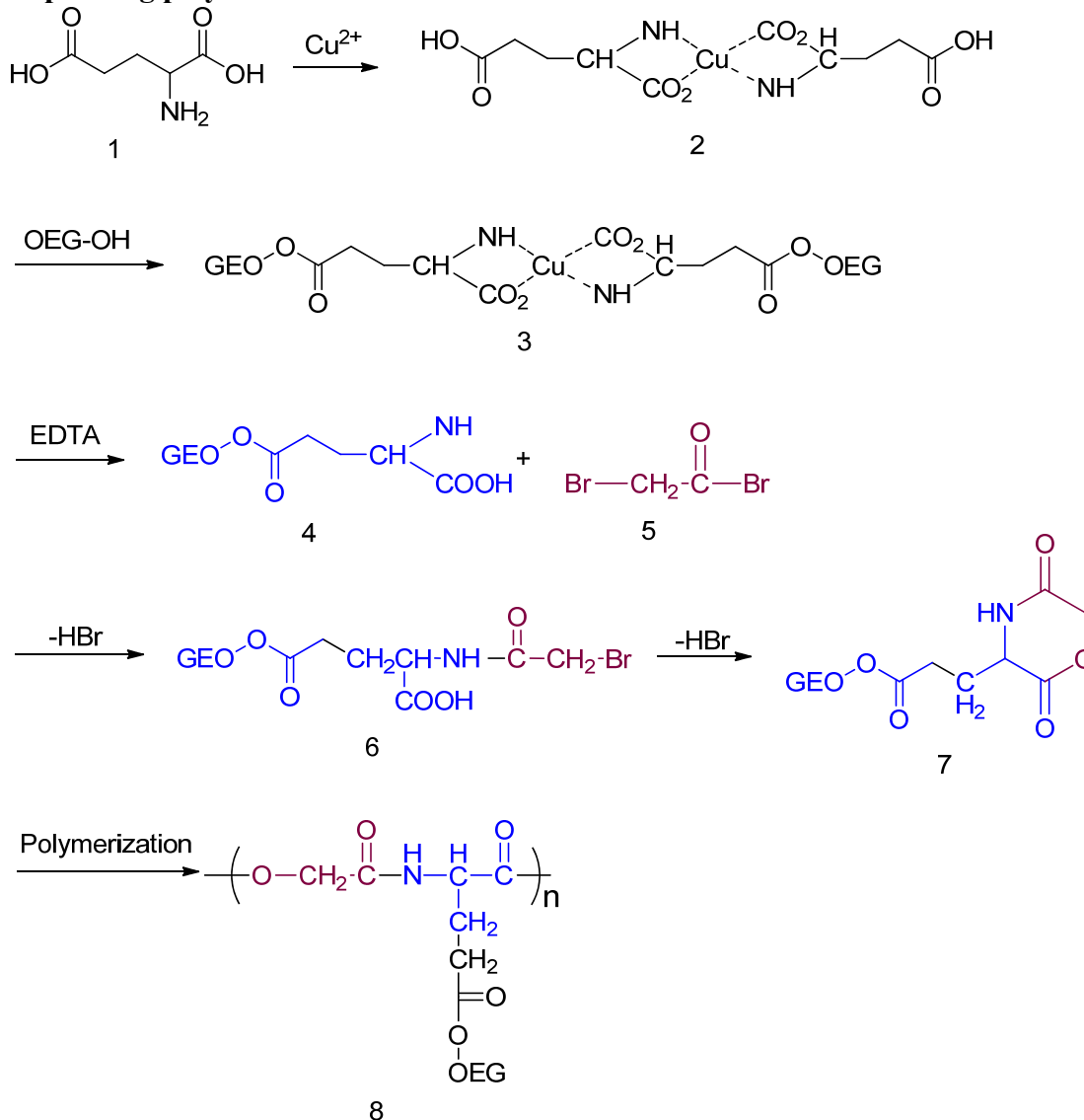
Based on the previous discussion, the difficulties of both pre- and post-grafting strategy were taken into consideration. Performing CuAAC before ROP may be first tried. However, possible decomposition should also be taken into consideration. Copper cations used as

catalysts in CuAAC are Lewis acidic and can bind to the oxygen of the carbonyl groups and make the ring of LA easier to open. All advantages and disadvantages will be judged and weighted for selecting the “grafting onto” bridge molecule and grafting OEG before or after ROP.

B. Synthetic route for poly(lactide-amino acid)

As discussed in the introduction, bioactive polypeptides can be used on surface coating because they are a kind of antibiofouling materials that can give an inherent communicative understanding between surfaces and foreign body giant cells.⁵ Synthesis of OEG modified morpholione-2,5-dione is the new strategy that combines of the non-fouling PEG moiety with the biomimetic polypeptide and biodegradable poly(lactic acid) sequences.

Scheme 21. Synthetic route for OEG modified morpholione-2,5-dione and corresponding polymer



Starting from commercially available glutamic acid (**1**, Scheme 19), α -amino and carboxylic acid groups will first be protected by coordination to copper(II). Then oligo(ethylene glycol) with hydroxyl end group can react with the γ -carboxylic acid group. Ethylenediaminetetraacetic acid (EDTA) will be used to deprotect α -amino and carboxylic acid groups. In the next two steps of the ring closing reaction, **4+5** to **6** and **6** to **7**, a basic

environment is required to eliminate the byproduct, HBr and promote the equilibrium in the direction to form the six membered ring product. The organic base triethylamine (TEA) will be selected to maintain a homogeneous reaction mixture. It had been demonstrated that both TBD OAc and Sn(Oct)₂ are effective catalysts for the ROP of morpholione-2,5-dione but tin is expected to function better cooperating with surface hydroxyl initiators to graft **7** onto silicon substrate (mechanism of SIP of LA catalyzed by tin salt, see Scheme 8 in the Results and Discussion section). At the end, the new hybrid polymeric brushes constituted of peptide and ester bonds with OEG side chains on the backbone will be formed on surfaces. Characterization via ellipsometry water contact angle measurement, ATR-FTIR and AFM image collection, and protein adhesion studies will be performed on these new surfaces.

References:

- (1) Iha, R. K.; Wooley, K. L.; Nyström, A. M.; Burke, D. J.; Kade, M. J.; Hawker, C. J. *Chemical Reviews* **2009**, *109*, 5620.
- (2) Riva, R.; Schmeits, S.; Jérôme, C.; Jérôme, R.; Lecomte, P. *Macromolecules* **2007**, *40*, 796.
- (3) Yu, Y.; Zou, J.; Yu, L.; Ji, W.; Li, Y.; Law, W.-C.; Cheng, C. *Macromolecules* **2011**, *44*, 4793.
- (4) Jiang, X.; Vogel, E. B.; Smith, M. R.; Baker, G. L. *Macromolecules* **2008**, *41*, 1937.
- (5) Franz, S.; Rammelt, S.; Scharnweber, D.; Simon, J. C. *Biomaterials* **2011**, *32*, 6692.

EXPERIMENTAL SECTION

A. General Considerations

All the reactions described here were carried out under nitrogen protection or in a nitrogen-filled glovebox if indicated. Solvents were of reagent grade and dried with 4 Å molecular sieves before use. All commercially available chemicals were used without further purification unless indicated. ^1H and ^{13}C NMR analyses were carried out at room temperature on a Varian Mercury 300 or 400 spectrometer, with the chemical shifts reported in ppm and referenced to signals from residual protons in the solvent. FT-IR spectra were acquired using a Bruker Vertex 80V infrared spectrometer equipped with a Platinum™ diamond ATR attachment.

N-Bromosuccinimide (NBS) was purchased from Alfa Aesar. NBS (50 g) was dissolved in 500 mL of boiling water and filtered through a fluted filter paper into a flask. After 2 hours, crystals and solvent were filtered through Buchner Funnel and NBS crystals were further dried under vacuum over P_2O_5 . L-lactide was purchased from Sigma-Aldrich. It was purified by recrystallization twice from anhydrous toluene.

O-benzyl-L-serine (15 g) was purchased from VWR International. Diethylene glycol monomethyl ether (50 g) was purchased from Sigma-Aldrich. Diethyl oxalate (500 g) was purchased from Alfa Aesar. Sodium hydride (50 g) was purchased from Alfa Aesar and used directly in a nitrogen-filled glovebox. All the heterogeneous hydrogenation catalysts, including Palladium on charcoal (5, 10 wt. %), Platinum on charcoal (10 wt. %) and $\text{Pd}(\text{OH})_2$ on charcoal, were purchased from Sigma-Aldrich. Chromatography employed two kinds of silica gels. For the crude isolation performed in short columns, Sorbent Tech Standard Grade Silica (porosity 60 Å, particle size 40-63 μm (230 X 400 mesh), surface area 500-600 m^2/g , pH range 6.5-7.5) was used; while Biotage SNAP Ultra cartridges (size 10 g, pressure rating 100 psi, resolution 10,000 N/m, media 25 micron spherical silica) were used for separation of diastereomers **8** (version II). Decomposition of the cyclic compound **8** was observed during chromatography using the Sorbent Tech Standard Grade Silica Gel.

B. Reproduced Growth and Degradation Curve of Poly(lactic acid)

B.1. Growth of PLA on silicon surface

PLA was successfully grown from Si substrate given thickness of ca. 10nm under optimized reaction condition.¹ To generally restate the experimental procedure, L-lactide and Sn(Oct)₂ were purchased from Sigma-Aldrich, lactide was purified by recrystallization twice in anhydrous toluene to remove little amount of water. Sn(Oct)₂ was distilled at 80°C under vacuum of 10 millitorr. The purified products were stored in the dry box. Silicon substrates were cut into 5mm×5mm small chips and cleaned in Piranha solution (a 70/30 v/v mixture of concentrated sulfuric acid and 30 % aqueous hydrogen peroxide) for 7 hours. Then the chips were rinsed with large amount of DI water and ethanol sequentially, sonicated for 10min in ethanol, rinse with ethanol again and dried under nitrogen. Then ultraviolet-ozone (UVO) cleaner was used to prepare silica layer on silicon substrate. The solution of Sn(Oct)₂ in freshly distilled THF (0.25 M) was prepared before use.

The fresh silicon chips in small vials were transferred into glovebox. For each sample, 20μl catalyst solution and lactide (72 mg, 0.25 M) in 5ml fresh THF were added. The grafted samples were rinsed and sonicated with ethanol for 10 min. The clean samples were dried with nitrogen flowing before characterization.

The thickness grown on surface was measured by Rudolph Research/AutoEL ellipsometry facility. Before and after grafting, each sample was measured twice and the difference determined the thickness of PLA brushes. No special storage method was employed.

B.2. Degradation of PLA brushes

It had been successfully demonstrated that when exposed to aqueous solutions, PLA brushes on silicon surfaces decrease with time and the optimized condition, which gave the fastest degradation rate, is 37°C and pH=8.² The degradation curve provided the approach to dynamic surfaces. To generally restate the experimental procedure, the samples of silicon substrate with PLA brushes were immersed into 10ml phosphate buffer solution at PH=8 and

kept in incubator set 37°C as constant temperature. Single sample was taken out from buffer solution, rinsed with ethanol, dried under nitrogen before each ellipsometry measurement (Rudolph Research/AutoEL) ellipsometry facility at various time points.

C. PEG₆-Grafted PLA: Monomer synthesis and polymerization (All the numbers of molecules are referred to Scheme 10)

C.1. Synthesis of Hexaethylene Glycol Methyl Ether 1,2,3- Δ^2 -Triazoline-spiro[6-methyl-1,4-dioxane-2,5-dione-3,2'-bicyclo-[2.2.1]heptanes, PEG₆ Spirolactide

C.1.1. (3S, 6S)-3-Bromo-3,6-dimethyl-1,4-dioxane-2,5-dione (1)

Benzene (124 mL), recrystallized lactide (24.92 g, 0.173 mol) and N-bromosuccinimide (33.91 g, 0.191 mol) were added to a three necked round bottom flask. After the mixture was brought to reflux, benzoyl peroxide (0.837 g, 3.45 mmol) in benzene (12 mL) was added drop wise through a dropping funnel over the course of 20 m. The color of the reaction mixture changed to red orange within 30 m. After the lactide was consumed (as monitored by thin layer chromatography, mobile phase: ethyl acetate and hexane 1:1), the reaction mixture was cooled to room temperature and filtered. The filtrate was evaporated to give a yellow solid. Dichloromethane (186 mL) was added to dissolve the solid and the solution was washed with saturated sodium bisulfite solution three times and saturated sodium chloride solution once sequentially in a separation funnel. The organic solution was dried over magnesium sulfate overnight and evaporated to dryness. Crude (3S, 6S)-3-Bromo-3,6-dimethyl-1,4-dioxane-2,5-dione was recrystallized from ethyl acetate and hexane (1:1) to give 17.33 g of white crystals (45% yield). ¹H NMR(CDCl₃): δ 5.48 (q, 1H) 2.32 (s, 3H), 1.72 (d, 3H) matched that reported previously.³ (Figure 17)

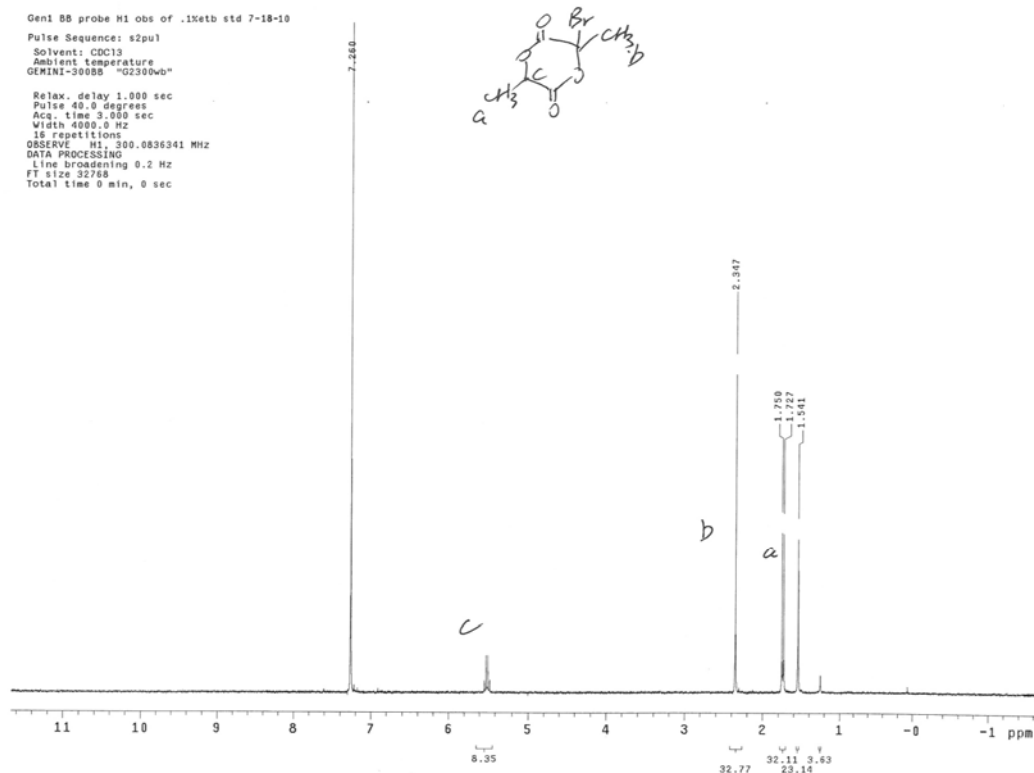


Figure 17. ^1H NMR spectrum of (3S, 6S)-3-Bromo-3,6-dimethyl-1,4-dioxane-2,5-dione (CDCl_3)

C.1.2. (6S)-3-Methylene-6-methyl-1,4-dioxane-2,5-dione (2)

Dichloromethane (111 mL) and (3S, 6S)-3-Bromo-3,6-dimethyl-1,4-dioxane-2,5-dione (17.3 g, 777 mmol) were added to a round bottomed flask. The flask was flushed with nitrogen and immersed into an ice bath. The reaction was run subsequently under nitrogen atmosphere. Triethylamine (11.9 mL, 85 mmol) was added drop wise via a syringe. The color of the reaction mixture changed to dark orange within 5m. After 1h the ice bath was removed and the reaction was continued at room temperature for another hour. Then the mixture was then washed with hydrochloric acid (1M) 3 times and saturated sodium chloride once sequentially in a separatory funnel. After the organic solution was dried over magnesium sulfate overnight,

it was evaporated to dryness. The resulting yellow solid was purified by column chromatography on silica gel eluting with dichloromethane (DCM) to afford a white solid. The white solid was further purified by sublimation at 45°C under vacuum to give 4.77 g (43% yield) of product. $^1\text{H NMR}(\text{CDCl}_3)$: δ 5.94 (d, 1H), 5.54 (d, 1H), 5.02 (q, 1H), 1.70 (d, 3H) matched that reported previously³ (Figure 18).

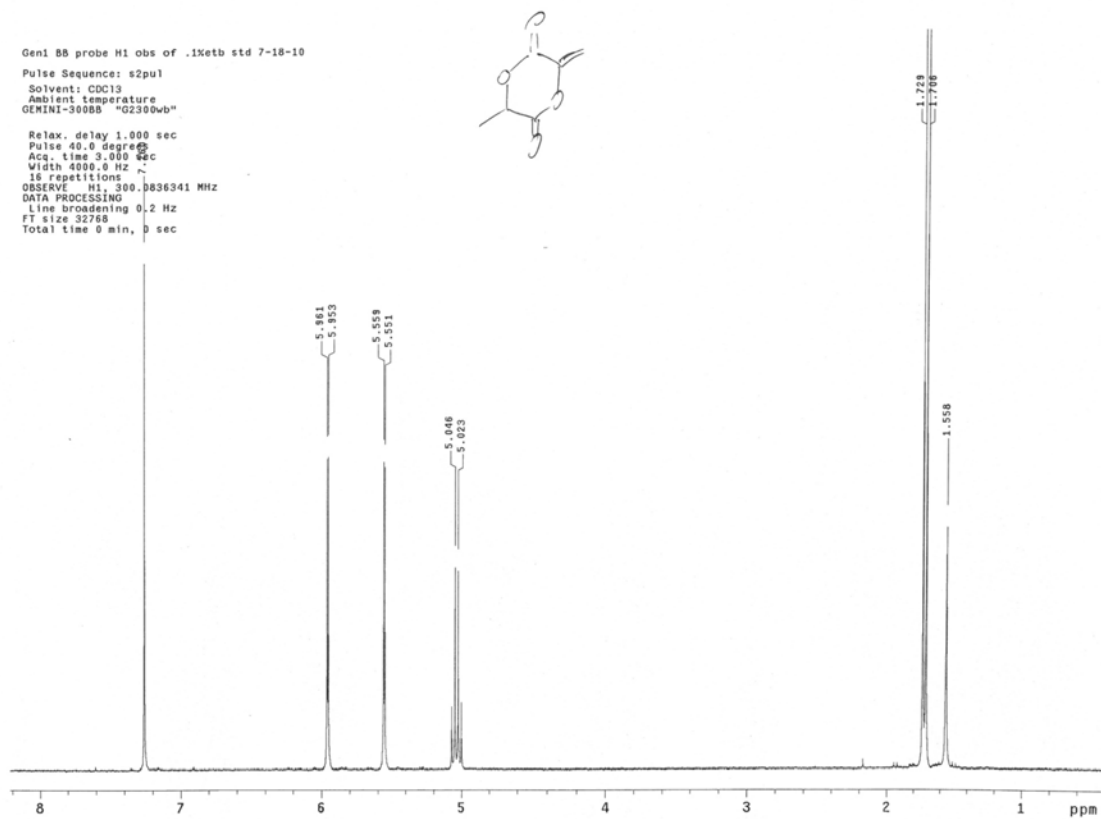


Figure 18. $^1\text{H NMR}$ spectrum of (6S)-3-Methylene-6-methyl-1,4-dioxane-2,5-dione (CDCl_3)

C.1.3. Spiro[6-methyl-1,4-dioxane-2,5-dione-3,2'-bicyclo[2.2.1]hept[5]ene] (3)

Dicyclopentadiene (ca. 10 g) was placed in a 50 mL round bottomed flask. Under nitrogen protection, the material was heat to 210 °C, and kept refluxing using a sand bath. A 1 mL forerun was discarded then cyclopentadiene was collected at -78 °C using dry ice/acetone bath. (6S)-3-Methylene-6-methyl-1,4-dioxane-2,5-dione (4.77 g, 33.6 mmol), freshly distilled cyclopentadiene (4.44 g, 67.2 mmol) and benzene (31 mL) was added into a 100 mL round bottom flask. Oil bath was used to keep the mixture refluxing overnight under inert gas protection. Benzene and extra cyclopentadiene was eliminated through concentration after the reaction was cooled down to room temperature. The crude product was purified by column chromatography on silica gel eluting with hexane first then dichloromethane to afford a white solid. The white solid was further purified by sublimation at 50°C under vacuum to give 3.8g (54.37% yield) of product. ¹H NMR(CDCl₃): δ 6.56 (m, 1H), 6.05 (m, 1H), 5.15 (m, 1H), 3.44-3.16 (m, 1H), 3.09–3.03 (m, 1H), 2.85–2.03 (m, 1H), 2.02–1.85 (m, 1H), 1.82–1.60 (m, 4H), 1.50 (dd, 1H) matched that reported previously³ (Figure 19).

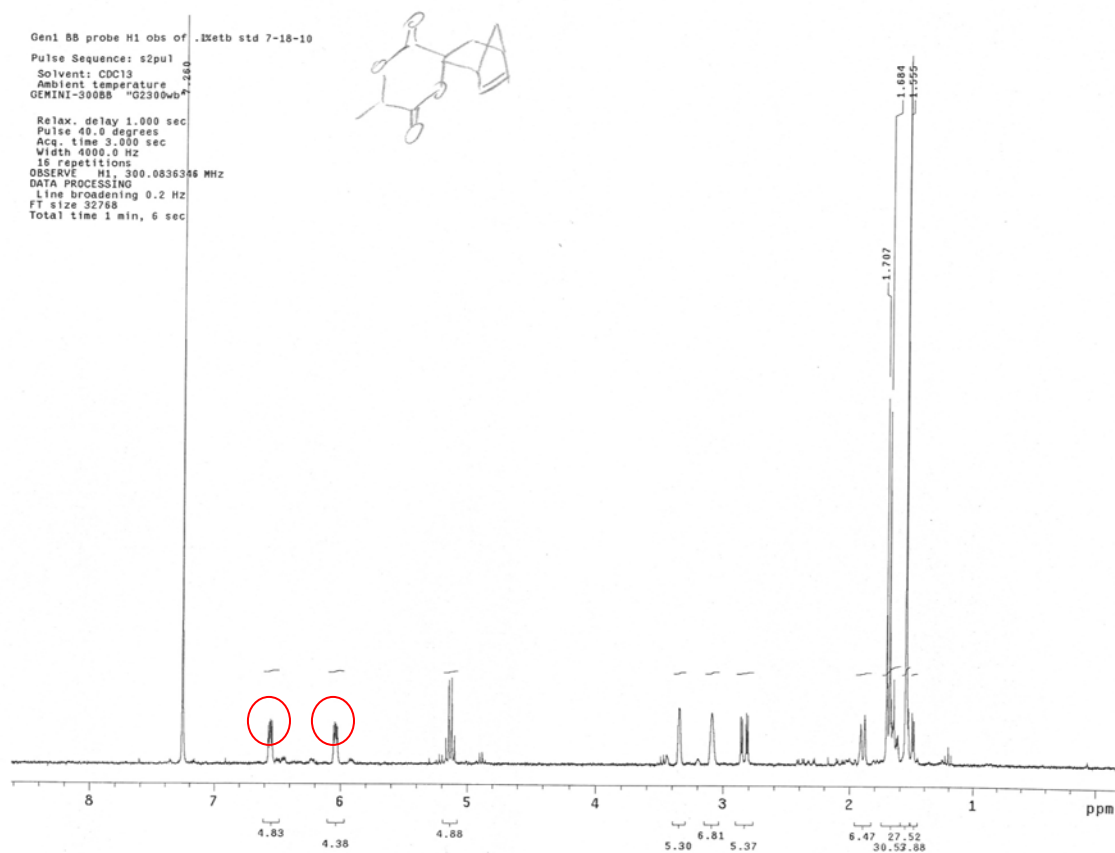


Figure 19. ^1H NMR spectrum of Spiro[6-methyl-1,4-dioxane-2,5-dione-3,2'-bicyclo[2.2.1]hept[5]ene] (CDCl_3)

C.1.4. Heptaethylene glycol monomethyl ether tosylate (5)

Heptaethylene glycol monomethylether (**4**) (ca. 10 g, 28.6 mmol) and freshly distilled tetrahydrofuran (57.28 mL) were added into a 150 mL round bottom flask. A solution of sodium hydroxide (1.6 g) in 7.16 mL of deionized water was added and ice bath was used to keep the reaction at 0°C . Then a solution of p-toluene sulfonyl chloride (6.538 g, 34.23 mmol) in 10.74 mL of tetrahydrofuran was added drop wise while kept the reaction temperature below 5°C . Then the mixture was kept in ice bath for another 2.5h. After the reaction was complete, the organic layer was separated using a separatory funnel, dried over anhydrous

C.1.5. Azido-poly(ethylene glycol) monomethyl ethers (6)

Heptaethylene glycol monomethyl ether tosylate (8.83 g, 16.9 mmol), sodium azide (5.44 g, 83.7 mmol) and dimethylformamide (63.1 mL) were added into a 100 mL round bottom flask. The reaction mixture was stirred under 50°C for 5h. Then 5 mL of deionized water and dichloromethane was added sequentially to extract the organic product. The DCM solution was washed with brine in a separatory funnel and separated. After dried over sodium sulfate and concentrated, the liquid product azido-poly(ethylene glycol) monomethyl ethers was obtained. The isolated yield was 4.57g (72.2%). ¹H NMR (CDCl₃): δ 3.31 (s, 3H, OCH₃); 3.32-3.7 (m, 28H, glycol protons) matched that reported previously⁴ (Figure 21).

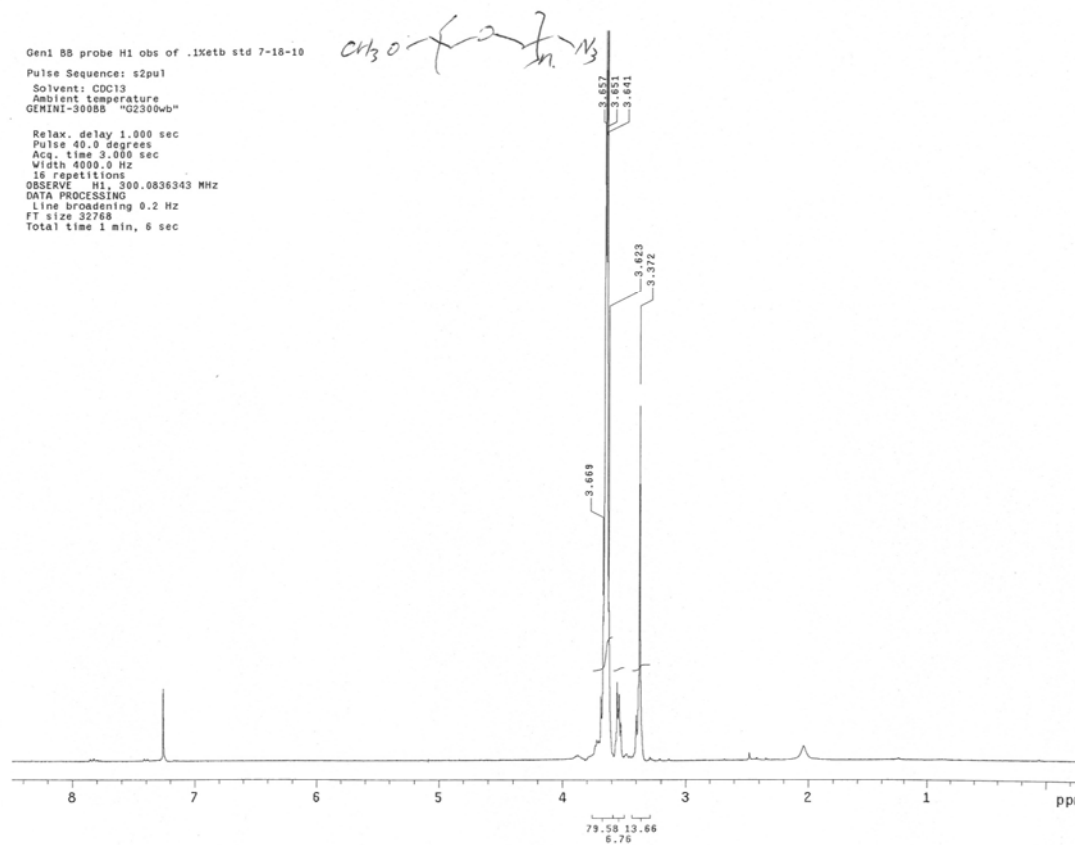


Figure 21. ¹H NMR spectrum of azido-poly(ethylene glycol) monomethyl ether (CDCl₃)

C.1.6. Hexaethylene Glycol Methyl Ether 1,2,3-Δ²-Triazoline-spiro[6-methyl-1,4-dioxane-2,5-dione-3,2'-bicyclo-[2.2.1]heptanes, PEG₆ Spirolactide (7)

Azido-poly(ethylene glycol) monomethyl ether (4.57 g, 12.2 mmol), Spiro[6-methyl-1,4-dioxane-2,5-dione-3,2'-bicyclo[2.2.1]hept[5]ene] (2.54g, 12.2 mmol) and ethyl acetate (68.5 mL) were added into a 150 mL round bottom flask. The reaction mixture was kept refluxing under nitrogen protection for 5 days. After the reaction was complete, the crude product was concentrated by rotary evaporator to give deep yellow oil. The oil was further purified by column chromatography on silica gel eluting with ethyl acetate:hexane=7:3 (volume ratio) to give 2.04 g (42% yield) light yellow oil. ¹H NMR (CDCl₃, 400 MHz, data shown for major

isomer): $\delta = 5.18$ (q, $J = 6.7$ Hz, 1H, -CH- of LA unit), 4.90 (d, $J = 9.8$ Hz, 1H, -CH- of triazolone unit), 3.82 (m, 2H), 3.75-3.61 (PEG chain, 34H), 3.53 (m, 3H), 3.35(m, 3H, CH₃-PEG-), 3.09 (s, 1H), 2.75 (dd, $J = 14.0$ Hz, $J = 4.9$ Hz, 1H), 2.63 (d, $J = 4.7$ Hz, 1H), 1.78 (m, 1H) (dd, $J = 11.6$ Hz, $J = 1.5$ Hz, 1H), 1.69 (d, $J = 6.7$ Hz, 3H, CH₃- of LA unit), 1.54 (dd, $J = 14.1$ Hz, $J = 3.6$ Hz, 1H), 1.26-1.23 (m, 1H). ¹³C NMR (CDCl₃, 100MHz, data shown for major isomer): $\delta = 167.9, 167.1, 85.7, 78.7, 73.0, 72.1, 70.8, 70.7$ (x2), 70.2, 62.7, 59.2, 48.9, 48.3, 41.0, 38.2, 31.5, 16.7. MS calcd for C₂₆H₄₄N₃O₁₁ 583; found 574.3. matched that reported previously³ (Figure 22, 23 and 24)

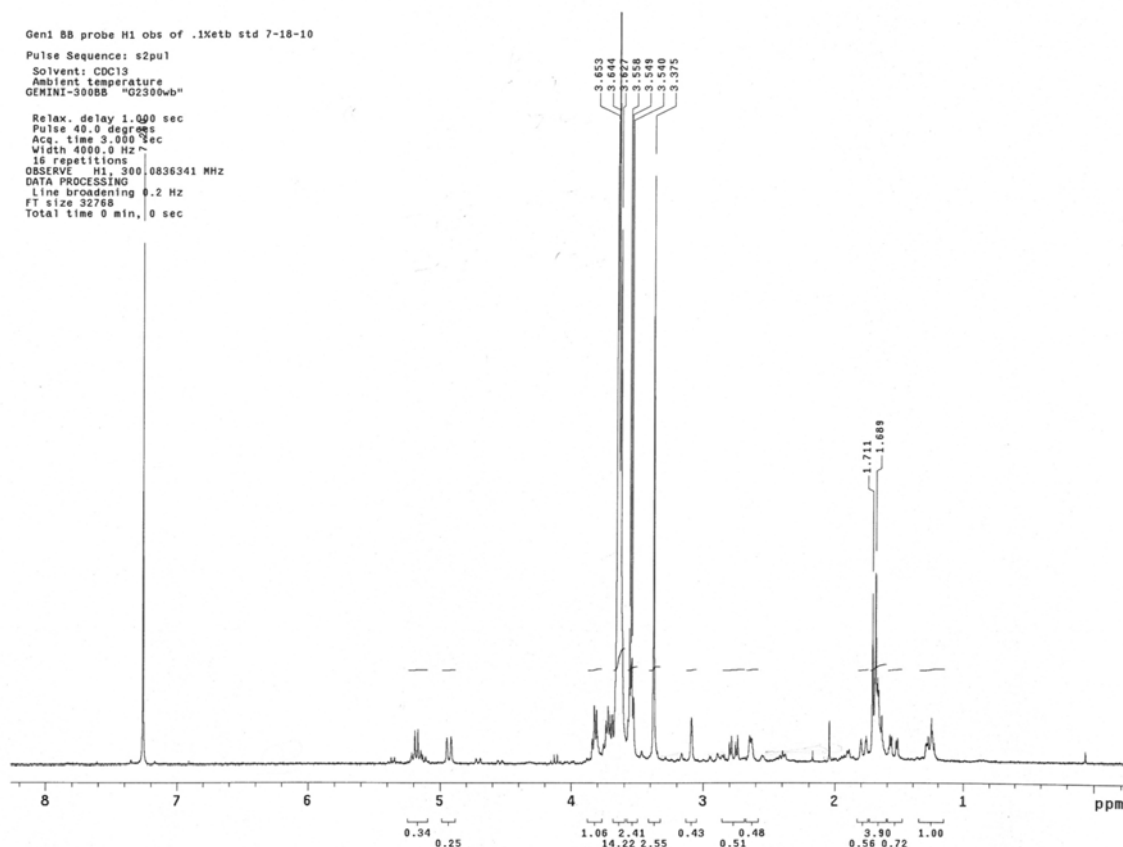


Figure 22. ¹H NMR spectrum of PEG₆-spiro-lactide (CDCl₃, molecular structure of 7 refers to scheme 10)

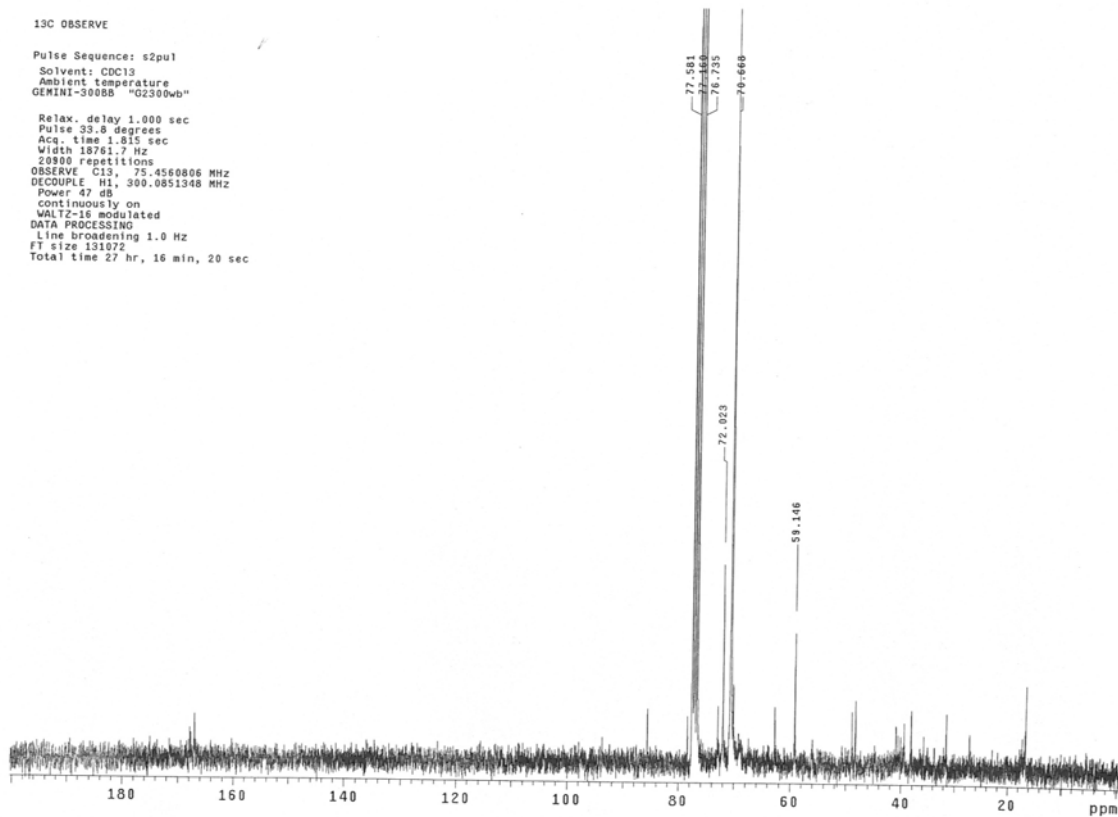


Figure 23. ¹³C NMR spectrum of PEG₆-spiro-lactide (CDCl₃, molecular structure of 7 refers to scheme 10)

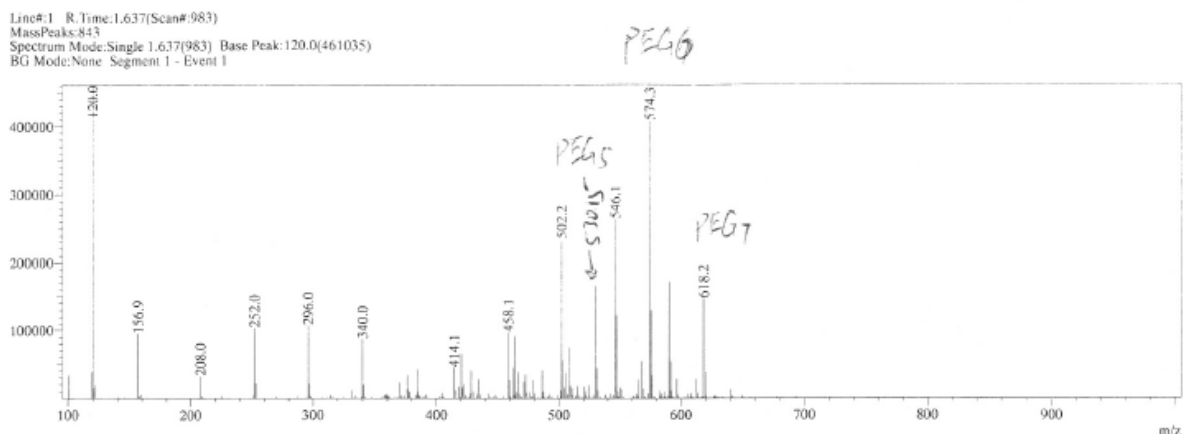


Figure 24. Mass Spectrum of PEG₆-spirolactide (molecular structure of 7 refers to scheme 10)

C.1.7. PEG₆-Grafted PLA (8)

The monomer was triply recrystallized from ethyl acetate/hexane and then was frozen in freshly distilled benzene and lyophilized three times. A catalyst/initiator solution was prepared by adding 1,5,7-triazabicyclo[4.4.0]dec-5-ene (TBD, 18 mg, 0.126 mmol) and benzyl alcohol (26 μ L, 0.215 mmol) into anhydrous dichloromethane (25 mL). 730 μ L of the freshly prepared solution was added into the Schlenk flask with monomer (425 mg). The initial molar ratio was monomer 100 equiv, TBD 0.5 equiv and BnOH 1 equiv. After 24h, the crude reaction was concentrated by rotary evaporator and purified by dialysis (MWCO 1000) from dichloromethane. The polymeric product was isolated as yellow oil and the yield was 373 mg (49%). ¹H NMR (acetone-d₆): δ = 5.35-4.55 (m, 2H, -CH- of LA unit and -CH- of triazoline unit), 3.85 (m, 1H), 3.72 (m, 4H), 3.59 (PEG chain, 30H), 3.48 (m, 3H), 3.30 (s, 4H, including CH₃-PEG-), 3.24-2.95 (m, 1H), 2.75-2.54 (m, 2H), 1.75 (m, 1H), 1.59 (m, 5H, including CH₃- of LA unit), 1.36 (m, 1H), 1.11 (m, 1H). ¹³C NMR (acetone-d₆): δ = 170.9, 170.7, 85.2, 80.6, 70.6, 63.0, 55.1, 48.9, 42.4, 41.9, 29.9, 17.0 matched that reported previously³ (Figure 25 and 26).

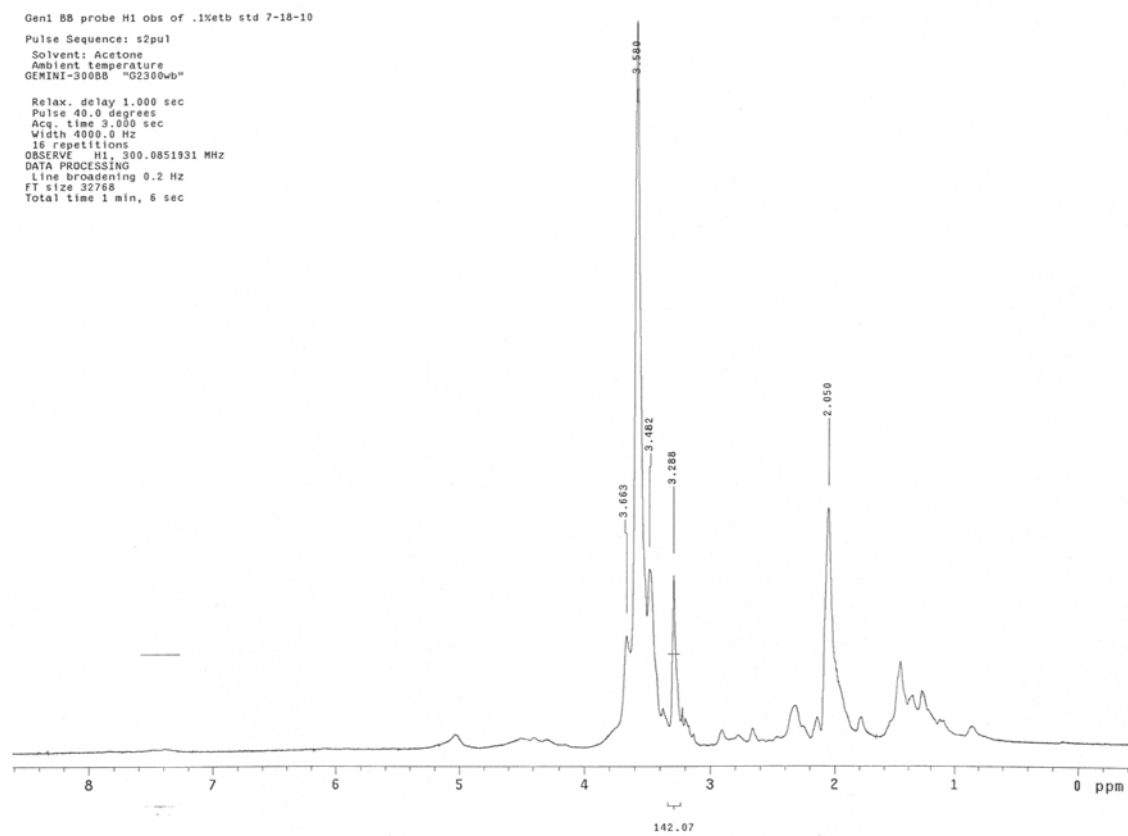


Figure 25. ^1H NMR spectrum of $\text{PEG}_6\text{-spiro-PLA}$ (acetone- d_6 , molecular structure of 8 refers to scheme 10)

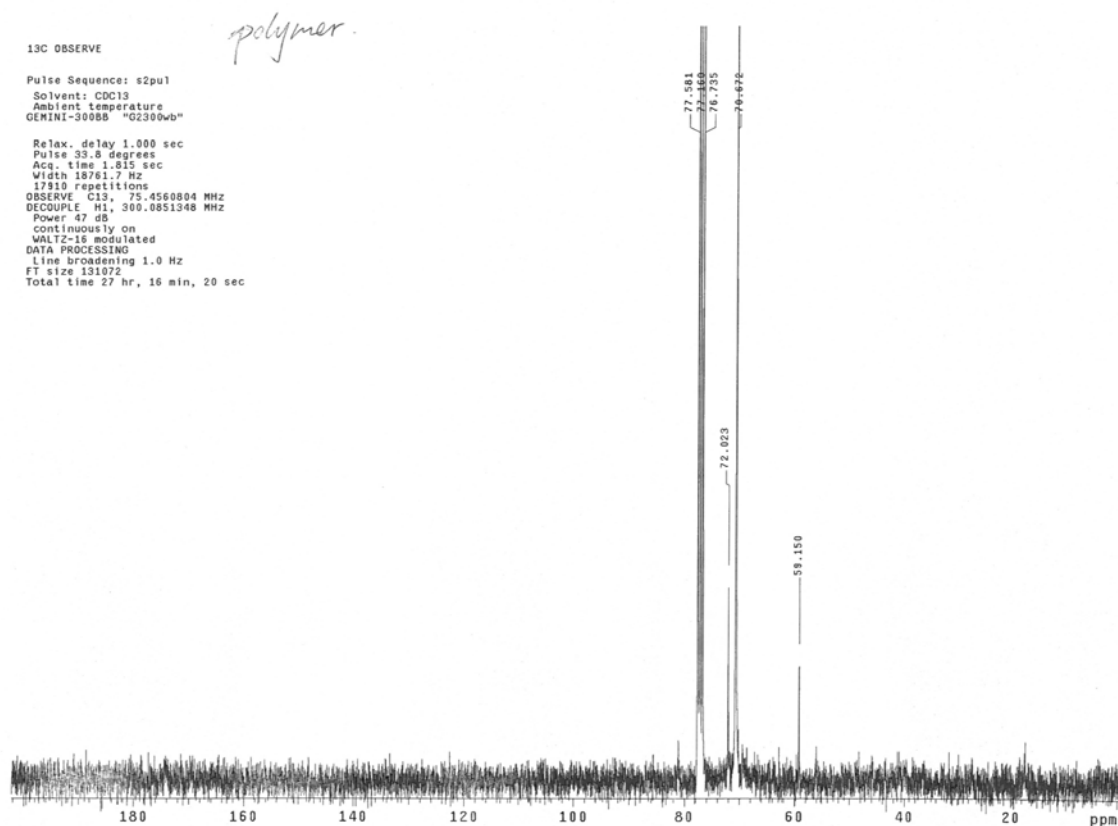


Figure 26. ^{13}C NMR spectrum of PEG₆-spiro-PLA (CDCl_3 , molecular structure of **8** refers to scheme 10)

D. Synthesis and polymerization of 5-Phenyl-1,3-dioxolane-2,4-dione [*O*-carboxyanhydride (OCA)]

D.1. Synthesis of 5-Phenyl-1,3-dioxolane-2,4-dione

Mandelic acid (2.90 g, 13.7 mmol) and freshly distilled tetrahydrofuran (31.4 mL) was added into a 150 mL round bottom flask. A solution of trichloromethyl chloroformate (diphosgene, 1.65 mL) in 10.45 mL tetrahydrofuran was prepared using Schlenk technique. That solution was added into the reaction flask drop wise. After being refluxed for 6h, the mixture was

concentrated to viscous colorless oil using rotary evaporator. Hexane was added into the oil and the mixture was kept under 0°C overnight. The solid crude product was further washed with hexane several times and crystallized from diethyl ether to give dioxolanedione. The product was further recrystallized from diethyl ether and hexane and purified by column chromatography on silica gel eluting with hexane first then ethyl acetate to give a 1.50 g (61.5% yield) white solid. $^1\text{H NMR}$ (CDCl_3): δ 5.99 (s, 1H, CH); 7.38-7.58 (m, 5H, Ar) matched that reported previously⁵ (Figure 27)

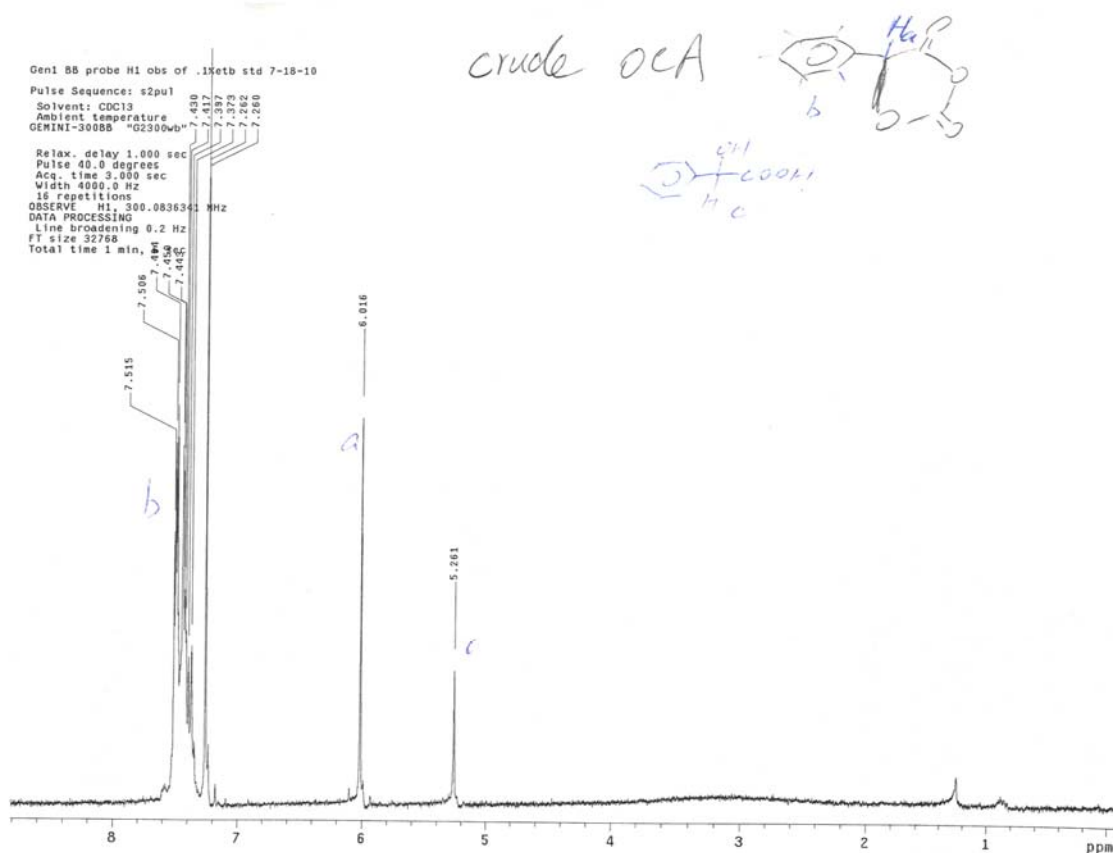


Figure 27. $^1\text{H NMR}$ spectrum of crude OCA (CDCl_3) showing the methane protons of the starting material, mandelic acid and the product

D.2. Test of water sensitivity of 5-Phenyl-1,3-dioxolane-2,4-dione

5-Phenyl-1,3-dioxolane-2,4-dione (mg level) was dissolved by CDCl_3 in a NMR tube. A drop of D_2O was added. The NMR tube was kept under room temperature. ^1H NMR spectroscopy of the mixture was taken at certain time point to observe the speed of ring opening reaction. Because the diagnostic peaks of mandelic acid in ^1H NMR are at 4.9 and 7.38-7.58 ppm while ones of OCA are at 5.99 and 7.38-7.58 ppm, increasing peak at 4.9 and decreasing peak at 5.9 indicated the ring opening reaction of OCA. Most OCA turned back to mandelic acid after hydrolyzed by D_2O for 66h.

D.3. Polymerization of 5-Phenyl-1,3-dioxolane-2,4-dione

In a glove box, 5-Phenyl-1,3-dioxolane-2,4-dione (178 mg, 1 mmol) and dry DCM taken from solvent column (10 mL) was added to a DCM solution (2 mL) of 4-Dimethylaminopyridine (DMAP, 1.22 mg, 10 μmol) and benzyl alcohol (1.08 mg, 10 μmol) at room temperature. The reaction was monitored by FTIR and the disappearance of the anhydride peak of OCA at 1810 cm^{-1} showed the completion of polymerization. The polymer was precipitated with ether and the precipitate was dried under vacuum. The isolated yield was 0.21 g (over 100%). ^1H NMR (CDCl_3): δ 7.3 (m, Ph); 5.9 (m, CH)

E. OEG-Grafted PLA (Version II): Monomer Synthesis and Characterization (All the numbers of molecules are referred to Scheme 16)

E.1. Syntheses of 3-(Benzyloxymethyl)-6-methyl-1,4-dioxane-2,5-dione (9)

E.1.1. Synthesis of 3-Benzyloxy-2-hydroxypropionic Acid (2)

O-benzyl-L-serine (10 g, 51.25 mmol) was dissolved in a solution of trifluoroacetic acid in deionized water (0.7 M, 100 mL). A solution of NaNO_2 (5.3 g, 76.85 mmol) in water (50 mL) was added dropwise via syringe pump over 3 h at $25\text{ }^\circ\text{C}$. The reaction was left at $25\text{ }^\circ\text{C}$ for another 3 h, then NaCl (10 g) was added into the mixture and the crude product was extracted into ethyl acetate. The organic layers of the crude product in EtOAc were isolated and washed with a saturated solution of NaCl in water and dried over MgSO_4 . After removing

EtOAc, and further drying under vacuum to afford a yellow oil, the crude product was purified by column chromatography on silica gel (standard grade) eluting with a mixed solvent system of CH₂Cl₂, MeOH and AcOH (97:2:1) to give a pale yellow oil (6.44 g, 70%).
¹H NMR (300 MHz, CDCl₃) δ: 7.25-7.35 (m, 5H), 4.5 (s, 1H), 4.3 (t, 1H), 3.7-3.8 (m, 2H);
¹³C NMR (300 MHz, CDCl₃) δ: 173.4, 138.8, 128.4, 127.7, 127.6, 73, 72, 71 matched that reported previously⁶. (Figure 28)

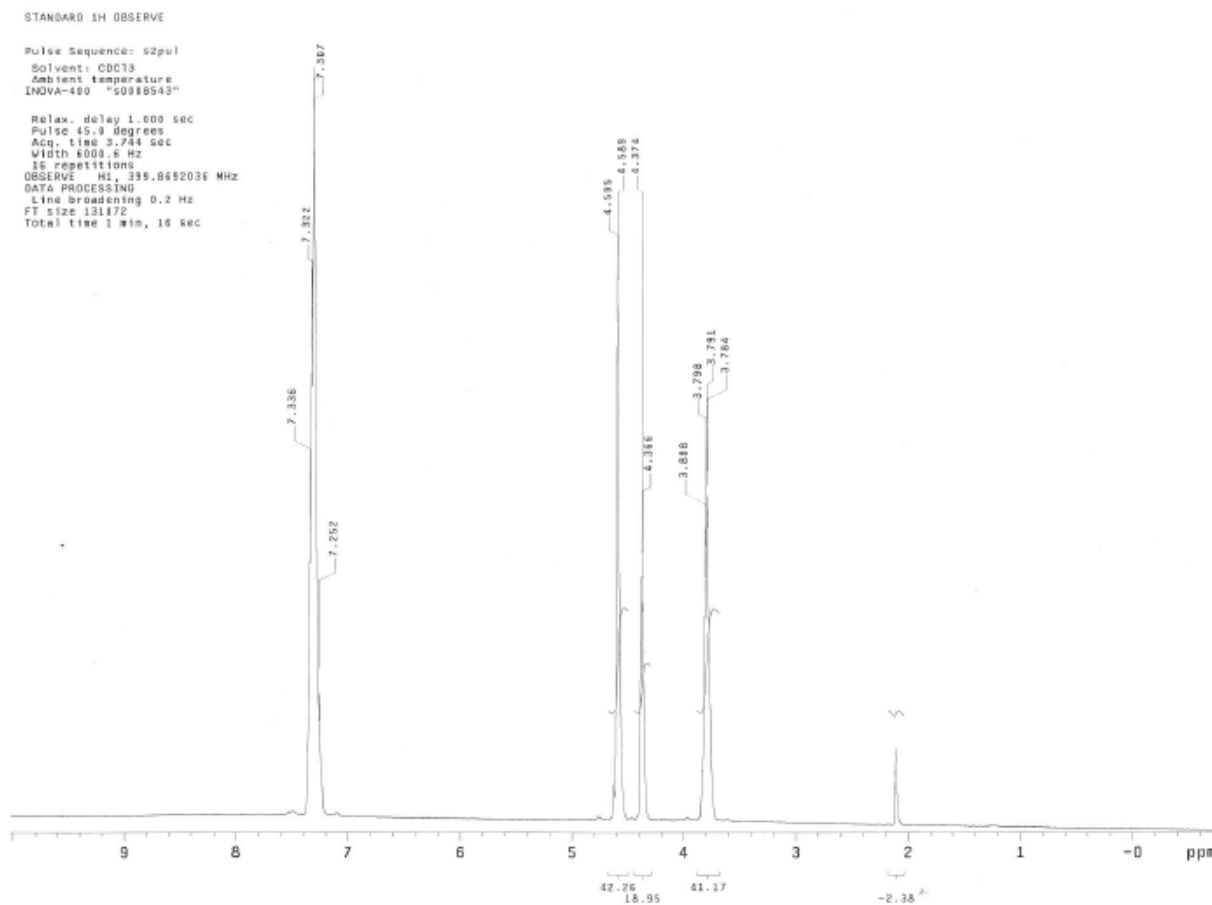


Figure 28. ¹H NMR spectrum of 3-Benzyloxy-2-hydroxypropionic Acid (CDCl₃, refer to scheme 16)

E.1.2. Synthesis of L- α -Bromopropionyl Chloride (5)

L-Alanine (molecule **3**, 10 g, 112 mmol) was dissolved in the solution of HBr (48 wt%, 116 mL) in water (160 mL). After adding some cracked ice, NaNO₂ (20.8 g, 302 mmol) and Na₂SO₄ (140 g) were added slowly and sequentially into the solution to avoid effervescing. When the temperature reached 15 °C, the reaction was terminated and, after filtration, the solution was divided into several portions and each was extracted with Et₂O. All the organic layers were combined and dried over Na₂SO₄ and CaCl₂ sequentially. After evaporating Et₂O, low pressure distillation (110 °C, 25 Torr) was used to purify the product (molecule **4**, 10.28 g, 61%). Next, SOCl₂ was first refluxed with sulfur, then fractionally distilled twice and 6.92 mL of it was mixed with **4**. The reaction was kept under 60°C for 8 h and then left at room temperature overnight. Again, low pressure distillation (110 °C, 25 Torr) was employed to isolate the desired product (molecule **5**, 8.07 g, 69%). ¹H NMR (300 MHz, CDCl₃) δ : 1.93 (d, 3H, CH₃), 4.65 (q, 1H, CH) matched that reported previously⁵. (Figure 29)

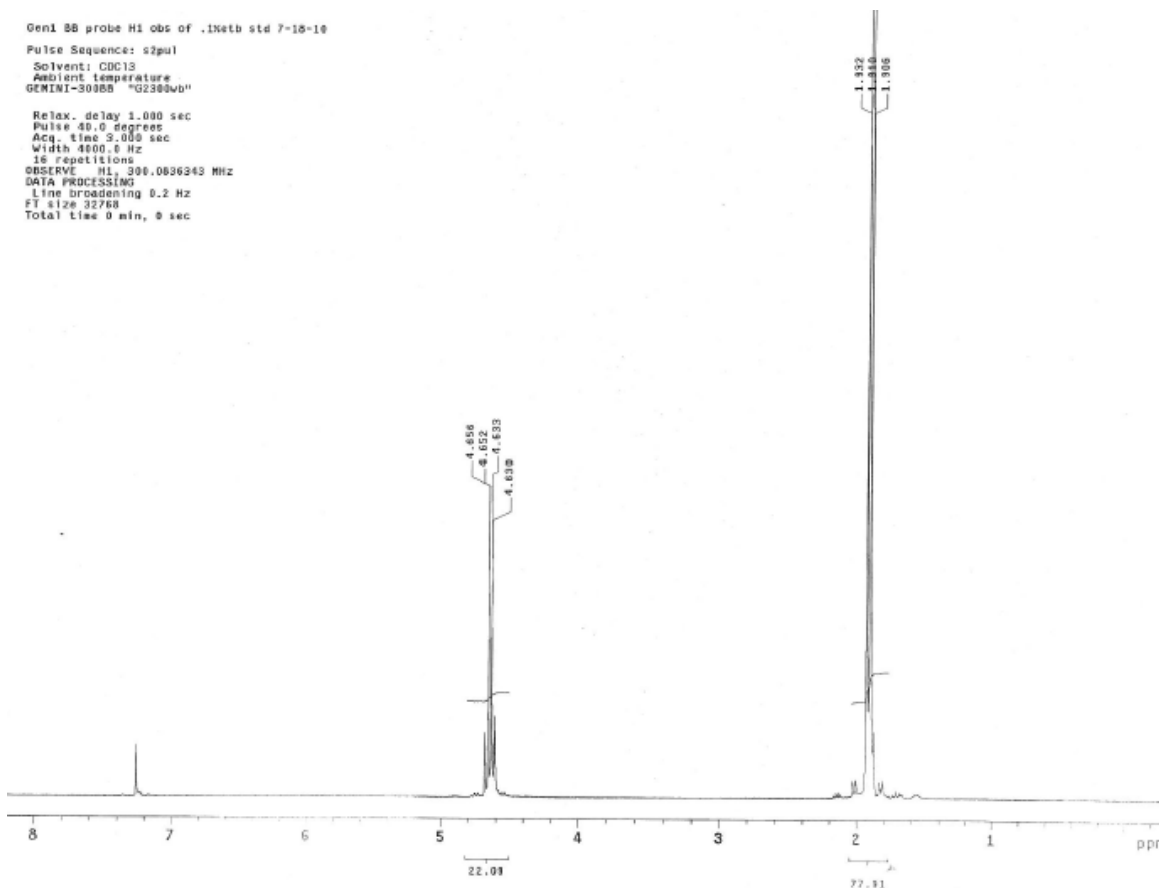


Figure 29. ^1H NMR spectrum of L- α -Bromopropionyl Chloride (CDCl_3 , scheme 16)

E.1.3. Synthesis of 3-(Benzyloxy)-2-(2-bromopropanoyloxy)propanoic Acid (6)

Before running the cyclization reaction, 3-Benzyloxy-2-hydroxypropionic Acid (**2**) was subject to one more purification. The residual water was removed azeotropically with toluene under low pressure. With no solvent added, L- α -Bromopropionyl chloride (3.44 g, molecule **5**) and 3-benzyloxy-2-hydroxypropionic acid (2.17 mL, molecule **2**) were placed in a three-necked, round bottomed flask equipped with a base trap (NaOH or KOH). The mixture was heated at 70 °C under N_2 atmosphere. After 6 h, the reaction was done, which could be monitored by thin layer chromatography (TLC, mobile phase: DCM). The resulting, dark brown oil was placed under vacuum and slightly heated (35 °C) overnight to remove excess molecule **2**. The crude product **6** was isolated by column chromatography on silica gel

(standard grade) eluting with a mixed solvent system of CH₂Cl₂, MeOH and AcOH (98:1.5:0.5). The purified product **6** was carried on to the next reaction directly (Figure 30).

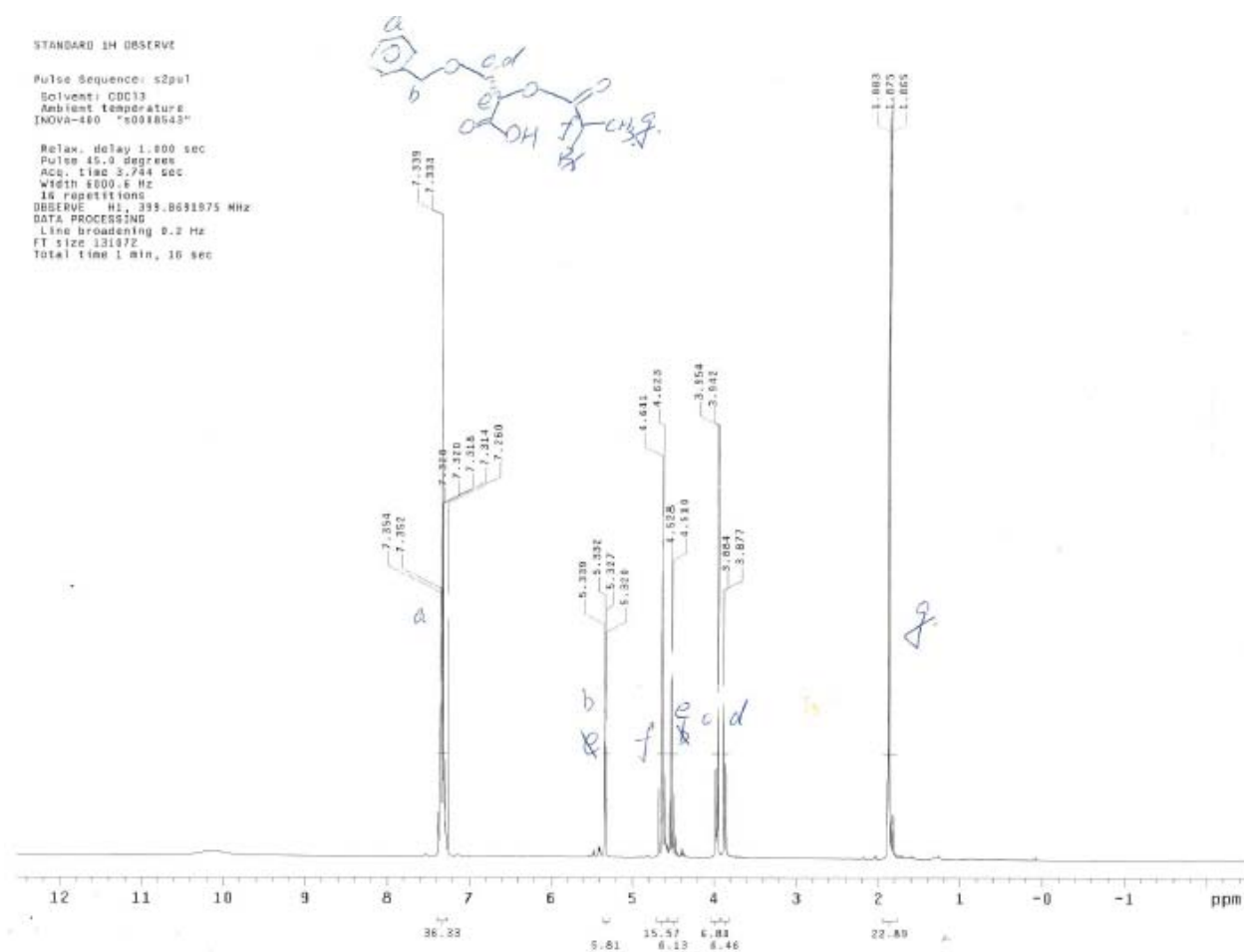


Figure 30. ¹H NMR spectrum of 3-(benzyloxy)-2-(2-bromopropanoyloxy)propanoic Acid (CDCl₃, scheme 16)

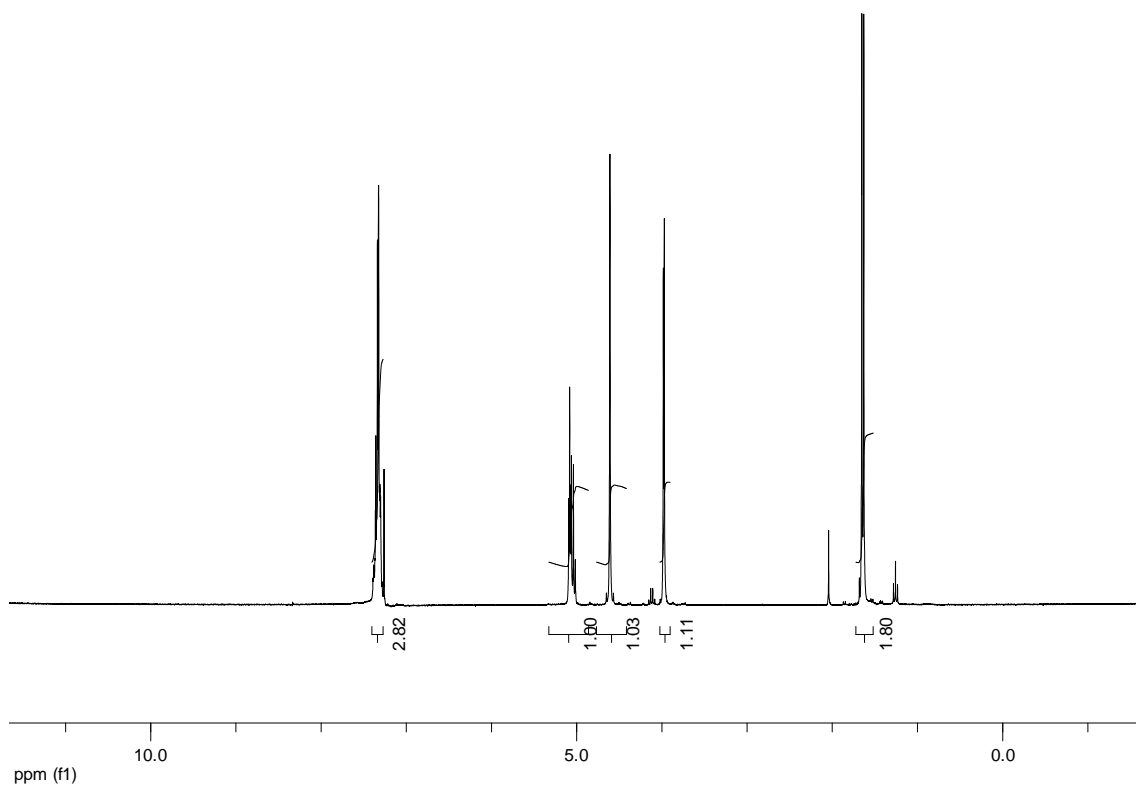
E.1.4. Halide Exchange

A solution of 3-(benzyloxy)-2-(2-bromopropanoyloxy)propanoic acid (1.01 g, molecule **6**) in dry acetone (25 mL) was heated to reflux with 10 equivalents of KI under N₂ atmosphere. After 12 h, the mixture was filtered through celite and the solvent was evaporated. The

product was redissolved in EtOAc and washed three times with a 2M Na₂S₂O₃ solution. The color of the solution was light yellow after washing. The organic layer was dried over MgSO₄ and the product **7** was isolated after removing the solvent under reduced pressure. Molecule **7** was used for the next reaction without further purifications.

*E.1.5. Synthesis of 3-(Benzyloxymethyl)-6-methyl-1,4-dioxane-2,5-dione (**8**)*

A solution of di-isopropyl ethyl amine (DIEA, 0.743 mL) in dry acetone (161 mL) was heated to reflux. A solution of molecule **7** (0.84 g) in dry DCM (16 mL) was added to the solution of DIEA dropwise over 8 h via a syringe pump (Adding rate was calculated individually by experimenter). After adding the solution of **7**, the reaction was kept refluxing for another hour. The solvent was removed under reduced pressure, then Et₂O (17 mL) was added to the crude product (brown) to precipitate out ammonium iodide. The mixture was filtered through celite and the crude product was isolated after removing solvent. It was first purified by column chromatography on silica gel (standard grade) eluting with mixed solvent system of hexane and EtOAc (3:1) to obtain a mixture of diastereomers. These were separated using another column (premium grade silica gel) eluting with a mixed solvent system of hexane and EtOAc (8:2). Each of the two isomers was isolated as a crystalline solid (0.22 g, 33% and 0.18 g, 28%). ¹H NMR (300 MHz, CDCl₃, only one diastereomer) δ: 7.2-7.4 (m, 5H), 5.1 (q, 1H), 5.0 (dd, 1H), 4.5 (s, 2H), 4.0 (dd, 1H), 3.9 (dd, 1H), 1.6 (d, 3H); ¹³C NMR (300 MHz, CDCl₃) δ: 166.0, 164.1, 136.4, 128.4, 128.1, 127.9, 76.0, 74.0, 73.1, 68.6, 17.8 matched that reported previously⁵. (Figure 31)



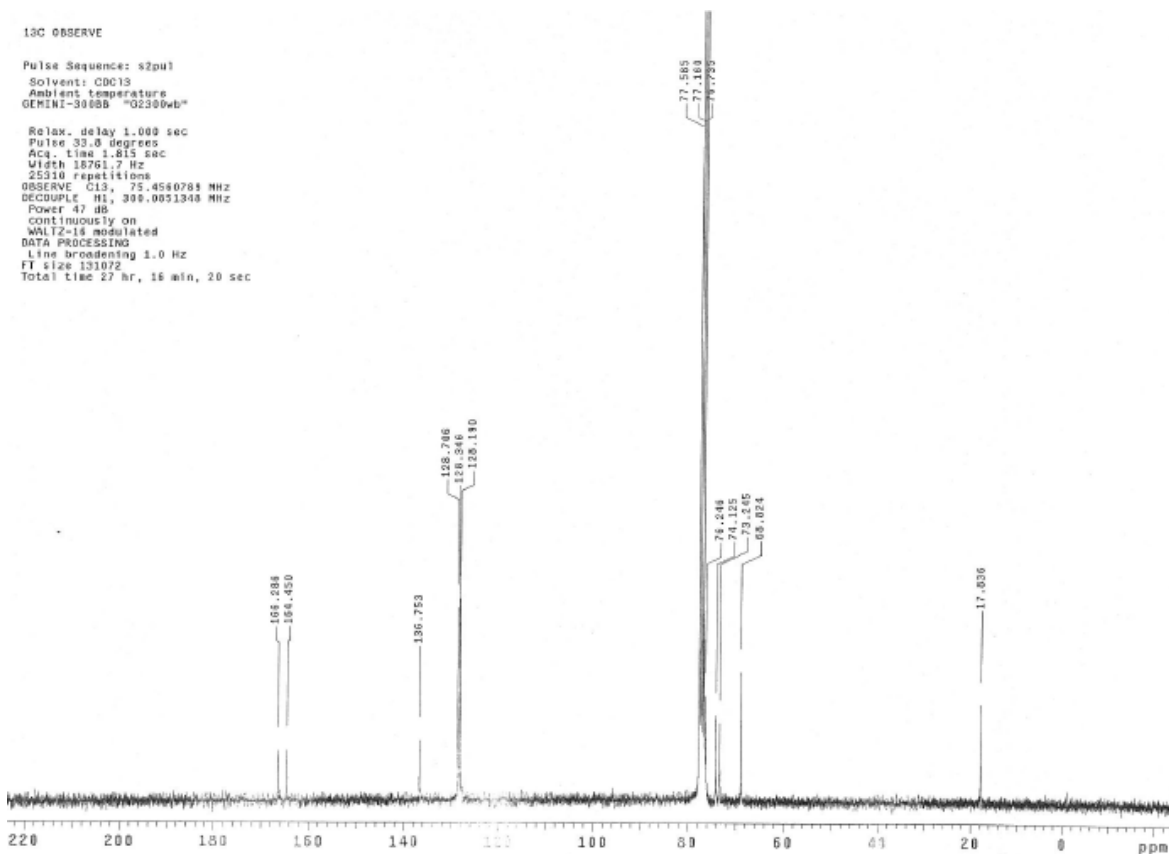


Figure 31. ^1H NMR and ^{13}C NMR spectra of 3-(Benzyloxy)-2-(2-bromopropanoyloxy)propanoic Acid (CDCl_3 , scheme 16)

E.2. Attempt at Syntheses of Oligo(ethylene glycol)-grafted Lactide (11)

E.2.1. Synthesis of Hydroxyl Functionalized Lactide (10)

A white solid of 0.22 g of molecule **9** was dissolved in one of several solvents (e.g. THF, 0.88 mL) and reaction was stirred with a heterogeneous catalyst (e.g. Pd/C, 23.47 mg, excess) under H_2 atmosphere for approximately 2 days. The carboxybenzyl group was deprotected after 2 days and leaving a white solid **10** (0.13 g, 94%). ^1H NMR (300 MHz, CDCl_3) δ : 5.2 (q, 1H), 5.1 (t, 1H), 4.2 (d, 2H), 1.7 (d, 3H). (Figure 32)

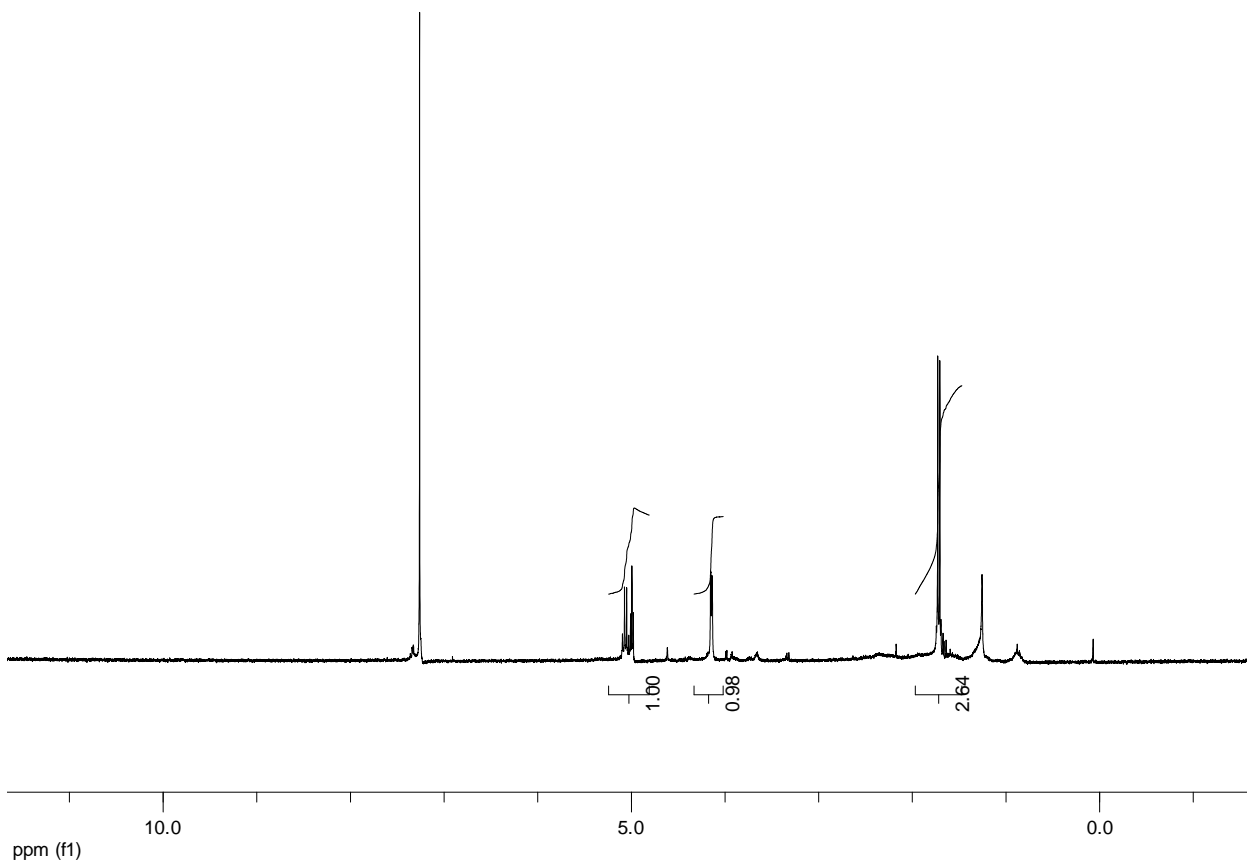


Figure 32. ^1H NMR spectrum of Hydroxyl Functionalized Lactide (CDCl_3 , scheme 16)

E.2.2. Attempt at Synthesis of tosylactide (11)

Molecule **10** (0.13 g) was dissolved in one of several basic solvents (e.g. dry pyridine, 0.5 mL) at 0 °C. Then, *p*-toluenesulfonyl chloride (1.1 eq) was added to the solution over 5 min with stirring. The mixture was then stirred continuously at 0 °C for 3 h. A solution of HCl (6 M) was added until the pH reach a value of 1 as determined by pH indicator strips. The mixture was extracted with EtOAc and dried over Na_2SO_4 . However, the ^1H NMR of the crude product indicated that the ring structure of lactide was no longer present. As little starting materials were left over, this synthesis was terminated here.

F. OEG-Grafted PLA (Version III): Monomer Synthesis and Characterization (All the numbers of molecules are referred to Scheme 17)

F.1. Synthesis of 1-Bromo-7,10,13-trioxatetradecane (16)

Dry THF (600 mL), 1,6-dibromohexane (50.8 g) and NaH (60% in mineral oil, 60 g) were added into a nitrogen-charged, two-necked reaction flask. The reaction was cooled to -35 °C (bath of ethylene glycol/ethanol and dry ice). A solution of freshly distilled diethylene glycol monomethyl ether (12.1 g) in dry THF (50 mL) was added dropwise into the stirred slurry over 5 h. After completing the addition, the reaction was stirred at 0 °C for 2 days. The crude product was purified by filtration, rotary evaporation and then fractional distillation. The distillate at 58-60 °C (50 mTorr) gave 1.5 g of 3 (61 %) as a colorless oil. ¹H NMR (300 MHz, CDCl₃) δ: 3.53 (m, 2H), 3.49 (m, 2H), 3.42 (t, 2H), 3.38 (t, 2H), 3.34 (s, 3H), 1.84 (p, 2H), 1.59 (p, 2H), 1.38-1.46 (m, 2H), 1.29-1.38 (m, 2H). ¹³C NMR δ: 71.93, 71.20, 69.95, 58.97, 33.71, 32.65, 29.33, 27.90, 25.22 matched that reported previously⁷. (Figure 33)

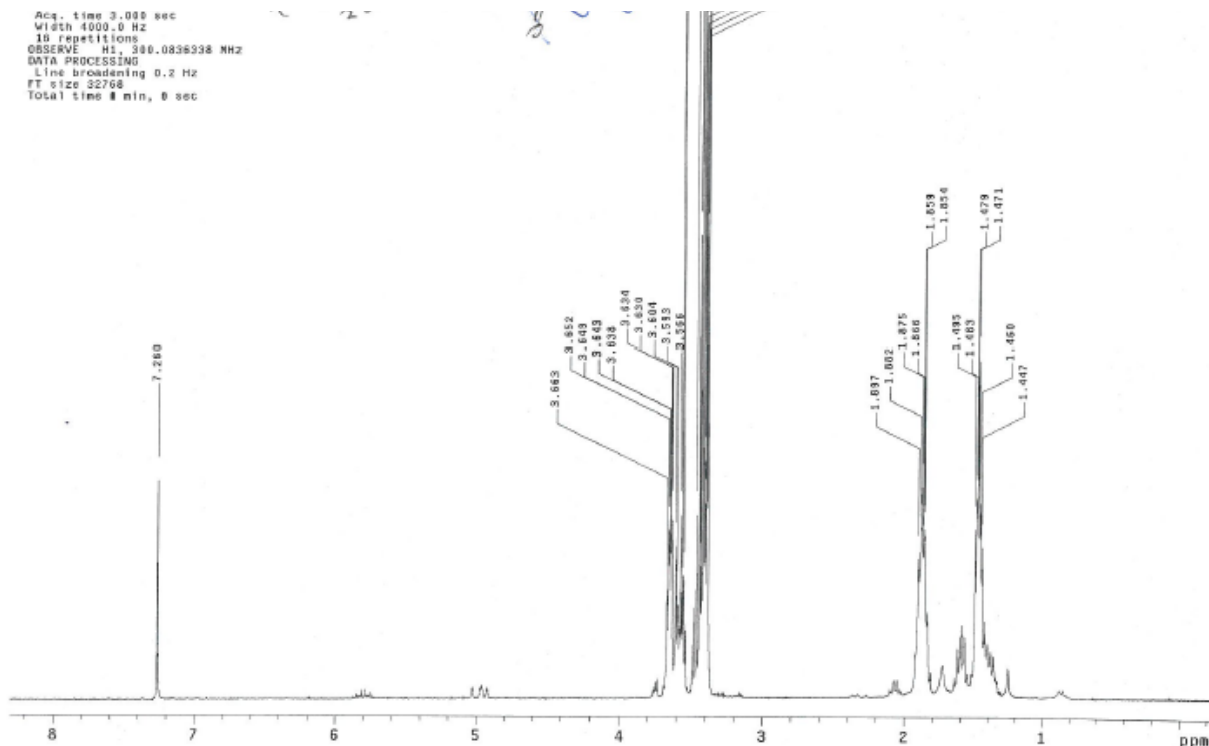


Figure 33. ^1H NMR spectrum of 1-Bromo-7,10,13-trioxatetradecane (CDCl_3 , scheme 17)
F.2. Synthesis of 2-Hydroxy-9,12-dioxatridecanoic Acid (18)

Magnesium turnings (0.33 g) were heated slightly with I_2 (catalytic amount) in a two-necked reaction flask. A solution of **16** (1.5 g) in dry THF (8.36 mL) was added dropwise via an additional funnel to the flask. A clear solution formed after the magnesium turnings disappeared. The reaction was protected by nitrogen and did not occur vigorously. The Grignard reagent was then added dropwise under nitrogen to a 1 L round-bottom flask containing a stirred solution of diethyl oxalate (0.772 g) in dry THF (7 mL) at $-80\text{ }^\circ\text{C}$. The mixture was stirred for an additional hour at $-80\text{ }^\circ\text{C}$ (liquid nitrogen), and the reaction was quenched by adding 4 mL of 2 M HCl. The aqueous layer was extracted with ether and the organic layer containing crude product **17** was dried over MgSO_4 . Filtration and removal of solvent gave a light brown oil (1.03 g, 64%). This was used without further purification (Figure 34)

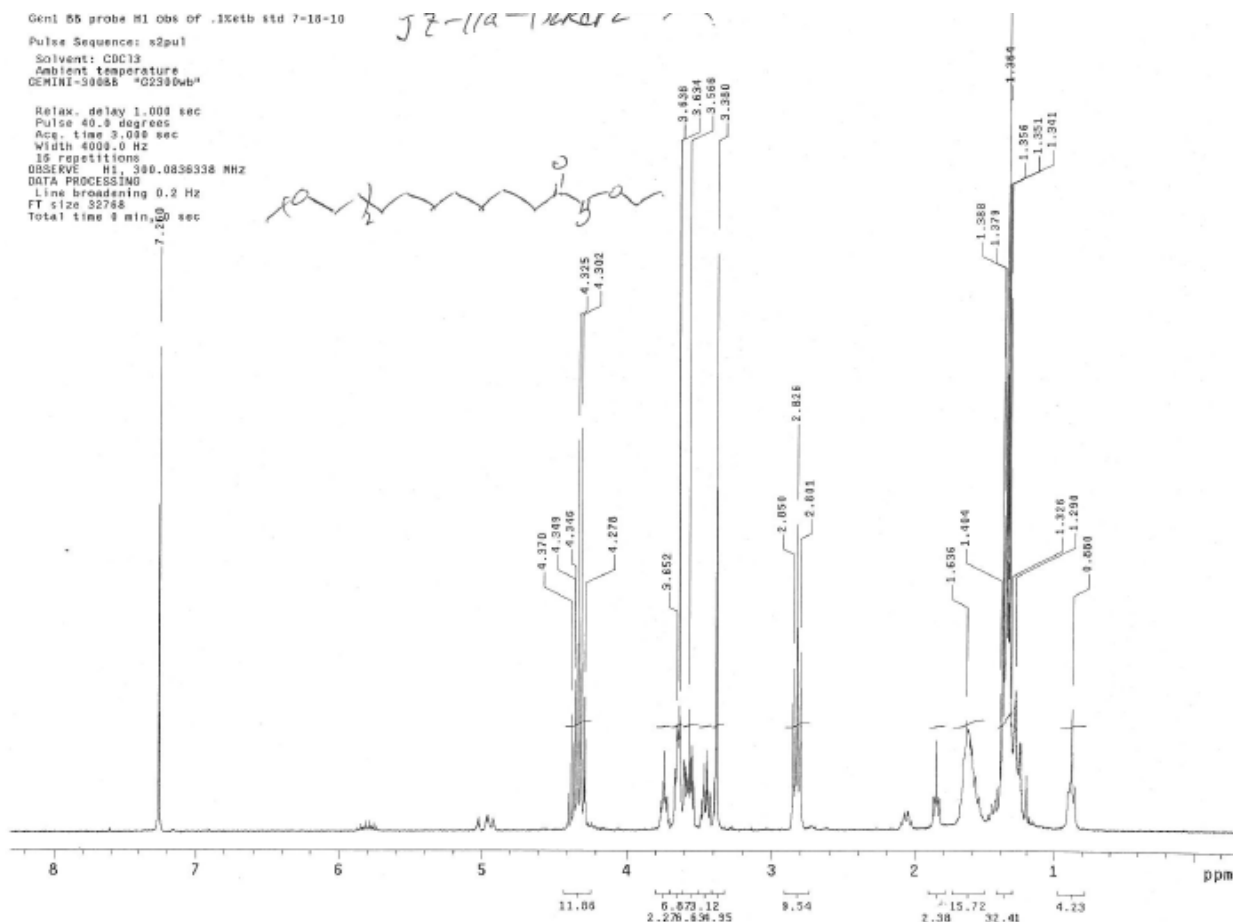


Figure 34. ^1H NMR spectra of α -keto ester **17** (CDCl_3 , scheme 17)

The α -keto ester **17** (1.03 g) was dissolved in ethanol (10 mL) and stirred at 0 °C. NaBH_4 (1.5 eq.) was dissolved in minimal amount of ethanol and added dropwise into the solution of **17**. After 30 min, the reaction was tracked by TLC (mobile phase: hexane: ethyl acetate 1:1) using dinitrophenyl hydrazine (DNP) as indicator and ^1H NMR. When ^1H NMR showed that α -keto ester had fully reacted (disappearance of the triplet at 3 ppm), the solids were removed by filtration and the solvent was evaporated to give a colorless oil. The oil was used for the next hydrolysis without further characterization (Figure 35).

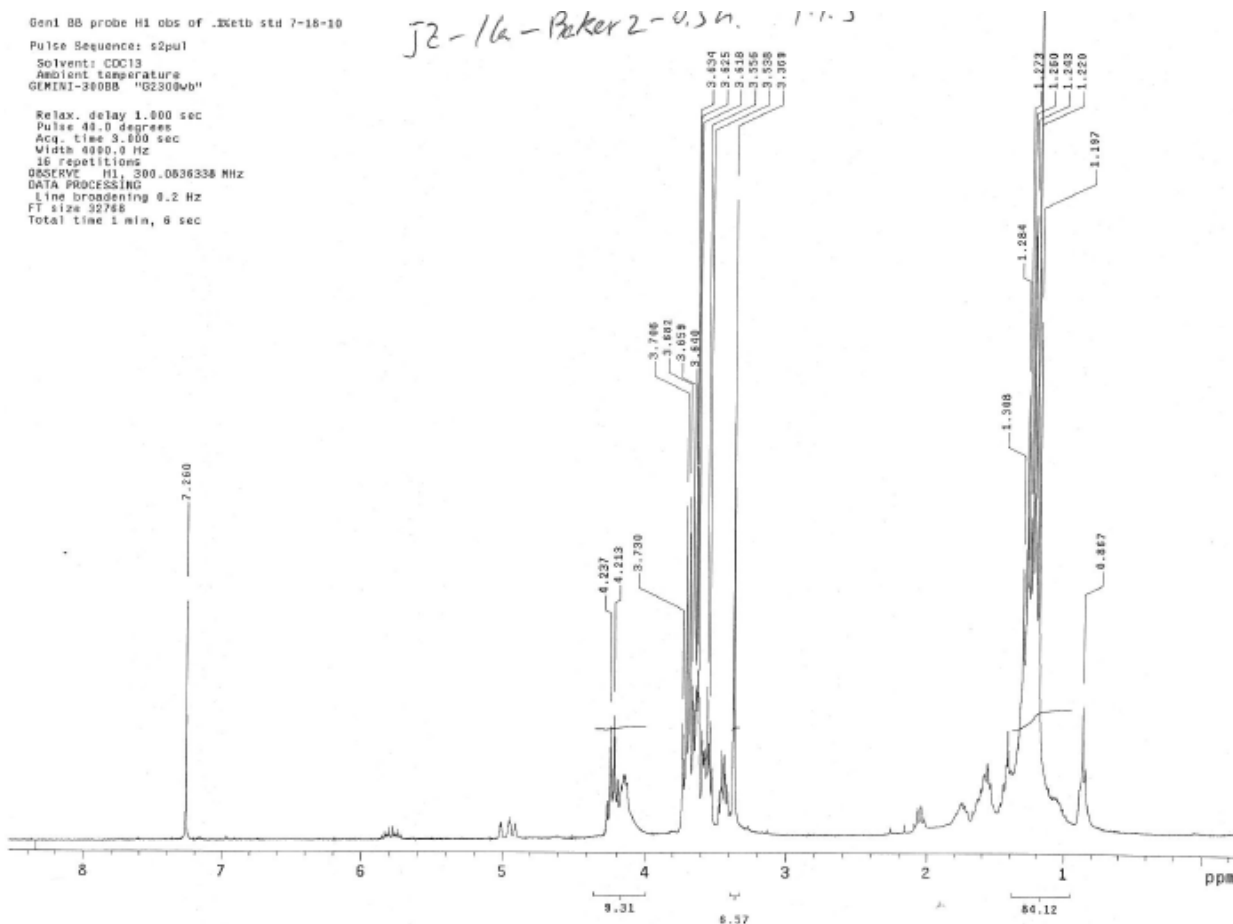
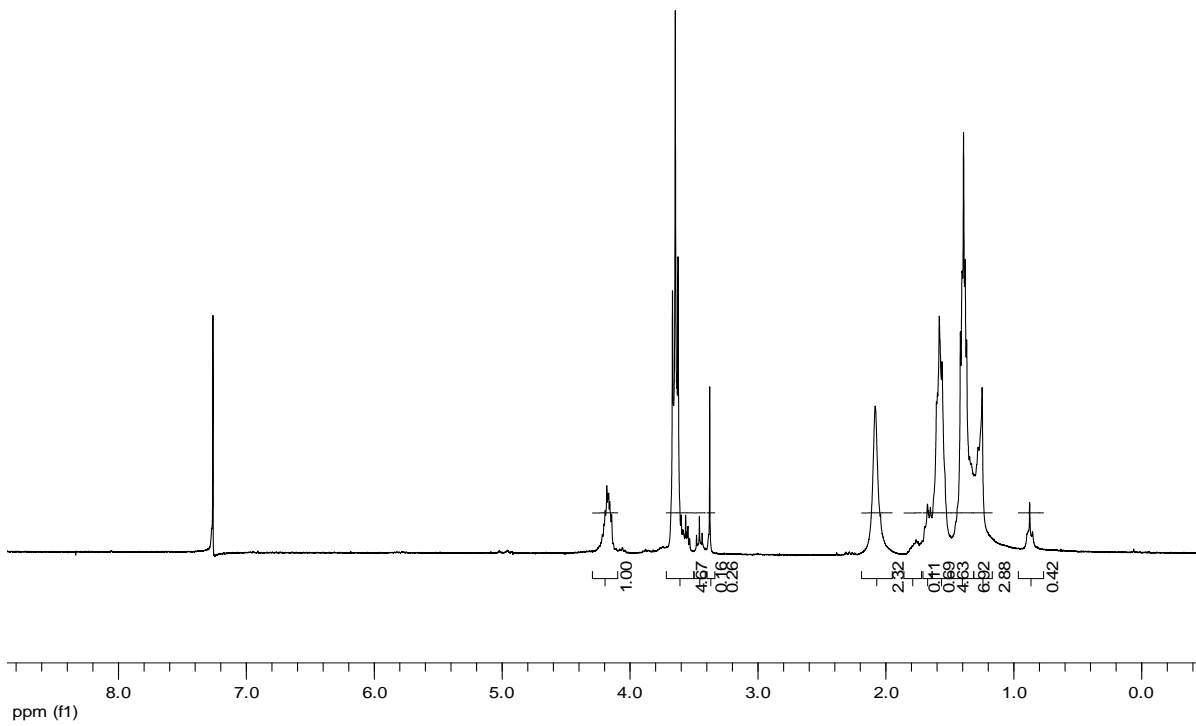


Figure 35. ^1H NMR spectrum of α -hydroxy ester (CDCl_3 , scheme 17)

Next, the oil was added to a solution of saturated NaHCO_3 in water (14 mL), and the mixture was heated to reflux for 3 days. When ^1H NMR showed the hydrolysis was complete (disappearance of the quartet at 4 ppm), the aqueous solution was extracted with ether for 24 h at room temperature. Only the aqueous layer was further used. It was acidified with HCl to $\text{pH}=1$. The acidic, aqueous solution was extracted with ether once again for 48 h through vigorous stirring of the two, immiscible solvents. This time, the ether layer was dried over MgSO_4 , filtered and evaporated to give **18** as a light brown oil. The crude product was triply recrystallized from ether at $-40\text{ }^\circ\text{C}$ to give a colorless oil (0.37 g, 47%). ^1H NMR (300 MHz, CDCl_3): δ : 4.20 (q, 1H), 3.62 (m, 4H), 3.56 (m, 4H), 3.43 (t, 2H), 3.35 (s, 3H), 1.78 (m, 1H), 1.66 (m, 1H), 1.55 (p, 2H), 1.24-1.48 (m, 6H) matched that reported previously⁷ (Figure 36).



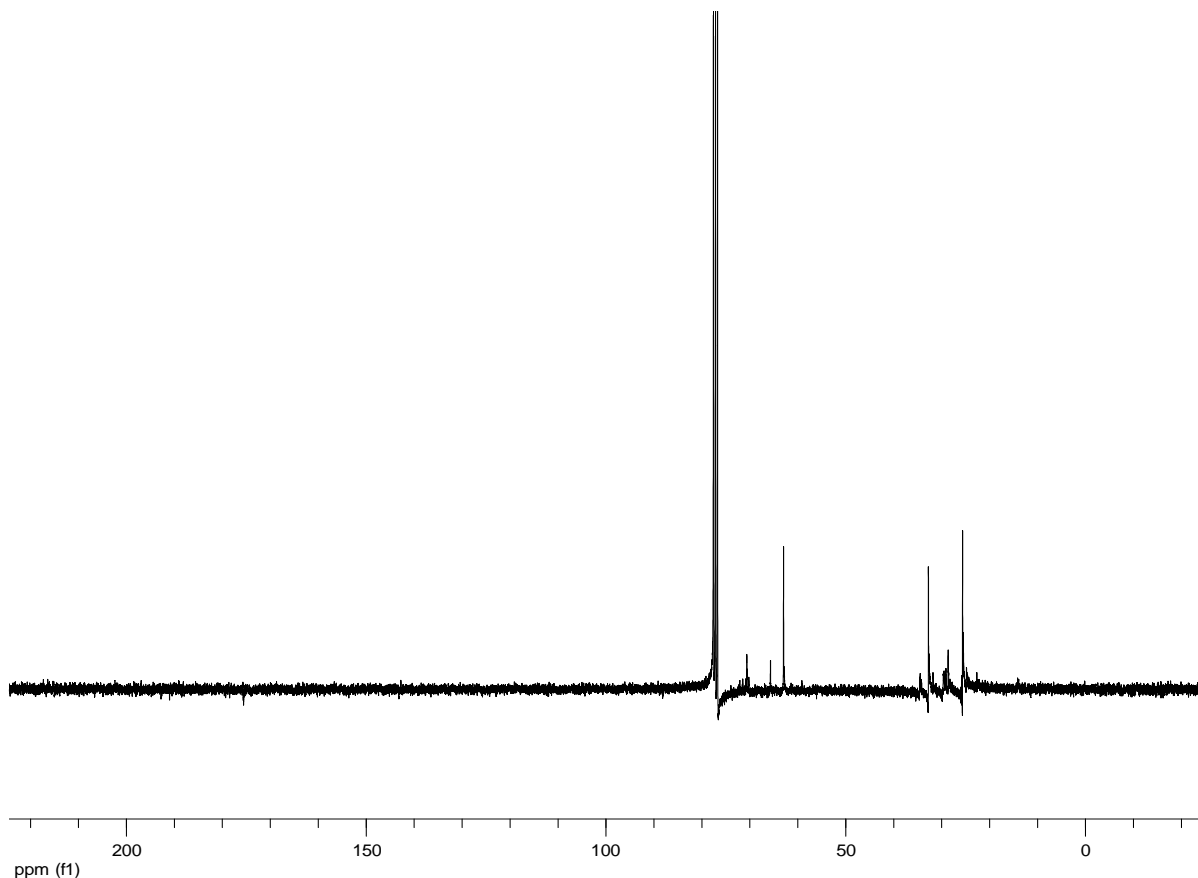


Figure 36. ^1H NMR and ^{13}C NMR spectrums of 2-Hydroxy-9,12-dioxatridecanoic Acid (CDCl_3 , scheme 17)

F.3. Synthesis of 3,6-Bis(7,10,13-trioxatetradecyl)-1,4-dioxane-2,5-dione (**19**)

2-Hydroxy-9,12-dioxatridecanoic acid (**18**) (0.37 g), *p*-toluenesulphonic acid (12.1 mg) and toluene (22 mL) were placed in a 100 mL round-bottomed flask. The reaction was heated to reflux for 3 days with a Barrett trap to remove any residual water azeotropically. After evaporating the solvent, the resulting oil was redissolved in ether, washed with saturated NaHCO_3 solution (aq) and dried over MgSO_4 . Filtration and evaporation of the solvent gave the crude product **19** as a yellow oil, which was recrystallized from ether at $-40\text{ }^\circ\text{C}$. Although the gel-like monomer **19** could be purified using reduced-pressure distillation ($180\text{ }^\circ\text{C}/3\text{ mTorr}$) in the literature, attempts to distill the monomer resulted in polymerization.

^1H NMR (300 MHz, CDCl_3): δ : 4.88 (q), 4.83 (q, 1H total for the signals at 4.88 and 4.83, diagnostic peak of lactide) matched that reported previously⁷. (Figure 37)

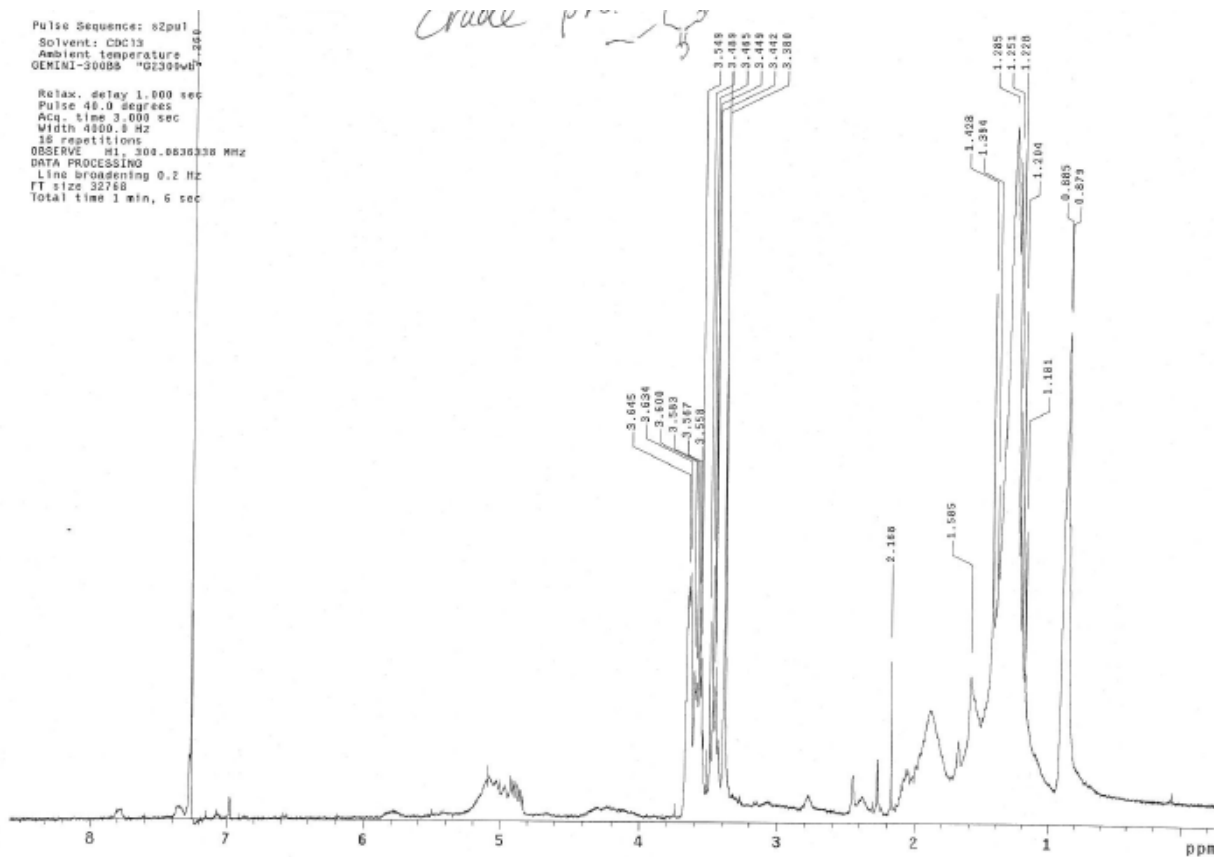


Figure 37. ^1H NMR spectrum of 3,6-Bis(7,10,13-trioxatetradecyl)-1,4-dioxane-2,5-dione (CDCl_3 , scheme 17)

References:

- (1) Xu, L.; Gorman, C. B. *Journal of Polymer Science Part A: Polymer Chemistry* **2010**, *48*, 3362.
- (2) Xu, L.; Crawford, K.; Gorman, C. B. *Macromolecules* **2011**, *44*, 4777.
- (3) Castillo, J. A.; Borchmann, D. E.; Cheng, A. Y.; Wang, Y.; Hu, C.; Garcia, A. J.; Weck, M. *Macromolecules* **2012**, *45*, 62.
- (4) Saha, A.; Ramakrishnan, S. *Macromolecules* **2009**, *42*, 4956.
- (5) Gerhardt, W. W.; Noga, D. E.; Hardcastle, K. I.; Garcia, A. J.; Collard, D. M.; Weck, M. *Biomacromolecules* **2006**, *7*, 1735.
- (6) Barrera, D. A.; Zylstra, E.; Lansbury, P. T.; Langer, R. *Macromolecules* **1995**, *28*, 425.
- (7) Jiang, X.; Smith III, M. R.; Baker, G. L. *Macromolecules* **2008**, *41*, 318-324.